



University of Stavanger

Faculty of Science and Technology

MASTER'S THESIS

Study program/ Specialization: Master of Science in Petroleum Engineering Reservoir Engineering	Spring semester, 2013 Open
Writer: Alex Rodrigo Valdés Pérez (Writer's signature)
Faculty supervisor: Leif Larsen	
External supervisor(s):	
Titel of thesis: “A New Double Porosity Fractal Model for Well Test Analysis with Transient Interporosity Transfer for Petroleum and Geothermal Systems”	
Credits (ECTS): 30	
Key words: Fractal Well Testing Naturally Fractured Reservoirs Double Porosity	Pages: 116 + enclosure: Stavanger, June 6th, 2013

Copyright

by

Alex Rodrigo Valdés Pérez

2013

*“...¿Qué mágicas infusiones
de los Indios herbolarios
de mi Patria, entre mis letras
el hechizo derramaron?...”*

Sor Juana Inés de la Cruz

*“I firmly believe that any man’s finest hour,
the greatest fulfilment of all that he holds dear,
is the moment when he has worked his heart out
in a good cause and lies exhausted on the
field of battle – victorious!”*

Vince Lombardi

Dedication

To México, this is also part of you.

*To my beloved parents Marta and Ismael,
without your help and support, I could not achieve this goal.*

To Valeria and Ian, our future is in your hands.

This page is intentionally left in blank.

Acknowledgements

I want to express my gratitude to Iván, Raúl and Javier Valdés, for their support in my norwegian adventure.

To my recommendators for this program Héber Cinco-Ley, Héctor Pulido, Fernando Samaniego and Rafael Rodriguez, for their invaluable help and contributions to the petroleum engineering.

The *SPE fellowship* which was awarded to me was crucial to successfully complete my studies here. The loan provided by *Banco de México* is greatly acknowledged.

I am also deeply thankful to my advisor Leif Larsen, for his advice, guidance and encouragement through the development of this thesis.

I am grateful to Frode Hveding who trusted me and gave me the opportunity to apply my knowledge in well test analysis.

I also want to thank to Hans Borge, who is always willing to help the students and is ally of us.

To my closest friends during this period of my life, Pablo and Miguel Luzuriaga,, Luisa Campiño, Roberto Pérez, Diana Pavón and Juan Andrade. Guys, it was very funny.

And last but not least, to Norway and to the University of Stavanger, for giving me the opportunity of studying, working and living outside my country. I will be always grateful with you.

This page is intentionally left in blank.

Abstract

A new double porosity model for Naturally Fractured Reservoirs (NFRs) assuming fractal fracture network behavior and its solution is presented. Primary porosity is idealized as Euclidian matrix blocks (slabs or spheres) and Secondary porosity is defined by any post-depositional geological phenomenon such as fractures and vugs.

In order to provide a framework, the generalized radial flow model solution for well test analysis for petroleum and geothermal systems in Laplace and Real space was developed. Development of an appropriate wellbore storage model for fractal reservoirs is also shown.

For this model, the dimensionless fractal fracture area parameter was developed. In addition, interporosity skin factor between matrix blocks and fractal fracture network is introduced. Relationship of convergence between interporosity skin under transient transference regime and pseudosteady state transference regime is discussed. An analytical general solution was obtained in Laplace space; besides, analytical solutions in real space that describe the behavior of NFRs at different stages and different cases of flow are also presented. Early, intermediate and late-time approximations are used to obtain reservoir and fractal fracture network parameters. A synthetic example is presented to illustrate the application of this model.

This page is intentionally left in blank.

Contents

Abstract	v
Contents	vii
Chapter I Basic Concepts	1
Chapter II Literature Review	11
II.1. Double porosity models	11
II.2. Fractal models	18
Chapter III Proposed model	25
III.1. Flow model development	25
III.2. Transformation to dimensionless variables for well test analysis	28
Chapter IV Model solutions for well test analysis	31
IV.1. General Solution in Laplace space	31
IV.2. Approximate solutions at short times: Total Expansion in the Fracture Network	34
IV.3. Approximate solutions at intermediate times: Interaction between porous media	39
IV.4. Approximate solutions at late times: Single System Behavior	44
Chapter V Validation and Application	45
Chapter VI Conclusions	55
References	57
Appendix A Generalized Radial Flow Model	61
Appendix B Pressure Transient Analysis of Fractal Reservoirs assuming Pseudo- Steady State Interporosity Transfer	67
Appendix C Pressure Transient Analysis of Fractal Reservoirs with Transient Interporous Transference (Olarewaju, 1996)	73
Appendix D Pressure Transient Analysis of Fractal Reservoirs assuming Free Interaction Interporosity Transfer	79
Appendix E Modified Transient Matrix-Response Model (Larsen, 2013)	93
Appendix F Wellbore Storage for Fractal Models	95
Appendix G Constant Rate Solutions with Boundary Effects	99

List of Figures

Fig. I.1.	Examples of flow dimension (figure taken from Doe, 1991)	4
Fig. II.1.	Log-log plot of the pressure and pressure derivative function behaviour of the model proposed by Cinco-Ley et al. (1982), assuming slabs .	12
Fig. II.2.	Semilog plot of the pressure behaviour and approximate solutions of the model proposed by Cinco-Ley et al. (1982), assuming slabs	13
Fig. II.3.	Log- log plot of the pressure and pressure derivative function behaviour of the model proposed by Serra et al. (1982)	15
Fig. II.4.	Log-log plot of the pressure and pressure derivative function behaviour of the model presented by Warren et al. (1963)	16
Fig. II.5.	Idealization of the interporous skin between the matrix and the fracture	17
Fig. II.6.	Log-log plot of the pressure and pressure derivative function behaviour of the model developed by Cinco-Ley et al. (1963), for different values of interporous skin, assuming slabs	17
Fig. II.7.	Plot of Barker's constant rate case solution, for $\nu = 1/2, \nu = 0$ and $\nu = -1/2$	19
Fig. II.8.	Sublinear and Hyperspherical Conduits (figure taken from Doe, 1991)	20
Fig. II.9.	Plot of sublinear ($\nu = 0.25$ and $\nu = -0.25$) and hyperspherical ($\nu = -0.75$) geometries)	20
Fig. II.10.	Log-log plot of the model proposed by Olarewaju (1996))	22
Fig. II.11.	Chang et al. (1990) solution (numerical solution); short- and long-time approximations for a fractal fractured reservoir with matrix participation (figure taken from Flamenco et al., 2003)	22
Fig. II.12.	Log-log plot of the free interporous transference, developed in Appendix D	24
Fig. V.1.	Pressure and pressure derivate function behavior for some values of D_{fb} , and θ without interporous skin and its convergence to the model proposed by Cinco-Ley et al., (1982)	45
Fig. V.2.	Semilog plot of the pressure behavior for some values of θ that satisfy the condition of $D_{fb} = \theta + 2$	46

Fig. V.3.	Impact of interporous skin in pressure and pressure derivative function, when $D_{fb} \neq \theta + 2$	47
Fig. V.4.	Impact of interporous skin in pressure and pressure derivative function, for $D_{fb} = \theta + 2$	47
Fig. V.5.	Behavior of pressure and pressure derivative function, when $D_{fb} \neq \theta + 2$, considering phenomena around wellbore	48
Fig. V.6.	Behavior of pressure and pressure derivative function, when $D_{fb} = \theta + 2$, considering phenomena around wellbore	48
Fig. V.7.	Convergence from the short, intermediate and long times solutions to the general solution, when $D_{fb} = \theta + 2$, with no interporous skin	49
Fig. V.8.	Convergence from the short, intermediate and long times solutions to the general solution, when $D_{fb} \neq \theta + 2$, with no interporous skin	50
Fig. V.9.	Convergence from the short, intermediate and long times solutions to the general solution, when $D_{fb} = \theta + 2$, with low interporous skin	50
Fig. V.10.	Convergence from the short, intermediate and long times solutions to the general solution, when $D_{fb} \neq \theta + 2$, with low interporous skin	51
Fig. V.11.	Convergence from the short, intermediate and long times solutions to the general solution, when $D_{fb} = \theta + 2$, with severe interporous skin (pseudosteady-state)	51
Fig. V.12.	Convergence from the short, intermediate and long times solutions to the general solution, when $D_{fb} \neq \theta + 2$, with severe interporous skin (pseudosteady-state)	52
Fig. V.13.	Pressure and pressure derivative function behavior for synthetic example	53
Fig. V.14.	Log-log plot of the late time pressure behavior for synthetic example	53
Fig. V.15.	Specialized plot for intermediate times of the pressure behavior for synthetic example	54

This page is intentionally left in blank.

Chapter I

Basic Concepts

The purpose of this chapter is to familiarize the reader with concepts used in applications of fractal theory in well test analysis. Besides, new definitions are presented in order to develop the flow model presented in this work.

Concepts related to the rock and fluid properties, such as *compressibility of rock, oil, gas, steam and water* in addition to the *fluid viscosity, formation volume factors and fluids saturations* are important in well test analysis. Therefore, it is assumed that the reader has prior knowledge of these concepts.

Bulk Volume: It is constituted by the volume of any kind of voids and solids contained in a rock. Considering three kinds of voids, i.e, pores, fractures and vugs, a mathematical representation for the volume of rock is:

$$V_b = V_{pores} + V_{fractures} + V_{vugs} + V_{solids} , \quad \text{I.1}$$

where:

V_{pores} = volume of pores;

$V_{fractures}$ = volume of fractures;

V_{solids} = volume of solids.

Prior definition is based on the components of the rock. However, *bulk volume* can be defined by its shape. For instance, if the rock would have a cubic shape, volume would be defined as:

$$V_b = L^3 , \quad \text{I.2}$$

where:

L = length of the base of the cubic rock;

or, if rock would be a sphere:

$$V_b = \frac{4\pi}{3} r^3 , \quad \text{I.3}$$

where:

r = radius of the rock.

If the rock does not show a regular shape, it can be represented by the *volume between two equipotential surfaces*, such region is defined as:

$$V_b = \alpha_{d_e} b^{3-d_e} r^{d_e-1} \Delta r, \quad \text{I.4}$$

where:

α_{d_e} = Area of a unit sphere of in d_e dimensions; it is defined as:

$$\alpha_{d_e} = \frac{2\pi^{d_e/2}}{\Gamma\left(\frac{d_e}{2}\right)}, \quad \text{I.5}$$

where:

$\Gamma(x)$ = gamma function of x .

Consider the region bounded by two equipotential surfaces which have radii r and $r + \Delta r$. These surfaces are the projections of d_e -dimensional spheres through three dimensional space by an amount b^{3-d_e} . For example, when d_e is equal to 2, the surfaces are finite cylinders of length b . A sphere of radius r has an area $\alpha_{d_e} r^{d_e-1}$.

In the realization of this thesis, it has found that, since the term Δr in eq. I.4 represents the width between the surfaces, the cross section (area exposed to the flow) between the two equipotential surfaces mentioned before, is given by:

$$A_{\text{exp. flow}} = \alpha_{d_e} b^{3-d_e} r^{d_e-1}, \quad \text{I.6}$$

where:

b = extent of the flow region.

Porosity: It is defined as the ratio of the porous volume divided by the rock volume:

$$\phi = \frac{\text{volume of pores}}{\text{total bulk volume}}. \quad \text{I.7}$$

When there is evidence of existence of non-intergranular pores into the rock in addition to the intergranular pores themselves (traditionally called *primary porosity*), e.g., fractures and/or vugs (*secondary porosity*), to distinguish and characterize such elements becomes very important for reservoir engineering and economical purposes.

Defining the total pore volume as:

$$V_{tp} = V_{pores} + V_{fractures} + V_{vugs}, \quad \text{I.8}$$

establishing that:

$$V_{sec} = V_{fractures} + V_{vugs}, \quad \text{I.9}$$

therefore:

$$V_{tp} = V_{pores} + V_{sec}. \quad \text{I.10}$$

Dividing previous eq. by bulk volume it results:

$$\phi_t = \phi_{ma} + \phi_{sec} , \quad \text{I.11}$$

where:

ϕ_t = total porosity,

ϕ_{ma} = matrix porosity (intergranular pores);

ϕ_{sec} = secondary porosity.

Total porosity is traditionally determined from logs; *matrix porosity* can be determined by core analysis. *Secondary porosity* can be estimated with the following model (Pulido et al., 2005):

$$\phi_{sec} = [1 - 0.74\phi_t] \phi_t^{m_{dp}} . \quad \text{I.12}$$

For a good understanding of the present work, I consider necessary to introduce the concept of *unitary fracture porosity*. Conceptually it represents the volumetric fraction occupied by a single fracture related to the total rock volume. It is given by:

$$\phi_{uf} = \frac{\text{unitary fracture volume}}{\text{total bulk volume}} = \frac{V_{uf}}{V_{bulk}} . \quad \text{I.13}$$

On the other hand, the concept *fractured bulk porosity* has been used previously in the literature. It represents the volumetric fraction of all fractures in the rock. It is defined as:

$$\phi_{fb} = \frac{\text{fracture network volume}}{\text{total bulk volume}} = \frac{V_{fb}}{V_{bulk}} . \quad \text{I.14}$$

Assuming fractures with the same characteristics all over the bulk, *fracture network volume*, can be expressed as:

$$V_{fb} = n_f(r) V_{uf} \Delta r , \quad \text{I.15}$$

where:

$n_f(r)$ = number of fractures into fractured bulk,

V_{uf} = unitary fracture volume.

Moreover, the *number of fractures into fractured bulk*, also known as *Site Density* can be expressed using a power-law model:

$$n_f(r) = ar^{D_{fb}-1} . \quad \text{I.16}$$

Therefore, fracture network volume is expressed as:

$$V_{fb} = ar^{D_{fb}-1} V_{uf} \Delta r . \quad \text{I.17}$$

Combining eq. I.4 and eq. I.17, *porosity of the fracture network* is given by:

$$\phi_{fb} = \frac{ar^{D_{fb}-1}V_{uf}\Delta r}{\alpha_{d_e}r^{d_e-1}b^{3-d_e}\Delta r} = \frac{ar^{D_{fb}-d_e}V_{uf}}{\alpha_{d_e}b^{3-d_e}}. \quad \text{I.18}$$

Geometry factor: This parameter was introduced by Chang et al. (1990); it was used to provide a relation of the symmetry. It was defined as:

$$G = \frac{aV_s}{\phi}, \quad \text{I.19}$$

where:

V_s = site volume. This parameter is equivalent to the unitary fracture volume, presented in this thesis.

In the present work, it was found that the geometry factor is equivalent to:

$$G = \frac{A_{\text{exp.flow}}}{r^{d_e-1}} = \alpha_{d_e}b^{3-d_e}. \quad \text{I.20}$$

Dimension in Well Testing: The term *dimension* suffers from having different but related meanings in reservoir analysis. Dimension may refer to units of measure, as in *dimensionless pressure*. Dimension also arises when we discuss the three Euclidian dimensions, since all real well tests occur in three-dimensional space. *Fractal Dimension* describes how patterns fill spaces. Dimension has also been used in reference to the symmetry of flow lines in a well test. For example, linear flow is considered one-dimensional; cylindrical flow, two dimensional and spherical flow, three-dimensional, see **Fig. I.1**.

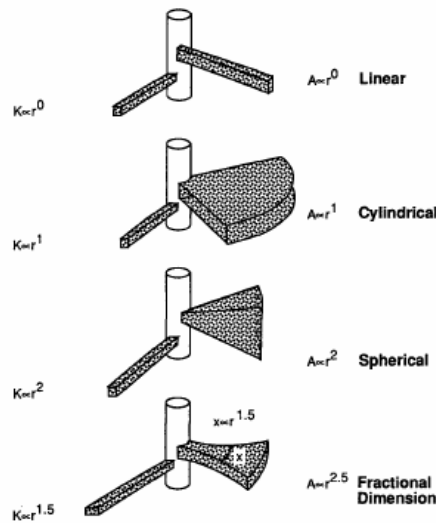


Fig. I.1. Examples of flow dimension (figure taken from Doe, 1991).

Spatial Dimension: The geometric property that defines spatial dimension is the change in conduit area with distance from a source point. In one-dimensional flow (linear flow) the area of the conduit is proportional to r^0 . The area does not change with distance. For cylindrical and spherical flow geometries, the areas are proportional to the r^1 and r^2 powers of distance, respectively. By extension of this logic, a conduit of fractional dimension is simply a conduit whose area is proportional to a non-integer power of distance from the source (Doe, 1991).

Fractal Permeability and Darcy's law in fractal form: According to Poiseuille's and Fanning's equations, a fluid's velocity through a capillary tube can be expressed as:

$$v_u = \frac{d_{uf}^2}{32\mu} \frac{\Delta p_{uf}}{\Delta L} \quad \text{I.21}$$

where:

d_{uf} = capillary tube diameter (pore, fracture or vug aperture);

μ = fluid viscosity;

Δp = pressure drop within the system;

ΔL = length of the capillary tube.

Fluid rate is given by:

$$\bar{q}_u = \bar{v}_u A_{uf}; \quad \text{I.22}$$

moreover, capillary tube area is:

$$A_{uf} = \pi r_{uf}^2. \quad \text{I.23}$$

Then, substituting capillary tube area and fluid velocity into fluid rate equation, it becomes: Hagen Pouisuelle

$$\bar{q}_u = \left[\frac{d_{uf}^2}{32\mu} \frac{\Delta p_{uf}}{\Delta L} \right] [\pi r_{uf}^2] = \frac{\pi r_{uf}^4}{8\mu} \frac{\Delta p}{\Delta L}. \quad \text{I.24}$$

Expressing prior equation in terms of radial coordinates and taking limits to zero:

$$\bar{q}_u = \frac{\pi r_{uf}^4}{8\mu} \frac{\partial p_{uf}}{\partial r}. \quad \text{I.25}$$

Previous equation provides the fluid rate in a single capillary tube considering n_p parallel tubes with the same characteristics, the total fluid rate can be expressed as:

$$\bar{q} = n_p \bar{q}_u = n_p \frac{\pi r_{uf}^4}{8\mu} \frac{\partial p_{fb}}{\partial r}, \quad \text{I.26}$$

where, the number of tubes is defined as follows:

$$n_p = \frac{V_{fb}}{V_{uf}} = \frac{n_f(r) V_{uf}}{V_{uf}} = n_f(r), \quad \text{I.27}$$

with:

V_{fb} = capillary tubes volume (fractured bulk volume);

V_{uf} = capillary tube volume (unitary fracture volume).

Equation I.28 can be expressed as:

$$n_p = \frac{V_{fb}}{\pi r_p^2 l} \frac{1}{l}. \quad \text{I.28}$$

Hence, the following expression can be deduced:

$$n_p = n_f(r) = \frac{V_{fb}}{\pi r_p^2 l} \frac{1}{l}. \quad \text{I.29}$$

Equation I.26 can be rewritten as follows:

$$\bar{q} = a r^{D_{fb}-1} \frac{\pi r_{uf}^4}{8\mu} \frac{\partial p_{fb}}{\partial r} = \frac{a \pi r_{uf}^4}{8\mu} r^{D_{fb}-1} \frac{\partial p_{fb}}{\partial r}. \quad \text{I.30}$$

assuming:

$$r_{uf}^4 = C_1 r^{4\Theta}, \quad \text{I.31}$$

where:

Θ = parameter describing the conductivity in a fractal object. Therefore, eq. I.30 is rewritten as:

$$\bar{q} = \frac{a \pi [C_1 r^{4\Theta}]}{8\mu} r^{D_{fb}-1} \frac{\partial p_{fb}}{\partial r} = \frac{a \pi C_1}{8\mu} r^{D_{fb}-\theta-1} \frac{\partial p_{fb}}{\partial r}, \quad \text{I.32}$$

where:

$\theta = 4\Theta$. It is defined as the anomaly in conductivity in a fractal object (O'Shaughnessy and Procaccia, 1985).

Defining:

$$C_2 = \frac{a \pi C_1}{8} = a C_1^*, \quad \text{I.33}$$

equation I.32 can be expressed as, similar to Chang et al. (1990):

$$\bar{q} = C_2 \frac{r^{D_{fb}-\theta-1}}{\mu} \frac{\partial p_{fb}}{\partial r}. \quad \text{I.34}$$

On the other hand, Darcy's law is given by (considering a variable permeability, through porous media):

$$\bar{v} = -\frac{k_{fb}(r)}{\mu} \frac{\partial p_{fb}}{\partial r}; \quad \text{I.35}$$

fractured bulk's fluid rate is given by:

$$\bar{q} = A_{fb} \bar{v}_f, \quad \text{I.36}$$

flowing area of fractured bulk is given by:

$$A_{fb} = \alpha_{d_e}^* b^{2-d_e} r^{d_e}, \quad \text{I.37}$$

and:

$$\alpha_{d_e}^* = \frac{2\pi^{\frac{d_e-1}{2}}}{\Gamma\left(\frac{d_e-1}{2}\right)}. \quad \text{I.38}$$

Therefore, fractured bulk's fluid rate is given by:

$$\bar{q} = \left[\alpha_{d_e}^* b^{2-d_e} r^{d_e} \left[-\frac{k_{fb}(r)}{\mu} \frac{\partial p_{fb}}{\partial r} \right] \right] = -\frac{k_{fb}(r) \alpha_{d_e}^* b^{2-d_e} r^{d_e}}{\mu} \frac{\partial p_{fb}}{\partial r}. \quad \text{I.39}$$

Comparing equations I.34 and I.39 it results:

$$-\frac{\alpha_{d_e}^* b^{2-d_e} r^{d_e} k_{fb}(r)}{\mu} = C_2 \frac{r^{D_{fb}-\theta-1}}{\mu} \frac{\partial p_{fb}}{\partial r}, \quad \text{I.40}$$

arraying:

$$-\alpha_{d_e}^* b^{2-d_e} r^{d_e} k_{fb}(r) = C_2 r^{D_{fb}-\theta-1} \frac{\partial p_{fb}}{\partial r}, \quad \text{I.41}$$

then, it can be concluded that:

$$k_{fb}(r) = -\frac{C_2}{\alpha_{d_e}^* b^{2-d_e}} r^{D_{fb}-\theta-d_e-1}. \quad \text{I.42}$$

Establishing the relationship:

$$C_2 = aC_1^*, \quad \text{I.43}$$

eq. I.42 becomes:

$$k_{fb}(r) = -\frac{aC_1^*}{\alpha_{d_e}^* b^{2-d_e}} r^{D_{fb}-\theta-d_e-1} = -C_1^* \frac{a}{\alpha_{d_e}^* b^{2-d_e}} r^{D_{fb}-\theta-d_e-1}. \quad \text{I.44}$$

On the other hand, defining:

$$C_1^* = \frac{k_{fb} V_{bulk}}{n_f(r)}, \quad \text{I.45}$$

then,

$$k_{fb}(r) = -\frac{ak_{fb}V_{bulk}}{\alpha_{d_e}^* b^{2-d_e} n_f(r)} r^{D_{fb}-\theta-d_e-1}, \quad \text{I.46}$$

according to definition:

$$V_{bulk} = \frac{n_f(r)V_{uf}}{\phi_{fb}}. \quad \text{I.47}$$

Therefore:

$$k_{fb}(r) = -\frac{ak_{fb}}{n_f(r)\alpha_{d_e}^* b^{2-d_e}} \frac{n_f(r)V_{uf}}{\phi_{fb}} r^{D_{fb}-\theta-d_e-1} = -\frac{aV_{uf}}{\alpha_{d_e}^* b^{2-d_e}} \frac{k_{fb}}{\phi_{fb}} r^{D_{fb}-\theta-d_e-1}, \quad \text{I.48}$$

and Darcy's equation results in:

$$\bar{q} = \left[\alpha_{d_e}^* b^{2-d_e} r^{d_e} \left[\frac{-\frac{aV_{uf}}{\alpha_{d_e}^* b^{2-d_e}} \frac{k_{fb}}{\phi_{fb}} r^{D_{fb}-\theta-d_e-1}}{\mu} \frac{\partial p_{fb}}{\partial r} \right] \right] = \left[\alpha_{d_e}^* b^{2-d_e} r^{d_e} \left[\frac{aV_{uf} k_{fb} r^{D_{fb}-\theta-d_e-1}}{\alpha_{d_e}^* b^{2-d_e} \phi_{fb} \mu} \frac{\partial p_{fb}}{\partial r} \right] \right]. \quad \text{I.49}$$

If:

$$\beta = D_{fb} - \theta - 1, \quad \text{I.50}$$

then, *Darcy's law in fractal form* is given by:

$$\bar{q} = \frac{aV_{uf} k_{fb} r^\beta}{\phi_{fb} \mu} \frac{\partial p_{fb}}{\partial r}. \quad \text{I.51}$$

Dimensionless variables: The use of dimensionless groups in well test analysis is very common. Dimensionless variables are defined differently depending on the phase flowing in the well and reservoir (oil and gas) and also, on the author.

The main advantages of using dimensionless variables, such as dimensionless pressure, p_D , dimensionless radius, r_D and dimensionless time, t_D , are:

- The use of such variables allows grouping known and unknown parameters of the fluid and the rock system.
- They make easier the mathematical work when solving the partial differential equations that governs the flow within the reservoir.
- The proper manipulation of dimensionless variables allows the use of the same models for different cases, e.g., different flowing phases in the reservoir.

The Inverse Chow Pressure Group: For a dimensionless solution $p_D(r_D, t_D)$, the *Chow pressure group* is defined by the identity:

$$\frac{p_D}{\partial p_D / \partial \ln t_D} = \frac{p_D}{p'_D t_D}. \quad \text{I.52}$$

and the *inverse Chow derivative of pressure group* by the identity

$$\frac{\partial p_D / \partial \ln t_D}{p_D} = \frac{p'_D t_D}{p_D}. \quad \text{I.53}$$

Dimensionless storativity ratio: This parameter relates the total expansion in the fracture network to the total expansion in the system. It is defined as:

$$\omega = \frac{\phi_{fb} c_{ifb}}{\phi_{fb} c_{ifb} + \phi_{ma} c_{ima}}. \quad \text{I.54}$$

Matrix-fracture interaction parameter: This parameter is used in all the double porosity models assuming pseudosteady-state interporous transference and in some transient interporous transference models. It is a dimensionless parameter, defined as the relation of permeabilities of the two media:

$$\lambda = \frac{\sigma k_{ma} r_w^2}{k_{fb}}, \quad \text{I.55}$$

where:

σ = shape factor that reflects the geometry of the matrix elements and controls the flow between porous media. It has dimensions reciprocal to the area.

r_w = wellbore radius.

Dimensionless matrix hydraulic diffusivity: This parameter relates the hydraulic diffusivity in the matrix blocks to the total hydraulic diffusivity of the system. This parameter allows the consideration of any type of flow within the matrix (transient or pseudosteady-state).

$$\eta_{maD} = \frac{k_{ma} (\phi c)_t}{\phi_{ma} c_{ima} k_{fb}}; \quad \text{I.56}$$

Dimensionless block size:

$$H_D = \frac{h_{ma}^2}{r_w^2}; \quad \text{I.57}$$

h_{ma} = height of matrix blocks.

Dimensionless fracture area, A_{fD} : This parameter relates the area of fractures per unit of matrix volume and the fracture area per unit of bulk volume. It ranges from 2 to 6, depending on the flow dimensions of the matrix.

$$A_{fD} = \frac{A_{FB} h_{ma} V_b r_w^\theta}{V_{ma}}, \quad \text{I.58}$$

where:

A_{FB} = fracture area per unit of bulk volume,

V_b = bulk volume,

V_{ma} = matrix volume.

Chapter II

Literature Review

The purpose of this chapter is to provide a summary of the double porosity flow models and models assuming non-fixed flow geometry (fractal models) for well test analysis and the theories behind them.

It is important to point out that all the models presented in this chapter are expressed in their respective dimensionless variables, i.e., dimensionless variables are different for every model.

II.1 Double porosity models

Nature of flow in multi-porous systems obeys to the fact that flow in each porous medium behaves differently in terms of gradient pressure from the other media. Such behavior is known as *transient interporous flow*; this flow regime was studied previously by de Swaan (1976) and Najurieta (1980). Later in 1982, three research teams solved the problem - in different ways - of the transient interporous transference between porous media, showing similar results.

Cinco-Ley et al. (1982) presented a flow model for double porosity systems, where the interaction between media was modeled by a convolution. It is given in dimensionless variables by:

$$\frac{\partial^2 p_{fD}(r_D, t_D)}{\partial r_D^2} + \frac{1}{r_D} \frac{\partial p_{fD}(r_D, t_D)}{\partial r_D} - [1 - \omega] A_{fD} \int_0^{t_D} \frac{\partial p_{fD}(\tau)}{\partial \tau} F(\eta_{maD}, t_D - \tau) = \omega \frac{\partial p_{fD}(r_D, t_D)}{\partial t_D}; \quad \text{II.1}$$

if slabs are assumed for matrix blocks:

$$F(\eta_{maD}, t_D - \tau) = 4\eta_{maD} \sum_{n=1}^{\infty} e^{-\eta_{maD}(2n+1)^2 \pi^2 [t_D - \tau]}, \quad \text{II.2}$$

or, for spheres:

$$F(\eta_{maD}, t_D - \tau) = 4\eta_{maD} \sum_{n=1}^{\infty} e^{-4\eta_{maD} n^2 \pi^2 [t_D - \tau]}. \quad \text{II.3}$$

In this study, Cinco-Ley et al. (1982) introduced the parameter A_{fD} , which is the *dimensionless fracture area*; its definition depends on the matrix block shape (slabs or spheres) and it is useful to estimate the area of fractures per volume of rock.

The general solution for eq. II.1, assuming an infinite reservoir and constant flow rate at wellbore, expressed in Laplace space, evaluated at wellbore is given by:

$$\bar{p}_{wD}(s) = \frac{K_0(\sqrt{sf(s)})}{s^{3/2} \sqrt{f(s)} K_1(\sqrt{sf(s)})}, \quad \text{II.4}$$

transference function is given by:

$$f(s) = \omega + [1 - \omega] A_{fD} f(\eta_{maD}, s), \quad \text{II.5}$$

where, for slabs:

$$f(\eta_{maD}, s) = \sqrt{\frac{\eta_{maD}}{s}} \tanh\left(\frac{1}{2} \sqrt{\frac{s}{\eta_{maD}}}\right). \quad \text{II.6}$$

and, for spheres:

$$f(\eta_{maD}, s) = \sqrt{\frac{\eta_{maD}}{s}} \left[\coth\left(\frac{1}{2} \sqrt{\frac{s}{\eta_{maD}}}\right) - 2 \sqrt{\frac{\eta_{maD}}{s}} \right]. \quad \text{II.7}$$

Fig. II.1 shows the pressure and derivative of pressure function of the solution given in eq. II.4. Storage and skin around wellbore is not considered.

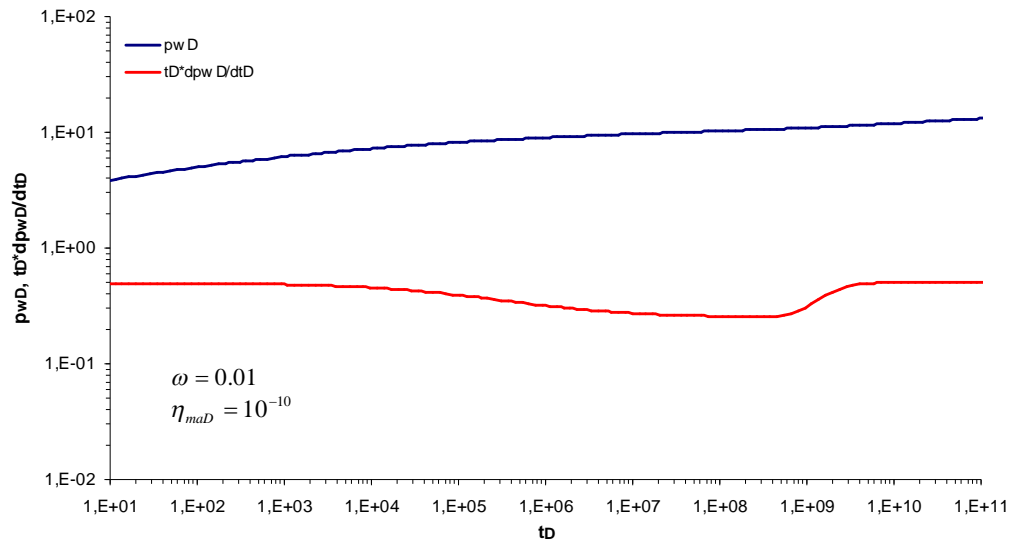


Fig. II.1. Log-log plot of the pressure and pressure derivative function behaviour of the model proposed by Cinco-Ley et al. (1982), assuming slabs.

In addition, Cinco-Ley et al. (1982) developed three solutions in real space that corresponds to the three periods of flow in double porosity media. The first flow period is dominated by a radial flow in the fracture network caused by the total expansion in the fractures. The solution in real space for such period is given by:

$$p_{wD}(t_D) = \frac{1}{2} \left[\ln\left(\frac{t_D}{\omega}\right) + 0.80907 \right]. \quad \text{II.8}$$

Second flowing period in double porosity systems is the one where the interactions between both mediums take place. Hence, second solution in real space is:

$$p_{wD}(t_D) = \frac{1}{4} \ln(t_D) - \frac{1}{2} \ln([1 - \omega] A_{fD} \sqrt{\eta_{maD}}) + 0.2602. \quad \text{II.9}$$

Finally, in the third flowing period the double porosity system acts as a single one. Provided solution for this flowing period is given by:

$$p_{wD}(t_D) = \frac{1}{2} [\ln(t_D) + 0.80907]. \quad \text{II.10}$$

Fig. II.2 shows a semilog plot of the pressure behaviour neglecting storage and skin around wellbore and the convergence of approximate solutions to the general solution.

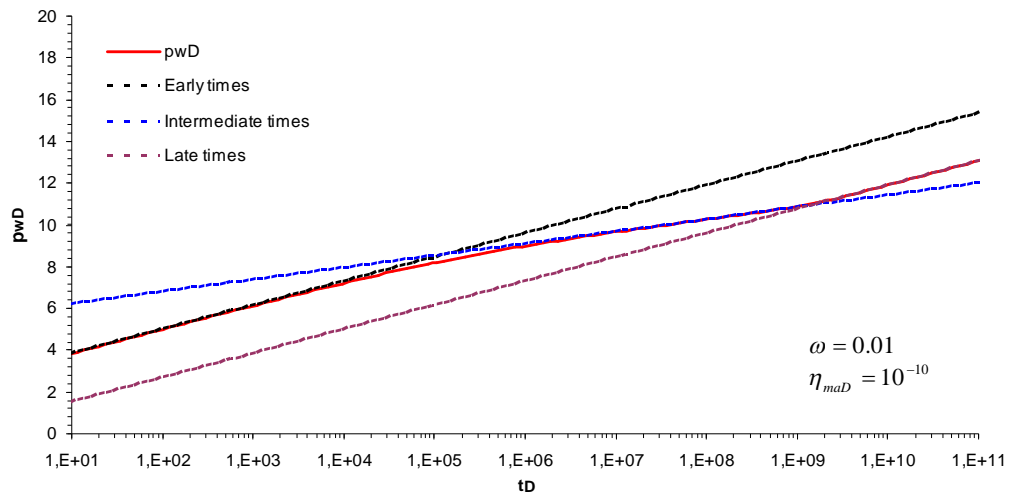


Fig. II.2. Semilog plot of the pressure behaviour and approximate solutions of the model proposed by Cinco-Ley et al. (1982), assuming slabs.

Streltsova (1982) presented a double porosity model assuming radial flow in fracture network and linear flow from matrix blocks to fractures. She solved this problem using Hankel transform. Radial flow model in fracture network, presented by Streltsova (1982) is given by:

$$\frac{\partial^2 \Delta p(r,t)}{\partial r^2} + \frac{1}{r} \frac{\partial \Delta p(r,t)}{\partial r} = \frac{\partial \Delta p(r,t)}{\partial t} + \frac{v_m}{T}, \quad \text{II.11}$$

where:

$$v_m = \frac{k_m}{\mu} \left. \frac{\partial \Delta p_m}{\partial z} \right|_{z=0}, \quad \text{II.12}$$

and:

$$T = \sum_{i=1}^n \left(\frac{k_f h}{\mu} \right)_i = \frac{2nk_f h}{\mu} = \frac{kh_t}{\mu}. \quad \text{II.13}$$

Solution evaluated at wellbore of eq. II.11 presented by Streltsova (1982) in real space, expressed in dimensionless drop of pressure is given by:

$$\Delta p_D = \ln \left(\frac{4\eta' t}{1.781 r_w^2} \right) + \ln \left(\frac{H}{(1.781 \eta_m t)^{1/2}} \right) + 2 \sum_{n=1,3,5}^{\infty} \frac{1}{n} \operatorname{erfc} \left(\frac{nH}{(\eta_m t)^{1/2}} \right), \quad \text{II.14}$$

where:

$$\Delta p_D = \frac{2\pi T}{q} \Delta p. \quad \text{II.15}$$

Serra et al. (1982) presented a flow model assuming slabs as matrix blocks, in terms of the parameters used previously by Warren et al. (1963). This model was developed by solving two partial differential equations: one for the fracture network and other for the matrix blocks. Partial differential equation that describes the flow in fracture network has the shape:

$$\frac{\partial^2 p_{fD}(r_D, t_D)}{\partial r_D^2} + \frac{1}{r_D} \frac{\partial p_{fD}(r_D, t_D)}{\partial r_D} - \frac{\lambda'}{3} \frac{\partial p_{maD}(z_D = 1, t_D)}{\partial z_D} = \frac{\partial p_{fD}(r_D, t_D)}{\partial t_D}. \quad \text{II.16}$$

And the partial differential equation that describes linear flow in the matrix blocks is given by:

$$\frac{\partial^2 p_{maD}(z_D, t_D)}{\partial z_D^2} = \frac{3\omega'}{\lambda'} \frac{\partial p_{maD}(z_D, t_D)}{\partial t_D}. \quad \text{II.17}$$

Solution of eq. II.16 coupled with eq. II.17, assuming constant flow rate at wellbore, infinite fracture network for eq. II.16 on one hand, and free interaction and closed boundary for eq. II.17 on the other, is given by:

$$\bar{p}_{wD}(s) = \frac{K_0 \left(\left(1 + \sqrt{\frac{\lambda' \omega'}{3s}} \tanh \left(\sqrt{\frac{3s}{\lambda' \omega'}} \right) \right)^{1/2} \sqrt{s} \right)}{s^{3/2} \left(1 + \sqrt{\frac{\lambda' \omega'}{3s}} \tanh \left(\sqrt{\frac{3s}{\lambda' \omega'}} \right) \right)^{1/2} K_1 \left(\left(1 + \sqrt{\frac{\lambda' \omega'}{3s}} \tanh \left(\sqrt{\frac{3s}{\lambda' \omega'}} \right) \right)^{1/2} \sqrt{s} \right)}. \quad \text{II.18}$$

Fig. II.3 shows the plot of the pressure and derivative of pressure function in log-log scale, where at intermediate times, a smooth transition in the slope of the pressure derivate function is observed.

Moreover, Serra et al. (1982) developed solutions for the three flowing periods for drawdown and build-up tests. Since build-up solutions are developed from the superposition principle, only drawdown solutions will be presented. For short times:

$$p_{wD}(t_D) = 1.151[\log(t_D) + 0.351] + s. \quad \text{II.19}$$

For intermediate times, real time approximation is given by:

$$p_{wD}(t_D) = 0.5756 \left[\log(t_D) + 0.452 - \log\left(\frac{\lambda' \omega'}{3}\right) \right] + s, \quad \text{II.20}$$

and, for late times:

$$p_{wD}(t_D) = 1.151[\log(t_D) + 0.351 - \log(1 + \omega')] + s. \quad \text{II.21}$$

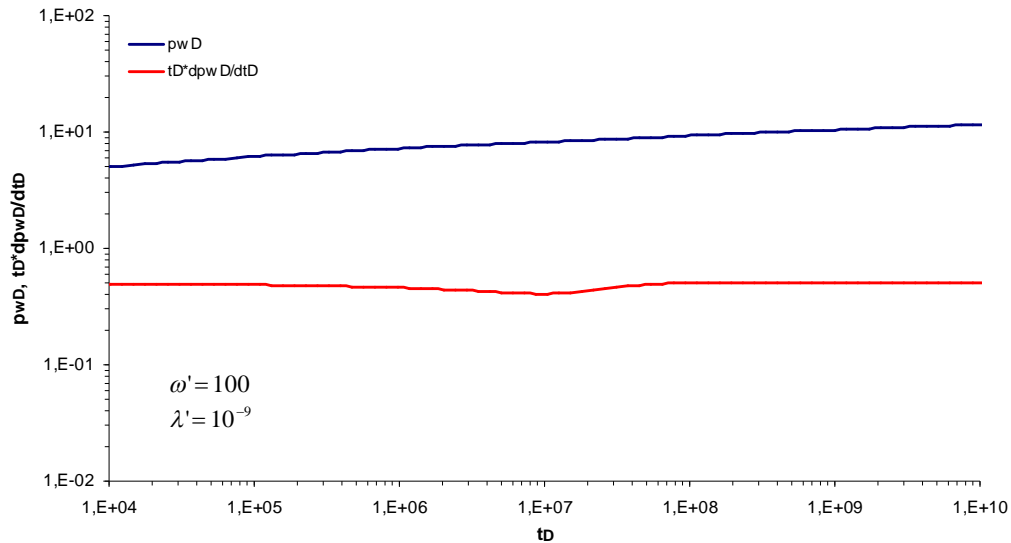


Fig. II.3. Log-log plot of the pressure and pressure derivative function behaviour of the model proposed by Serra et al. (1982).

However, practice has shown that apparently pressure gradients act homogeneously in all porous media which goes against the physics and the transient transfer theory. Such flow transfer is known as *pseudosteady-state flow*. Warren et al. (1963) using the formulation similar to Barenblatt et al. (1960), developed a radial flow model for double porosity systems; neglecting the variation regarding the angle, such model has the shape:

$$\frac{\partial^2 p_{rD}(r_D, \theta, t_D)}{\partial r_D^2} + \frac{1}{r_D} \frac{\partial p_{rD}(r_D, \theta, t_D)}{\partial r_D} = \omega \frac{\partial p_{rD}(r_D, \theta, t_D)}{\partial t_D} + [1 - \omega] \frac{\partial p_{mD}(r_D, t_D)}{\partial t_D}, \quad \text{II.22}$$

where, matrix source term is given by:

$$[1-\omega]\frac{\partial p_{mD}(r_D, t_D)}{\partial t_D} = \lambda[p_{fD}(r_D, t_D) - p_{mD}(r_D, t_D)]. \quad \text{II.23}$$

Solution of eq. II.22 assuming infinite reservoir and constant flow rate at wellbore and taking into account condition imposed by eq. II.23 is given by:

$$\bar{p}_{wD}(s) = \frac{K_0(\sqrt{sh(s)})}{s\sqrt{sh(s)}K_1(\sqrt{sh(s)})}, \quad \text{II.24}$$

Where:

$$h(s) = \frac{\omega[1-\omega]s + \lambda}{[1-\omega]s + \lambda}. \quad \text{II.25}$$

Fig. II.4 shows the log-log plot of the pressure and derivative of pressure function of the model presented by Warren et al. (1963), where at intermediate times, an abrupt transition in the slope of the pressure derivate function is observed.

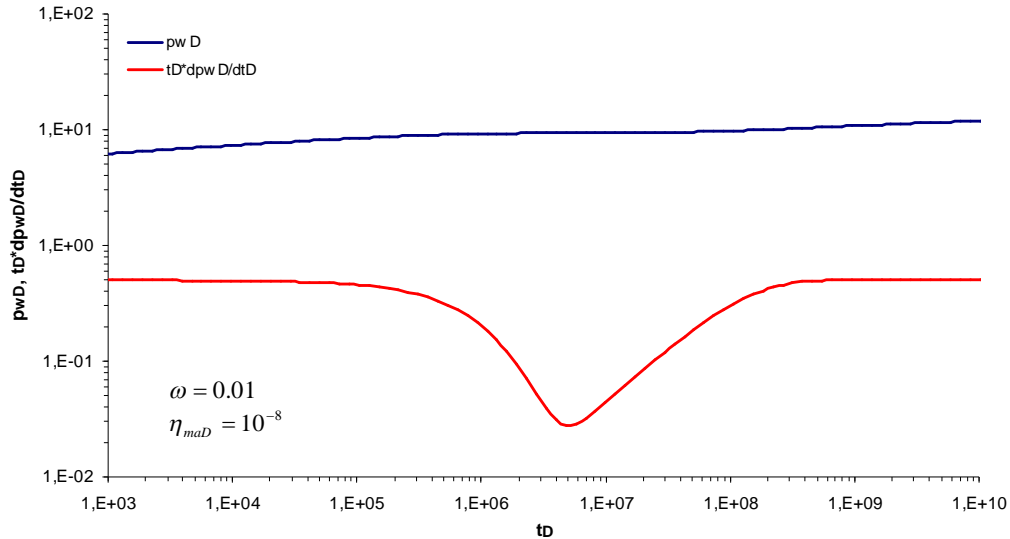


Fig. II.4. Log-log plot of the pressure and pressure derivative function behaviour of the model presented by Warren et al. (1963).

Cinco-Ley et al. (1985) showed that the apparent pseudosteady-state transference behavior seen in tests can be attributed to a presence of interporous skin between matrix and fracture network. Such interporous skin is produced by a film created by mineralization or interaction between fluids in the face of the matrix blocks. Mineralization has been observed in outcrops, where precipitation and other chemical phenomena create a skin between different porous media. General solution for this flow model has the same shape of eq. II.4, except for the transference function, which is given by:

$$f(s) = \frac{A_{fD}[1-\omega]f(\eta_{maD}s)}{1 + \frac{S_{ma-fbD}}{\eta_{maD}}f(\eta_{maD},s)s} + \omega, \quad \text{II.26}$$

And interporous skin is defined as:

$$S_{maD} = \frac{k_{ma}x_d}{k_d h_{ma}}. \quad \text{II.27}$$

Fig. II.5 shows the idealization of a matrix block with interporous skin between the matrix and the fracture.

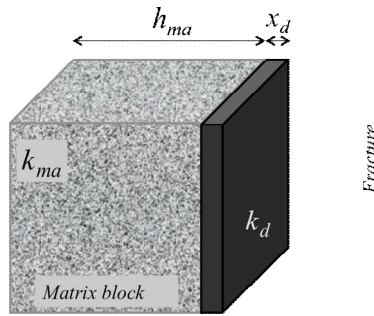


Fig. II.5. Idealization of the interporous skin between the matrix and the fracture.

Cinco-Ley et al. (1985) showed that a high interporous skin causes the apparent pseudosteady-state behaviour, and a relationship between interporous skin and the interporous flow parameter used in pseudosteady-state models was found:

$$\lambda = \frac{A_{fD}\eta_{maD}}{S_{maD}}. \quad \text{II.28}$$

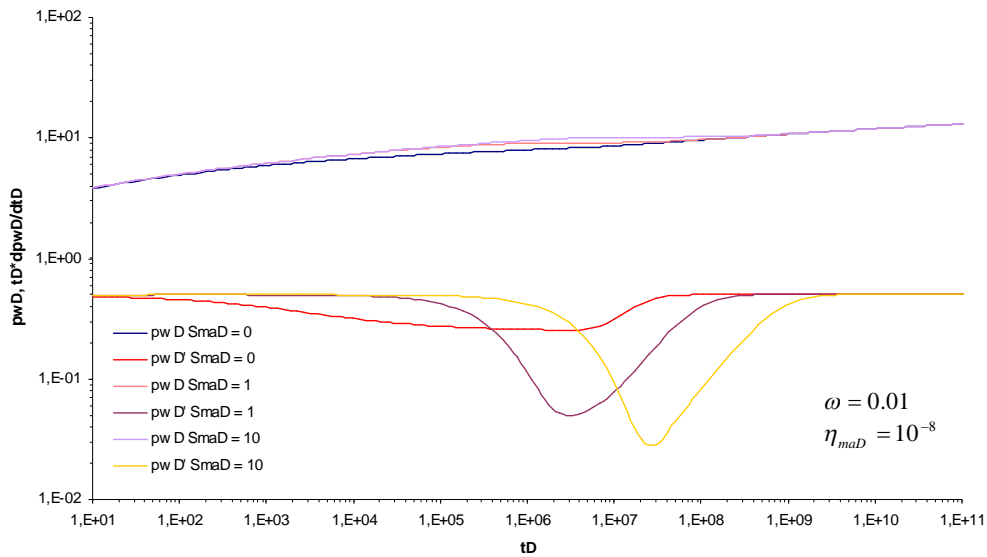


Fig. II.6. Log-log plot of the pressure and pressure derivative function behaviour of the model developed by Cinco-Ley et al. (1985), for different values of interporous skin, assuming slabs.

II.2 Fractal models

In order to understand the fractal theory applied to well test analysis, the first reference that must be consulted is the publication of Barker in 1988. Barker presented mathematical solutions for the diffusivity equation expressed as a *Generalized Radial Flow Model (GRF)*. The theory was developed for hydraulic test, but it can be used for petroleum well testing applying some modifications. Development of GRF and its solution for constant rate case is presented in Appendix A.

Barker (1988) developed a model where a variable parameter governing the Euclidean dimension of flow at wellbore was introduced. Such parameter is expressed in the present work as d_e . GRF adapted for petroleum well testing, in dimensionless variables is:

$$\frac{\partial^2 p_D(r_D, t_D)}{\partial r_D^2} + \frac{d_e - 1}{r_D} \frac{\partial p_D(r_D, t_D)}{\partial r_D} = \frac{\partial p_D(r_D, t_D)}{\partial t_D}. \quad \text{II.29}$$

It can be verified that, when $d_e = 1$, eq. II.29 takes the form of the diffusivity equation for linear flow (Miller, 1962); when $d_e = 2$ GRF takes the form of the diffusivity equation for radial flow (van Everdingen and Hurst, 1949) and, when $d_e = 3$, it takes the form of the spherical flow model (Chatas, 1966). Main assumptions made by Barker on this model are:

- Flow obeys Darcy's law;
- Flow is radial into a reservoir which is homogeneous and isotropic and fills an n-dimensional space;
- The source is an n-dimensional sphere (for example a cylinder for two dimensional flow or a sphere for three-dimensional flow).

Although Barker developed a model assuming a fractured rock, the assumption of a homogeneous and isotropic reservoir allows its application into non fractured media.

The constant rate solution assuming an infinite reservoir for eq. II.29 in Laplace space is detailed in Appendix A. Such solution is given by:

$$\bar{p}_{wD}(s) = \frac{K_v(\sqrt{s})}{s^{3/2} K_{\nu-1}(\sqrt{s})}, \quad \text{II.30}$$

where:

$$\nu = 1 - \frac{d_e}{2}. \quad \text{II.31}$$

Fig II.7 shows the plot of eq. II.30 and its derivative using Stehfest's Algorithm (Stehfest, 1970), when $\nu = \frac{1}{2}$, $\nu = 0$ and $\nu = -\frac{1}{2}$, which correspond to the linear, radial and spherical flows, respectively.

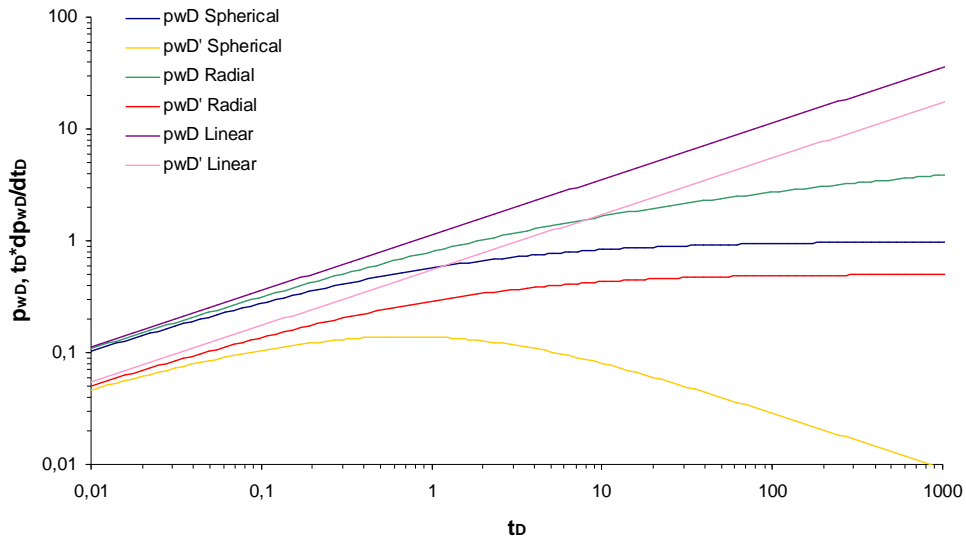


Fig. II.7. Plot of Barker's constant rate case solution, for $\nu = 1/2$, $\nu = 0$ and $\nu = -1/2$.

Doe (1991) presented methods for analyzing transient flow-rate data from constant-pressure well tests, where the spatial dimension is variable. Such analysis can be applied for the constant flow rate case.

Doe (1991) stated that, by definition of spatial dimension, the test dimension is not limited to the range of the Euclidian dimensions, that is between 1 and 3. Conduits may decrease in area by a power law of distance; hence their dimension is less than 1. Such a case may be termed *sublinear*. Similarly, a conduit whose area changes by a power greater than 2 has a dimension greater than 3, and may be called *hyperspherical*. Examples of these conduits are shown in **Fig. II.8**.

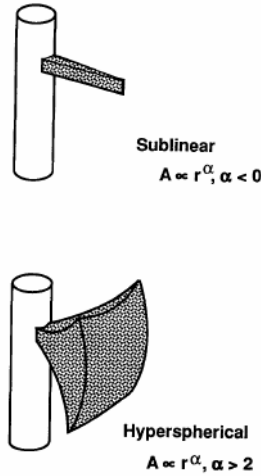


Fig. II.8 Sublinear and Hyperspherical Conduits (figure taken from Doe, 1991).

Fig. II.9 shows the transient pressure responses for the geometries established by Doe (1991).

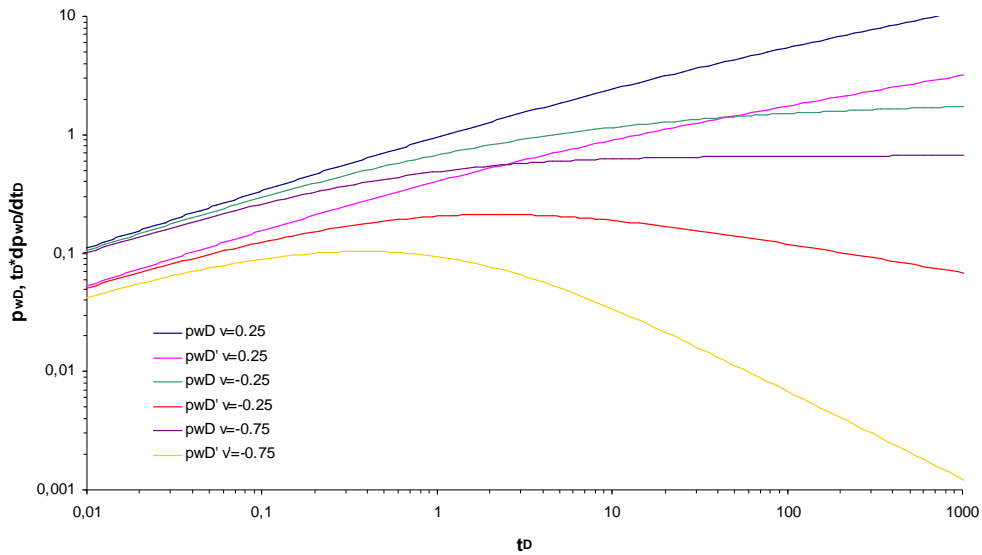


Fig. II.9. Plot of sublinear ($\nu = 0.25$ and $\nu = -0.25$) and hyperspherical ($\nu = -0.75$) geometries.

Chang et al. (1990) presented a flow model for a fractal reservoir, with single and double porosity. For the double porosity case, they assumed pseudo-steady state interaction between matrix and fractures. Appendix B shows the general development for this model. Diffusivity equation presented by Chang and Yortsos in its dimensionless form is given by:

$$\frac{1}{r_D^{D_{fb}-1}} \frac{\partial}{\partial r_D} \left(r_D^\beta \frac{\partial p_{fbD}(r_D, t_D)}{\partial r_D} \right) = r_D^{d_e - D_{fb}} [1 - \omega] \frac{\partial p_{maD}(r_D, t_D)}{\partial t_D} + \omega \frac{\partial p_{fbD}(r_D, t_D)}{\partial t_D}, \quad \text{II.32}$$

where:

$$\beta = D_{fb} - \theta - 1; \quad \text{II.33}$$

D_{fb} = mass fractal dimension of fractures;

d_e = Euclidean dimension.

θ = conductivity index (spectral dimension).

Later, Olarewaju (1996) presented a model and its solution in Laplace space for a transient interaction between matrix and fracture network. Model developed by Olarewaju in its dimensionless form is:

$$\frac{\partial^2 p_{fbD}(r_D, t_D)}{\partial r_D^2} + \frac{\beta}{r_D} \frac{\partial p_{fbD}(r_D, t_D)}{\partial r_D} + \frac{r_D^\theta \lambda}{3} \frac{\partial p_{maD}(z_D, t_D)}{\partial z_D} = r_D^\theta \omega^* \frac{\partial p_{fbD}(r_D, t_D)}{\partial t_D}, \quad \text{II.34}$$

where *interporosity flow coefficient*, λ is given by:

$$\lambda = \frac{12k_{ma} r_w^{\theta+2}}{h_{ma} k_{fb}}, \quad \text{II.35}$$

and *dimensionless storativity ratio*:

$$\omega^* = \frac{c_{ifb}}{\phi_{ma} c_{ima} + c_{ifb}}. \quad \text{II.36}$$

Neglecting skin and wellbore storage effects, solution in Laplace space for Olarewaju's model, assuming constant flow rate and infinite reservoir, is:

$$\bar{p}_{wD}(s) = \frac{K_{\frac{1-\beta}{\theta+2}} \left(\frac{2}{\theta+2} \sqrt{sg(s)} \right)}{s^{3/2} \sqrt{g(s)} K_{\frac{D_{fb}}{\theta+2}} \left(\frac{2}{\theta+2} \sqrt{sg(s)} \right)}, \quad \text{II.37}$$

where:

$$g(s) = \omega^* + [1 - \omega^*] \sqrt{\frac{\lambda}{3s[1 - \omega^*]}} \tanh \left(\sqrt{\frac{3s[1 - \omega^*]}{\lambda}} \right). \quad \text{II.38}$$

Fig. II.37 shows the model proposed by Olarewaju (1996) with the inclusion of storage and skin around wellbore for different values of the fractal dimension of fracture network.

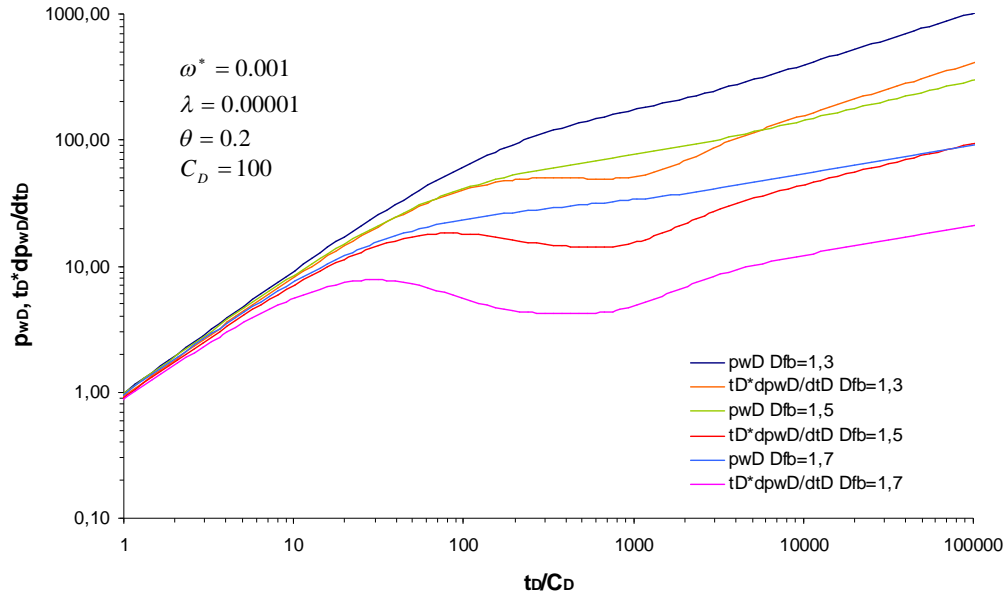


Fig. II.10. Log-log plot of the model proposed by Olarewaju (1996).

Flamenco et al. (2001) and Flamenco et al. (2003) presented approximated solutions for the early and late times periods of the models presented by Chang et al. (1990). The convergence of such solutions was tested against a numerical solution of the same model. **Fig. II.11** shows the convergence of the analytical and semi-analytical solutions to the numerical one, presented by these authors.

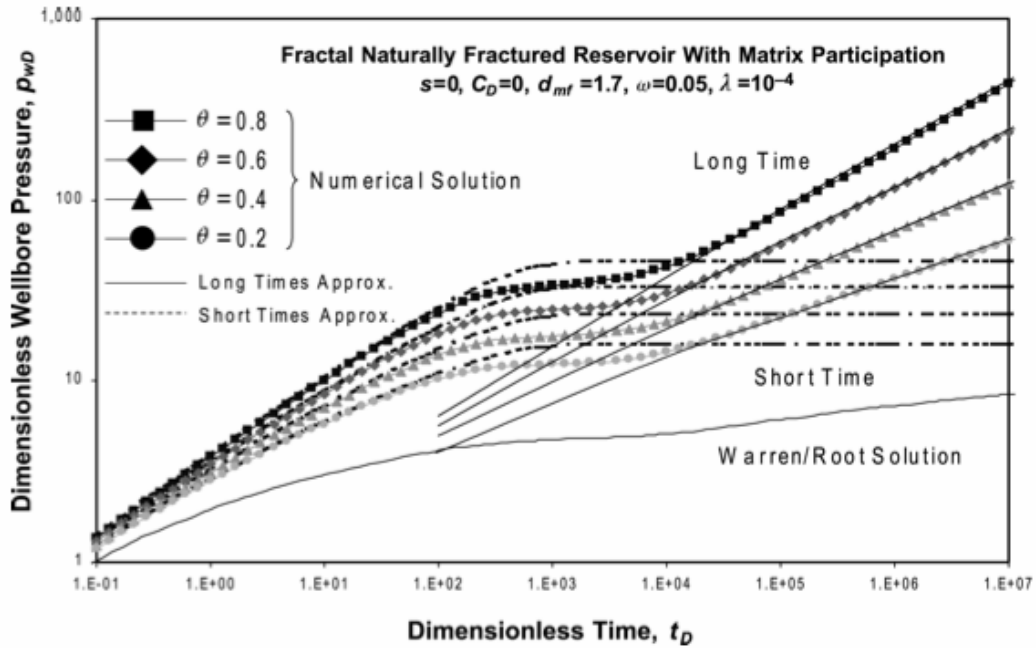


Fig. II.11. Chang et al. (1990) solution (numerical solution); short- and long-time approximations for a fractal fractured reservoir with matrix participation (figure taken from Flamenco et al., 2003).

In Appendix C of this thesis, a free interaction between matrix and fractures under transient pressure conditions was developed. With this development the concept of *dimensionless fracture area*, A_{fD} , (Cinco-Ley and Samaniego, 1982) was introduced into fractal reservoir theory. Moreover, with this model, it is possible to assume slabs and spherical shape for matrix blocks. Developed diffusivity equation for this model is:

$$\begin{aligned} & \frac{\partial^2 p_{fbD}(r_D, t_D)}{\partial r_D^2} + \frac{\beta}{r_D} \frac{\partial p_{fbD}(r_D, t_D)}{\partial r_D} - r_D^\theta A_{fD} [1 - \omega] \int_0^{t_D} \frac{\partial p_{fbD}(r_D, \tau)}{\partial \tau} F(\eta_{maD}, H_D, t_D - \tau) d\tau = \\ & = r_D^\theta \omega \frac{\partial p_{fbD}(r_D, t_D)}{\partial t_D} \end{aligned} \quad , \quad \text{II.39}$$

where:

A_{fD} = dimensionless fractal fracture area, and it is defined as:

$$A_{fD} = \frac{A_{fb} h_{ma} V_b r_w^\theta}{V_{ma}} . \quad \text{II.40}$$

Fluid transference functions, assuming slabs is given by:

$$F(\eta_{maD}, H_D, t_D - \tau) = \frac{4\eta_{maD}}{H_D} \sum_{n=1}^{\infty} e^{-\frac{\eta_{maD}(2n+1)^2 \pi^2 [t_D - \tau]}{H_D}} , \quad \text{II.41}$$

or, if spheres as matrix blocks, fluid transference function is:

$$F(\eta_{maD}, H_D, t_D - \tau) = \frac{4\eta_{maD}}{H_D} \sum_{n=1}^{\infty} e^{-\frac{4\eta_{maD} n^2 \pi^2 [t_D - \tau]}{H_D}} . \quad \text{II.42}$$

Solution in Laplace Space for eq. II.39 under constant flow rate and infinite reservoir conditions is given by:

$$\bar{p}_{wD}(s) = \frac{K_{\frac{1-\beta}{\theta+2}} \left(\frac{2}{\theta+2} \sqrt{sf(s)} \right)}{s^{3/2} \sqrt{f(s)} K_{\frac{D_{fb}}{\theta+2}} \left(\frac{2}{\theta+2} \sqrt{sf(s)} \right)} , \quad \text{II.46}$$

where:

$$f(s) = A_{fD} [1 - \omega] \bar{F}(\eta_{maD}, H_D, s) - \omega . \quad \text{II.47}$$

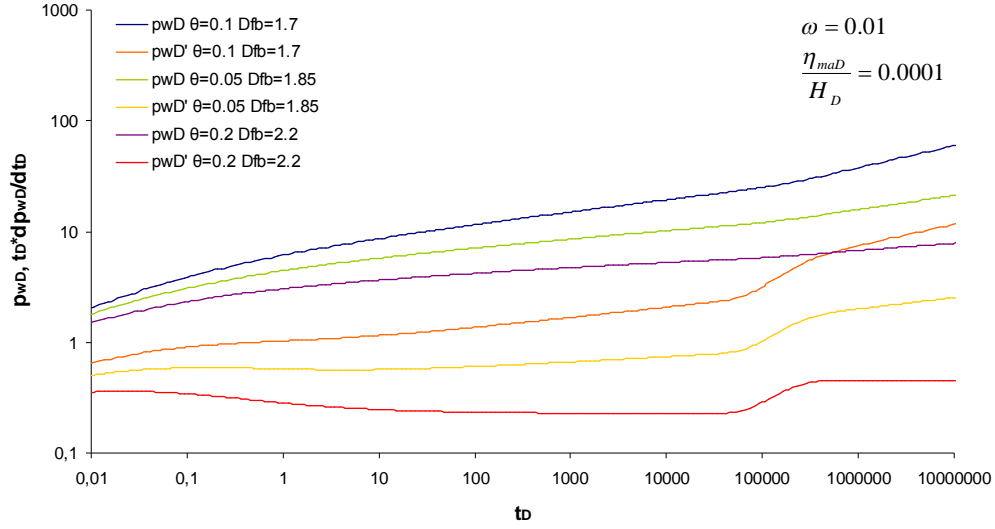


Fig. II.12. Log-log plot of the free interporous transference, developed in Appendix C.

Larsen (2013) developed a modified fractal model for small values of the dimensionless storativity ratio by combining models presented previously by Chang et al. (1990) and Olarewaju (1996). Such modification yields the equation in Laplace space:

$$\frac{1}{r_D^{\beta-\theta}} \frac{d}{dr_D} \left(r_D^\beta \frac{d\bar{p}_{fbD}(r_D, t_D)}{dr_D} \right) = \frac{\lambda}{3} r_D^{d-D_{fb}} \sqrt{\alpha s} \tanh(L_D \sqrt{\alpha s}) \bar{p}_{fbD}(r_D, t_D). \quad \text{II.48}$$

Detailed development of this model is shown in Appendix D.

Other relevant papers regarding this topic are the ones published by Acuña et al. (1995) and Camacho-Velázquez et al. (2008). In addition, Cossio (2012) and Cossio et al. (2013) presented a model that describes the behaviour of pressure within a finite conductivity fracture into a fractal reservoir, and a semi-analytical solution for it.

Chapter III

Proposed Model

III.1. Flow model development

Incoming fluid mass into an object is given by:

$$m_{in} = \rho_f q_f \Delta t ; \quad \text{III.1}$$

out coming fluid mass from the same object is:

$$m_{out} = \rho_f q_f \Delta t + \Delta(\rho_f q_f) \Delta t ; \quad \text{III.2}$$

oil mass contribution from the Euclidean matrix:

$$m_{ma} = \rho_f \bar{q}_{ma} \Delta t . \quad \text{III.3}$$

Then, cumulative fluid mass into the object is:

$$m_{cum} = m_{out} - m_{in} + \rho_f \bar{q}_{ma} \Delta t = \Delta(\rho_f q_f) \Delta t + \rho_f \bar{q}_{ma} \Delta t . \quad \text{III.4}$$

On the other hand, mass of fluid at a time t_1 is given by:

$$m_{t_1} = S_f \rho_f \phi_{fb} V_{bulk} , \quad \text{III.5}$$

at a time t_2 :

$$m_{t_2} = S_f \rho_f \phi_{fb} V_{bulk} + \Delta(S_f \rho_f \phi_{fb}) V_{bulk} , \quad \text{III.6}$$

and, cumulative fluid mass is given by:

$$m_{cum} = m_{t_2} - m_{t_1} = \Delta(S_f \rho_f \phi_{fb}) V_{bulk} . \quad \text{III.7}$$

Equating eq. III.4 and eq. III.7 results:

$$\Delta(\rho_f q_f) \Delta t + \rho_f \bar{q}_{ma} \Delta t = \Delta(S_f \rho_f \phi_{fb}) V_{bulk} . \quad \text{III.8}$$

Using definition of bulk volume (eq. I.4), eq. III.8 becomes:

$$\Delta(\rho_f q_f) \Delta t + \rho_f \bar{q}_{ma} \Delta t = \Delta(S_f \rho_f \phi_{fb}) [\alpha_{d_e} r^{d_e-1} b^{3-d_e} \Delta r] . \quad \text{III.9}$$

Arraying previous equation:

$$\frac{1}{\alpha_{d_e} r^{d_e-1} b^{3-d_e}} \frac{\Delta(\rho_f q_f)}{\Delta r} + \rho_f q_{ma}^* = \frac{\Delta(S_f \rho_f \phi_{fb})}{\Delta t} . \quad \text{III.10}$$

Where *Matrix flow rate per unit of bulk volume* is defined by:

$$q_{ma}^* = \frac{\bar{q}_{ma}}{V_{bulk}} . \quad \text{III.11}$$

Taking the limits Δr and Δt to zero, and arraying, equation III.10 becomes:

$$\frac{\partial(\rho_f q_f)}{\partial r} + \alpha_{d_e} r^{d_e-1} b^{3-d_e} \rho_f q_{ma}^* = \alpha_{d_e} r^{d_e-1} b^{3-d_e} \frac{\partial(S_f \rho_f \phi_{fb})}{\partial t} . \quad \text{III.12}$$

Inserting Darcy's equation in fractal form (eq.I.51) into previous equation, results:

$$\frac{\partial}{\partial r} \left(\rho_f \frac{aV_{uf}k_{fb}r^\beta}{\phi_{fb}\mu} \frac{\partial p_{fb}}{\partial r} \right) + \alpha_{d_e} r^{d_e-1} b^{3-d_e} \rho_f q_{ma}^* = \alpha_{d_e} r^{d_e-1} b^{3-d_e} \frac{\partial (S_f \rho_f \phi_{fb})}{\partial t}. \quad \text{III.13}$$

Applying the derivatives in eq. III.13:

$$\begin{aligned} & \frac{aV_{uf}k_{fb}}{\phi_{fb}\mu} \left[\rho_f r^\beta \frac{\partial^2 p_{fb}(r,t)}{\partial r^2} + \rho_f \beta r^{\beta-1} \frac{\partial p_{fb}(r,t)}{\partial r} + r^\beta \frac{\partial p_{fb}(r,t)}{\partial r} \frac{\partial \rho_f}{\partial r} \right] + \\ & + \alpha_{d_e} r^{d_e-1} b^{3-d_e} \rho_f q_{ma}^* = \alpha_{d_e} r^{d_e-1} b^{3-d_e} \left[\phi_{fb} \frac{\partial (S_f \rho_f)}{\partial t} + S_f \rho_f \frac{\partial (\phi_{fb})}{\partial t} \right]. \end{aligned} \quad \text{III.14}$$

According to chain rule:

$$\frac{\partial \rho_f}{\partial r} = \frac{\partial \rho_f}{\partial p_{fb}(r,t)} \frac{\partial p_{fb}(r,t)}{\partial r}, \quad \text{III.15}$$

$$\frac{\partial S_f \rho_f}{\partial t} = \frac{\partial S_f \rho_f}{\partial p_{fb}(r,t)} \frac{\partial p_{fb}(r,t)}{\partial t}, \quad \text{III.16}$$

$$\frac{\partial \phi_{fb}}{\partial t} = \frac{\partial \phi_{fb}}{\partial p_{fb}(r,t)} \frac{\partial p_{fb}(r,t)}{\partial t}. \quad \text{III.17}$$

Substituting eqs. III.15, III.16 and III.17 and using compressibility definitions, prior eq. is rewritten as follows:

$$\begin{aligned} & \frac{aV_{uf}k_{fb}}{\phi_{fb}\mu} \left[r^\beta \frac{\partial^2 p_{fb}(r,t)}{\partial r^2} + \beta r^{\beta-1} \frac{\partial p_{fb}(r,t)}{\partial r} + r^\beta c_f \left(\frac{\partial p_{fb}(r,t)}{\partial r} \right)^2 \right] + \alpha_n r^{n-1} b^{3-n} q_{ma}^* = \\ & = \alpha_n r^{n-1} b^{3-n} \phi_{fb} S_f [c_f + c_{fb}] \frac{\partial p_{fb}(r,t)}{\partial t} \end{aligned} \quad \text{III.18}$$

If single phase flow is assumed, then total compressibility is defined as:

$$c_{ifb} = c_f + c_{fb}, \quad \text{III.19}$$

therefore eq. III.18 is written as:

$$\begin{aligned} & \frac{aV_{uf}k_{fb}}{\phi_{fb}\mu} \left[r^\beta \frac{\partial^2 p_{fb}(r,t)}{\partial r^2} + \beta r^{\beta-1} \frac{\partial p_{fb}(r,t)}{\partial r} + r^\beta c_f \left(\frac{\partial p_{fb}(r,t)}{\partial r} \right)^2 \right] + \alpha_{d_e} r^{d_e-1} b^{3-d_e} q_{ma}^* = \\ & = \alpha_{d_e} r^{d_e-1} b^{3-d_e} \phi_{fb} c_{ifb} \frac{\partial p_{fb}(r,t)}{\partial t} \end{aligned} \quad \text{III.20}$$

Neglecting quadratic gradient pressure and according to *porosity of the fracture network* definition, prior equation becomes:

$$r^\beta \frac{\partial^2 p_{fb}(r,t)}{\partial r^2} + \beta r^{\beta-1} \frac{\partial p_{fb}(r,t)}{\partial r} + r^{D_{fb}-1} \frac{\mu}{k_{fb}} q_{ma}^* = r^{D_{fb}-1} \frac{c_{ifb} \phi_{fb} \mu}{k_{fb}} \frac{\partial p_{fb}(r,t)}{\partial t}. \quad \text{III.21}$$

On the other hand, *matrix flow rate per unit of bulk* can be expressed as:

$$q_{ma}^* = - \frac{k_{ma} A_{fb}}{\mu} \int_0^t \frac{\partial p_{ma}(\tau)}{d\tau} (\nabla \Delta p_{uma})_{sur} d\tau. \quad \text{III.22}$$

If slab matrix blocks are assumed, area exposed to flow is defined as:

$$A_{fb} = \frac{2}{h_{ma} + h_f}; \quad \text{III.23}$$

or, if cube matrix blocks are assumed:

$$A_{fb} = \frac{6h_{ma}^2}{(h_{ma} + h_f)^3}. \quad \text{III.24}$$

Substituting eq. III.22 into III.21, the *diffusivity equation for a double porosity fractal reservoir with transient interporosity transfer* is obtained:

$$r^\beta \frac{\partial^2 p_{fb}(r,t)}{\partial r^2} + \beta r^{\beta-1} \frac{\partial p_{fb}(r,t)}{\partial r} - r^{D_{fb}-1} \frac{k_{ma} A_{fb}}{k_{fb}} \int_0^t \frac{\partial p_{ma}(\tau)}{d\tau} (\nabla \Delta p_{uma})_{sur} d\tau = \frac{r^{D_{fb}-1}}{\eta_{fb}} \frac{\partial p_{fb}(r,t)}{\partial t}, \quad \text{III.25}$$

where hydraulic diffusivity coefficient in field units is defined as:

$$\eta_{fb} = \frac{0.00026367 k_{fb}}{\phi_{fb} \mu c_{ifb}}. \quad \text{III.26}$$

In compact form, eq. III.25 is written as:

$$\frac{1}{r^{D_{fb}-1}} \frac{\partial}{\partial r} \left(r^\beta \frac{\partial p_{fb}(r,t)}{\partial r} \right) - \frac{k_{ma} A_{fb}}{k_{fb}} \int_0^t \frac{\partial p_{ma}(\tau)}{d\tau} (\nabla \Delta p_{uma})_{sur} d\tau = \frac{1}{\eta_{fb}} \frac{\partial p_{fb}(r,t)}{\partial t}. \quad \text{III.27}$$

In order to have a homogeneous partial differential equation and an easier way to manage unknowns related to eq. III.27, it is necessary to expressed in dimensionless variables.

III.2 Transformation to dimensionless variables for well test analysis

In order to transform eq. III.27 to a dimensionless expression, following dimensionless variables has been stated:

Dimensionless radius:

$$r_D = \frac{r}{r_w}, \quad \text{III.28}$$

dimensionless time:

$$t_D = \frac{0.00026367k_{fb}}{(\phi c_t)_t \mu r_w^{2+\theta}} t, \quad \text{III.29}$$

where:

$$(\phi c_t)_t = \phi_{fb} c_{t_{fb}} + \phi_{ma} c_{t_{ma}}. \quad \text{III.30}$$

For an oil-filled system, dimensionless pressure in the fracture network:

$$p_{fbD}(r_D, t_D) = \frac{\alpha_{D_{fb}} (0.03281)^\theta}{887.22} \frac{aV_{uf} k_{fb} [p_i - p_{fb}(r, t)]}{qB_o \mu r_w^{1-\beta} \phi_{fb}}. \quad \text{III.31}$$

And, dimensionless pressure in the matrix:

$$p_{maD}(r_D, t_D) = \frac{\alpha_{D_{fb}} (0.03281)^\theta}{887.22} \frac{aV_{uf} k_{fb} [p_i - p_{ma}(r, t)]}{qB_o \mu r_w^{1-\beta} \phi_{fb}}. \quad \text{III.32}$$

For gas reservoirs, dimensionless pressure in the fracture network:

$$p_{fbD}(r_D, t_D) = \frac{\alpha_{D_{fb}} (0.03281)^\theta}{8937.2} \frac{aV_{uf} k_{fb} \Delta m(p_{fb})}{q_g \mu_g Z T r_w^{1-\beta} \phi_{fb}}, \quad \text{III.33}$$

where:

$$\Delta m(p_{fb}) = p_i^2 - p_{fb}^2(r, t). \quad \text{III.34}$$

and dimensionless pressure in the matrix:

$$p_{maD}(r_D, t_D) = \frac{\alpha_{D_{fb}} (0.03281)^\theta}{8937.2} \frac{aV_{uf} k_{fb} \Delta m(p_{ma})}{q_g \mu_g Z T r_w^{1-\beta} \phi_{fb}}, \quad \text{III.35}$$

where:

$$\Delta m(p_{ma}) = p_i^2 - p_{ma}^2(r, t). \quad \text{III.36}$$

For geothermal reservoirs (steam), dimensionless pressure in the fracture network:

$$p_{fbD}(r_D, t_D) = \frac{\alpha_{D_{fb}} (0.03281)^\theta}{81361} \frac{aV_{uf} k_{fb} \Delta m(p_{fb})}{W \mu_s Z T r_w^{1-\beta} \phi_{fb}}, \quad \text{III.37}$$

where:

$$\Delta m(p_{fb}) = p_i^2 - p_{fb}^2(r, t). \quad \text{III.38}$$

and, dimensionless pressure in the matrix:

$$p_{maD}(r_D, t_D) = \frac{\alpha_{D_{fb}} (0.03281)^\theta}{81361} \frac{aV_{uf} k_{fb} \Delta m(p_{ma})}{W\mu_s ZTr_w^{1-\beta} \phi_{fb}}, \quad \text{III.39}$$

and:

$$\Delta m(p_{ma}) = p_i^2 - p_{ma}^2(r, t). \quad \text{III.40}$$

The procedures for transformation to dimensionless variables of eq. III.25, for the oil, gas and steam reservoirs are similar, therefore only the oil-filled reservoir is shown.

Using chain rule, first derivative of pressure in the fracture network regarding the radius can be written as follows:

$$\frac{\partial p_{fb}(r, t)}{\partial r} = \frac{\partial p_{fb}(r, t)}{p_{fbD}(r_D, t_D)} \frac{dr_D}{dr} \frac{\partial p_{fbD}(r_D, t_D)}{\partial r_D}. \quad \text{III.41}$$

Based on dimensionless pressure definition, first derivative of pressure regarding dimensionless pressure in fracture network is:

$$\frac{\partial p_{fb}(r, t)}{\partial p_{fbD}(r_D, t_D)} = - \frac{887.22}{\alpha_{D_{fb}} (0.03281)^\theta} \frac{qB_o \mu r_w^{1-\beta} \phi_{fb}}{aV_{uf} k_{fb}}. \quad \text{III.42}$$

Based on the dimensionless radius definition, derivative of dimensionless radius regarding radius is:

$$\frac{dr_D}{dr} = \frac{1}{r_w}, \quad \text{III.43}$$

Substituting eq. III.42 and III.43 into eq. III.41 results:

$$\frac{\partial p_{fb}(r, t)}{\partial r} = - \frac{887.22}{\alpha_{D_{fb}} (0.03281)^\theta} \frac{qB_o \mu r_w^{-\beta} \phi_{fb}}{aV_{uf} k_{fb}} \frac{\partial p_{fbD}(r_D, t_D)}{\partial r_D}. \quad \text{III.44}$$

Taking second derivative regarding radius of eq. III.44:

$$\frac{\partial^2 p_{fb}(r, t)}{\partial r^2} = - \frac{887.22}{\alpha_{D_{fb}} (0.03281)^\theta} \frac{qB_o \mu r_w^{-\beta-1} \phi_{fb}}{aV_{uf} k_{fb}} \frac{\partial^2 p_{fbD}(r_D, t_D)}{\partial r_D^2}. \quad \text{III.45}$$

Analogously to the first derivative of pressure in the fracture network regarding the radius, first derivative of pressure in the fracture network regarding the time is given by:

$$\frac{\partial p_{fb}(r, t)}{\partial t} = \left[- \frac{887.22}{\alpha_{D_{fb}} (0.03281)^\theta} \frac{qB_o \mu r_w^{1-\beta} \phi_{fb}}{aV_{uf} k_{fb}} \right] \left[\frac{0.00026367k_{fb}}{(\phi c_t)_t \mu r_w^{2+\theta}} \right] \frac{\partial p_{fbD}(r_D, t_D)}{\partial t_D}. \quad \text{III.46}$$

Besides,

$$\frac{\partial p_{ma}(r, \tau)}{\partial \tau} = \frac{\partial p_{ma}(r, \tau)}{p_{maD}(r_D, \tau)} \frac{\partial p_{maD}(r_D, t_D)}{\partial \tau}, \quad \text{III.47}$$

hence:

$$\frac{\partial p_{ma}(r, \tau)}{\partial \tau} = \left[-\frac{887.22}{\alpha_{D_{fb}} (0.03281)^\theta} \frac{qB_o \mu r_w^{1-\beta} \phi_{fb}}{aV_{uf} k_{fb}} \right] \frac{\partial p_{maD}(r_D, t_D)}{\partial \tau}. \quad \text{III.48}$$

Substituting III.28, III.44, III.45, III.46, III.48 in III.25 and arraying it, results:

$$\begin{aligned} & \frac{\partial^2 p_{fbD}(r_D, t_D)}{\partial r_D^2} + \frac{\beta}{r_D} \frac{\partial p_{fbD}(r_D, t_D)}{\partial r_D} - r_D^\theta A_{fD} [1 - \omega] \int_0^{t_D} \frac{\partial p_{maD}(r_D, \tau)}{\partial \tau} F(\eta_{maD}, H_D, t_D - \tau) d\tau = \\ & = r_D^\theta \omega \frac{\partial p_{fbD}(r_D, t_D)}{\partial t_D} \end{aligned} \quad \text{III.49}$$

where, *dimensionless storativity ratio*, ω is defined as:

$$\omega = \frac{\phi_{fb} c_{ifb}}{(\phi c_t)_t}; \quad \text{III.50}$$

dimensionless matrix hydraulic diffusivity:

$$\eta_{maD} = \frac{k_{ma} (\phi c_t)_t}{\phi_{ma} c_{ima} k_{fb}}; \quad \text{III.51}$$

dimensionless block size, for slabs:

$$H_D = \frac{r_w^2}{h_{ma}^2}; \quad \text{III.52}$$

and for spheres:

$$H_D = \frac{r_w^2}{d_{ma}^2}; \quad \text{III.53}$$

dimensionless fractal fracture network area, A_{fD} :

$$A_{fD} = \frac{A_{fb} h_{ma} V_b r_w^\theta}{V_{ma}}. \quad \text{III.54}$$

Fluid transfer function, assuming slabs:

$$F(\eta_{maD}, H_D, t_D - \tau) = \frac{4\eta_{maD}}{H_D} \sum_{n=1}^{\infty} e^{-\frac{\eta_{maD}(2n+1)^2 \pi^2 [t_D - \tau]}{H_D}}, \quad \text{III.55}$$

or, if spheres as matrix blocks, fluid transfer function is:

$$F(\eta_{maD}, H_D, t_D - \tau) = \frac{4\eta_{maD}}{H_D} \sum_{n=1}^{\infty} e^{-\frac{4\eta_{maD} n^2 \pi^2 [t_D - \tau]}{H_D}}. \quad \text{III.56}$$

Chapter IV

Model solutions for well test analysis

IV.1. General Solution in Laplace space

In Chapter III the diffusivity equation for a double porosity reservoir assuming fractal fracture network and Euclidean matrix blocks was developed:

$$\begin{aligned} & \frac{\partial^2 p_{fbD}(r_D, t_D)}{\partial r_D^2} + \frac{\beta}{r_D} \frac{\partial p_{fbD}(r_D, t_D)}{\partial r_D} - r_D^\theta A_{fD} [1 - \omega] \int_0^{t_D} \frac{\partial p_{maD}(r_D, \tau)}{\partial \tau} F(\eta_{maD}, H_D, t_D - \tau) d\tau = \\ & = r_D^\theta \omega \frac{\partial p_{fbD}(r_D, t_D)}{\partial t_D} \end{aligned} \quad \text{IV.1}$$

In order to have a well test analysis model for the Fractal Reservoir Model assuming transient interporous transference between matrix and fractures, the following conditions have been set:

$$\text{initial condition for fracture network:} \quad p_{fbD}(r_D, t_D = 0) = 0, \quad \text{IV.2}$$

$$\text{inner Boundary:} \quad r_D^\beta \frac{\partial p_{fbD}(1, t_D)}{\partial t_D} = -1, \quad \text{IV.3}$$

$$\text{outer boundary:} \quad \lim_{r_D \rightarrow \infty} (p_D(r_D, t_D)) = 0. \quad \text{IV.4}$$

Constant rate solutions assuming finite circular reservoir and constant pressure boundary are shown in Appendix G.

Applying Laplace transform to eq. IV.1 yields:

$$\begin{aligned} & \frac{d^2 p_{fbD}(r_D, t_D)}{dr_D^2} + \frac{\beta}{r_D} \frac{dp_{fbD}(r_D, t_D)}{dr_D} - r_D^\theta A_{fD} [1 - \omega] \bar{F}(\eta_{maD}, H_D, s) s \bar{p}_{maD}(r_D, s) = \\ & = r_D^\theta \omega [s \bar{p}_{fbD}(r_D, s) - p_{fbD}(r_D, 0)] \end{aligned} \quad \text{IV.5}$$

Similar to Cinco-Ley et al. (1985), dimensionless pressure in the matrix can be expressed as follows:

$$\bar{p}_{maD}(r_D, s) = \frac{\bar{p}_{fbD}(r_D, s)}{1 + \frac{H_D S_{ma-fbD}}{\eta_{maD}} \bar{F}(\eta_{maD}, H_D, s) s} \quad \text{IV.6}$$

where, for slab matrix blocks:

$$\bar{F}(\eta_{maD}, H_D, s) = \sqrt{\frac{\eta_{maD}}{H_D s}} \tanh\left(\frac{1}{2} \sqrt{\frac{H_D s}{\eta_{maD}}}\right), \quad \text{IV.7}$$

and, for spheres as matrix blocks:

$$\bar{F}(\eta_{maD}, H_D, s) = \sqrt{\frac{\eta_{maD}}{H_D s}} \left[\coth\left(\frac{1}{2} \sqrt{\frac{H_D s}{\eta_{maD}}}\right) - 2 \sqrt{\frac{\eta_{maD}}{H_D s}} \right]. \quad \text{IV.8}$$

Substituting eq. IV.6 into eq. IV.5 results:

$$\begin{aligned} & \frac{d^2 p_{fbD}(r_D, t_D)}{dr_D^2} + \frac{\beta}{r_D} \frac{dp_{fbD}(r_D, t_D)}{dr_D} - r_D^\theta A_{fD} [1 - \omega] s \frac{\bar{F}(\eta_{maD}, H_D, s)}{1 + \frac{H_D S_{ma-fbD}}{\eta_{maD}} \bar{F}(\eta_{maD}, H_D, s) s} \bar{p}_{fbD}(r_D, s) = \\ & = r_D^\theta \omega [s \bar{p}_{fbD}(r_D, s) - p_{fbD}(r_D, 0)] \end{aligned} \quad \text{IV.9}$$

Applying initial condition in eq. IV.9, and arraying:

$$r_D^2 \frac{d^2 \bar{p}_{fbD}(r_D, s)}{dr_D^2} + \beta r_D \frac{d\bar{p}_{fbD}(r_D, s)}{dr_D} - s r_D^{\theta+2} f(s) \bar{p}_{fbD}(r_D, s) = 0. \quad \text{IV.10}$$

Where the transference function is defined as:

$$f(s) = \frac{A_{fD} [1 - \omega] \bar{F}(\eta_{maD}, H_D, s)}{1 + \frac{H_D S_{ma-fbD}}{\eta_{maD}} \bar{F}(\eta_{maD}, H_D, s) s} + \omega. \quad \text{IV.11}$$

It can be verified that, if there is no restriction between matrix and fractures, i.e., $S_{ma-fbD} = 0$, prior transference function reduces to the free interaction fractal model, showed in Appendix D.

Parameter δ is established:

$$\delta = \frac{1 - \beta}{2}, \quad \text{IV.12}$$

then:

$$r_D^2 \frac{d^2 \bar{p}_{fbD}(r_D, s)}{dr_D^2} + [1 - 2\delta] r_D \frac{d\bar{p}_{fbD}(r_D, s)}{dr_D} - s r_D^{\theta+2} f(s) \bar{p}_{fbD}(r_D, s) = 0. \quad \text{IV.13}$$

The following transform function has been set:

$$\bar{p}_D(r_D, s) = \bar{G}_D(z), \quad \text{IV.14}$$

and the transformation variable:

$$z = \frac{2\sqrt{sf(s)}}{\theta + 2} r_D^{\frac{\theta+2}{2}}. \quad \text{IV.15}$$

Applying the variable transformations, the following expression is obtained:

$$z^2 \frac{\partial^2 \bar{G}_D(z)}{\partial z^2} + [1 - 2v]z \frac{\partial \bar{G}_D(z)}{\partial z} - z^2 \bar{G}_D(z) = 0, \quad \text{IV.16}$$

where:

$$v = \frac{1 - \beta}{\theta + 2}, \quad \text{IV.17}$$

To equalize the coefficient of the first derivative to one the following expression is proposed:

$$\bar{G}_D(z) = \frac{z^v}{\psi} B_D(z), \quad \text{IV.18}$$

where:

$$\psi = \left(\frac{2\sqrt{sf(s)}}{\theta + 2} \right)^{\frac{1-\beta}{\theta+2}}. \quad \text{IV.19}$$

Eq. IV.16 is expressed in terms of function IV.18 as:

$$z^2 \frac{d^2 B_D(z)}{dz^2} + z \frac{dB_D(z)}{dz} - [v^2 + z^2] B_D(z) = 0. \quad \text{IV.20}$$

Solution for eq. IV.20 is given by:

$$B_D(z) = c_1 I_v(z) + c_2 K_v(z), \quad \text{IV.21}$$

or, in terms of eq. IV.18:

$$\bar{G}_D(z) = \frac{z^v}{\psi} [c_1 I_v(z) + c_2 K_v(z)], \quad \text{IV.22}$$

and, in terms of $\bar{p}_D(r_D, s)$ and $r_D \sqrt{s}$, solution is:

$$\bar{p}_D(r_D, s) = r_D^{\frac{1-\beta}{2}} \left[c_1 I_{\frac{1-\beta}{\theta+2}} \left(\frac{2\sqrt{sf(s)}}{\theta+2} r_D^{\frac{\theta+2}{2}} \right) + c_2 K_{\frac{1-\beta}{\theta+2}} \left(\frac{2\sqrt{sf(s)}}{\theta+2} r_D^{\frac{\theta+2}{2}} \right) \right]. \quad \text{IV.23}$$

Applying outer boundary condition, it can be concluded that:

$$c_1 = 0, \quad \text{IV.24}$$

and, bounded solution is:

$$\bar{p}_D(r_D, s) = c_2 r_D^{\frac{1-\beta}{2}} K_{\frac{1-\beta}{\theta+2}} \left(\frac{2\sqrt{sf(s)}}{\theta+2} r_D^{\frac{\theta+2}{2}} \right). \quad \text{IV.25}$$

Applying inner boundary condition it is found that:

$$c_2 = -\frac{1}{s^{3/2} \sqrt{f(s)} K_{\frac{D_{fb}}{\theta+2}} \left(\frac{2\sqrt{sf(s)}}{\theta+2} \right)}, \quad \text{IV.26}$$

and, solution can be expressed as:

$$\bar{p}_D(r_D, s) = \frac{r_D^{\frac{1-\beta}{2}} K_{\frac{1-\beta}{\theta+2}} \left(\frac{2\sqrt{sf(s)}}{\theta+2} r_D^{\frac{\theta+2}{2}} \right)}{s^{3/2} \sqrt{f(s)} K_{\frac{D_{fb}}{\theta+2}} \left(\frac{2\sqrt{sf(s)}}{\theta+2} \right)}. \quad \text{IV.27}$$

Solution evaluated at wellbore is:

$$\bar{p}_{wD}(s) = \frac{K_{\frac{1-\beta}{\theta+2}} \left(\frac{2}{\theta+2} \sqrt{sf(s)} \right)}{s^{3/2} \sqrt{f(s)} K_{\frac{D_{fb}}{\theta+2}} \left(\frac{2}{\theta+2} \sqrt{sf(s)} \right)}. \quad \text{IV.28}$$

Phenomena around wellbore such as skin at wellbore and wellbore storage, can be incorporated as follows:

$$\bar{p}_{wD}(s, C_D, S_{well}) = \frac{\bar{p}_{wD}(s) + \frac{S_{well}}{s}}{1 + S_{well} s C_D + C_D s^2 \bar{p}_{wD}(s)}. \quad \text{IV.29}$$

A detailed description of the storage around wellbore phenomenon is described in Appendix F.

IV.2. Approximate solutions at short times: Total Expansion in the Fracture Network

It has been shown that at early times, only the fracture expansion acts in the reservoir (Cinco-Ley et al., 1982). It means that transference function can be approximated as:

$$f(s) \approx \omega, \quad \text{IV.30}$$

therefore, eq. IV.1 is reduced to:

$$\frac{\partial^2 p_{fbD}(r_D, t_D)}{\partial r_D^2} + \frac{\beta}{r_D} \frac{\partial p_{fbD}(r_D, t_D)}{\partial r_D} = r_D^\theta \omega \frac{\partial p_{fbD}(r_D, t_D)}{\partial t_D}. \quad \text{IV.31}$$

Establishing the following transformation function:

$$Z_{1D} = \omega (D_{fb})^2 \frac{[\theta+2]}{D_{fb}} p_{fbD}(r_D, t_D), \quad \text{IV.32}$$

and transformation variables:

$$\tau_1 = \frac{1}{D_{fb}} r_D^{D_{fb}}, \quad \text{IV.33}$$

and:

$$\kappa_1 = D_{fb}^{2-\frac{[\theta+2]}{D_{fb}}} t_D. \quad \text{IV.34}$$

Eq. 31 is expressed according to eqs. IV.32 to IV.34 as follows:

$$\tau_1^{2-\frac{2+\theta}{D_{fb}}} \frac{\partial^2 Z_{1D}}{\partial \tau_1^2} + \tau_1^{1-\frac{2+\theta}{D_{fb}}} \frac{[2D_{fb} - \theta - 2]}{D_{fb}} \frac{\partial Z_{1D}}{\partial \tau_1} = \omega \frac{\partial Z_{1D}}{\partial \kappa_1}. \quad \text{IV.35}$$

Similarly initial condition is given by:

$$Z_{1D}(\tau_1, 0) = 0; \quad \text{IV.36}$$

inner boundary condition:

$$\lim_{\tau_1 \rightarrow 0} \left(\tau_1^{2-\frac{[\theta+2]}{D_{fb}}} \frac{\partial Z_{1D}}{\partial \tau_1} \right) = -1, \quad \text{IV.37}$$

and outer boundary condition:

$$Z_{1D}(\infty, \kappa_1) = 0. \quad \text{IV.38}$$

Establishing the following transformation function:

$$Z_{1D} = U_{1D}(\xi_1) \kappa_1^{\frac{D_{fb}}{[\theta+2]}}, \quad \text{IV.39}$$

and:

$$\xi_1 = \tau_1 \kappa_1^{\frac{D_{fb}}{[\theta+2]}}. \quad \text{IV.40}$$

Applying the transformation variables, eq. IV.35 is rewritten as:

$$\xi_1^{2-\frac{2+\theta}{D_{fb}}} \frac{d^2 U_{1D}}{d\xi_1^2} - \xi_1^{1-\frac{2+\theta}{D_{fb}}} \left[\frac{\theta+2}{D_{fb}} \right] \frac{dU_{1D}}{d\xi_1} = \omega \left[-\frac{D_{fb}}{[\theta+2]} \xi_1 \frac{dU_{1D}}{d\xi_1} \right]. \quad \text{IV.41}$$

Prior eq. can be expressed as:

$$\left[\frac{\theta+2}{D_{fb}} \right] \frac{d}{d\xi_1} \left(\xi_1^{2-\frac{\theta+2}{D_{fb}}} \frac{dU_{1D}}{d\xi_1} \right) = -\omega \frac{d}{d\xi_1} (U_{1D} \xi_1), \quad \text{IV.42}$$

transforming inner boundary condition:

$$\lim_{\tau_1 \rightarrow 0} \left(\tau_1^{2-\frac{[\theta+2]}{D_{fb}}} \frac{\partial Z_{1D}}{\partial \tau_1} \right) = \lim_{\xi_1 \rightarrow 0} \left(\xi_1^{2-\frac{[\theta+2]}{D_{fb}}} \frac{dU_{1D}}{d\xi_1} \right) = 0, \quad \text{IV.43}$$

integrating eq. IV.42:

$$\frac{\theta+2}{D_{fb}} \xi_1^{2-\frac{\theta+2}{D_{fb}}} \frac{dU_{1D}}{d\xi_1} = -\omega (U_{1D} \xi_1) + A_1, \quad \text{IV.44}$$

it can be concluded, based on inner boundary condition:

$$A_1 = 0, \quad \text{IV.45}$$

therefore eq. IV.44 reduces to:

$$\frac{[\theta + 2]}{D_{fb}} \frac{dU_{1D}}{U_{1D}} = -\omega \xi_1^{\frac{\theta+2}{D_{fb}}-1} d\xi_1, \quad \text{IV.46}$$

integrating and arraying eq. IV.47:

$$U_{1D} = A_2 e^{-\left(\frac{D_{fb}}{\theta+2}\right)^2 \omega \xi_1^{\frac{\theta+2}{D_{fb}}}}, \quad \text{IV.47}$$

applying outer boundary:

$$\int_0^\infty U_{1D} d\xi_1 = A_2 \int_0^\infty e^{-\left(\frac{D_{fb}}{\theta+2}\right)^2 \omega \xi_1^{\frac{\theta+2}{D_{fb}}}} d\xi_1 = 1, \quad \text{IV.48}$$

hence:

$$A_2 = \frac{1}{\int_0^\infty e^{-\left(\frac{D_{fb}}{\theta+2}\right)^2 \omega \xi_1^{\frac{\theta+2}{D_{fb}}}} d\xi_1}, \quad \text{IV.49}$$

establishing the following transformation variable:

$$\xi_1 = \left(\frac{\gamma}{\omega}\right)^{\frac{D_{fb}}{\theta+2}}, \quad \text{IV.50}$$

taking the first derivative:

$$d\xi_1 = \omega^{-\frac{D_{fb}}{\theta+2}} \left[\frac{D_{fb}}{\theta+2} \gamma^{\frac{D_{fb}}{\theta+2}-1} d\gamma \right]. \quad \text{IV.51}$$

Hence, eq. IV.49 can be expressed as:

$$A_2 = \frac{\omega^{\frac{D_{fb}}{\theta+2}}}{\left[\frac{D_{fb}}{\theta+2} \right] \int_0^\infty e^{-\left(\frac{D_{fb}}{\theta+2}\right)^2 \gamma^{\frac{D_{fb}}{\theta+2}-1}} d\gamma}. \quad \text{IV.52}$$

Moreover, defining:

$$\gamma = \gamma_2 \left(\frac{D_{fb}}{\theta+2}\right)^{-2}, \quad \text{IV.53}$$

its first derivative is given by:

$$d\gamma = \left(\frac{D_{fb}}{\theta+2}\right)^{-2} d\gamma_2. \quad \text{IV.54}$$

Hence, eq. IV.52 becomes:

$$A_2 = \frac{\left(\frac{D_{fb}}{\theta+2}\right)^{\frac{2D_{fb}-1}{\theta+2}} \omega^{\frac{D_{fb}}{\theta+2}}}{\int_0^{\infty} e^{-\gamma_2} \gamma_2^{\frac{D_{fb}-1}{\theta+2}} d\gamma_2}. \quad \text{IV.55}$$

Gamma Function for this case is defined as:

$$\Gamma\left(\frac{D_{fb}}{\theta+2}\right) = \int_0^{\infty} e^{-\gamma_2} \gamma_2^{\frac{D_{fb}-1}{\theta+2}} d\gamma_2, \quad \text{IV.56}$$

hence:

$$A_2 = \frac{\left(\frac{D_{fb}}{\theta+2}\right)^{\frac{2D_{fb}-1}{\theta+2}} \omega^{\frac{D_{fb}}{\theta+2}}}{\Gamma\left(\frac{D_{fb}}{\theta+2}\right)}; \quad \text{IV.57}$$

subsequently eq. IV.47 becomes:

$$U_{1D} = \frac{\left(\frac{D_{fb}}{\theta+2}\right)^{\frac{2D_{fb}-1}{\theta+2}} \omega^{\frac{D_{fb}}{\theta+2}}}{\Gamma\left(\frac{D_{fb}}{\theta+2}\right)} e^{-\left(\frac{D_{fb}}{\theta+2}\right)^2 \omega \xi_1^{\frac{\theta+2}{D_{fb}}}}. \quad \text{IV.58}$$

Applying Duhamel's principle in eq. IV.39:

$$Z_{1D} = \int_0^{\kappa_1} U_{1D} \kappa_1^{-\frac{D_{fb}}{\theta+2}} d\kappa_1. \quad \text{IV.59}$$

Substituting eq. IV.58 in eq. IV.59:

$$Z_{1D} = \frac{\left(\frac{D_{fb}}{\theta+2}\right)^{\frac{2D_{fb}-1}{\theta+2}} \omega^{\frac{D_{fb}}{\theta+2}}}{\Gamma\left(\frac{D_{fb}}{\theta+2}\right)} \int_0^{\kappa_1} e^{-\left(\frac{D_{fb}}{\theta+2}\right)^2 \omega \frac{\tau_1^{\frac{\theta+2}{D_{fb}}}}{\kappa_1}} \kappa_1^{-\frac{D_{fb}}{\theta+2}} d\kappa_1. \quad \text{IV.60}$$

Establishing the following variable transformation:

$$\kappa_1 = \omega \left(\frac{D_{fb}}{\theta+2}\right)^2 \frac{\tau_1^{\frac{\theta+2}{D_{fb}}}}{y}, \quad \text{IV.61}$$

and, taking the first derivate regarding y :

$$d\kappa_1 = -\omega \left(\frac{D_{fb}}{\theta+2}\right)^2 \frac{\tau_1^{\frac{\theta+2}{D_{fb}}}}{y^2} dy. \quad \text{IV.62}$$

Substituting eq. IV. 61 and IV.62 in IV.60:

$$Z_{1D} = -\frac{\omega \left(\frac{D_{fb}}{\theta + 2} \right)^{\frac{\theta+2}{D_{fb}}-1} \tau_1^{\frac{D_{fb}}{D_{fb}}-1}}{\Gamma \left(\frac{D_{fb}}{\theta + 2} \right)} \int_y^\infty e^{-y} y^{\frac{D_{fb}}{\theta+2}-2} dy. \quad \text{IV.63}$$

Incomplete function Gamma is defined as:

$$\Gamma(a, x) = \int_x^\infty t^{a-1} e^{-t} dt, \quad \text{IV.64}$$

then, eq. IV.63 becomes:

$$Z_{1D} = -\frac{\omega \left(\frac{D_{fb}}{\theta + 2} \right)^{\frac{\theta+2}{D_{fb}}-1} \tau_1^{\frac{D_{fb}}{D_{fb}}-1}}{\Gamma \left(\frac{D_{fb}}{\theta + 2} \right)} \Gamma \left(\frac{D_{fb}}{\theta + 2} - 1, \omega \left(\frac{D_{fb}}{\theta + 2} \right)^2 \frac{\tau_1^{\frac{D_{fb}}{D_{fb}}}}{\kappa_1} \right), \quad \text{IV.65}$$

therefore, solution of eq. IV.31 is given by:

$$p_{fbD}(r_D, t_D) = -\frac{r_D^{\theta+2-D_{fb}}}{(\theta + 2) \Gamma \left(\frac{D_{fb}}{\theta + 2} \right)} \Gamma \left(\frac{D_{fb}}{\theta + 2} - 1, \frac{\omega r_D^{\theta+2}}{(\theta + 2)^2 t_D} \right). \quad \text{IV.66}$$

In order to have simplified solutions relatively easy to use, two cases must be defined. The first case is given by the condition $D_{fb} = \theta + 2$. If that is the case, eq. IV.103 and evaluated in $r_D = 1$, it becomes:

$$p_{wD}(t_D) = -\frac{1}{(\theta + 2)} \Gamma \left(0, \frac{\omega}{(\theta + 2)^2 t_D} \right). \quad \text{IV.67}$$

According to incomplete gamma function convergences, prior expression can be expressed as:

$$p_{wD}(t_D) = -\frac{1}{(\theta + 2)} E_i \left(\frac{\omega}{(\theta + 2)^2 t_D} \right), \quad \text{IV.68}$$

where:

$E_i(x)$ = integral exponential.

For small arguments of the integral exponential, eq. IV.68 can be approximated as:

$$p_{wD}(t_D) = \frac{1}{(\theta + 2)} [\ln(t_D) + 2 \ln(\theta + 2) - \ln(\omega) - \gamma], \quad \text{IV.69}$$

where:

γ = Euler's constant.

It can be verified that, if $\theta = 0$, eq. IV.69 converges to the solution presented by Cinco-Ley et al. (1982).

On the other hand, for $D_{fb} \neq \theta + 2$ long time an approximation of incomplete gamma function is given by:

$$\Gamma(a, x) \approx \Gamma(a) - \frac{x^a}{a} + \frac{x^{a+1}}{[a+1]}, \quad \text{IV.70}$$

hence, incomplete gamma function for this problem is approximated as:

$$\Gamma\left(\frac{D_{fb}}{\theta+2} - 1, \frac{\omega r_D^{\theta+2}}{(\theta+2)^2 t_D}\right) = \Gamma\left(\frac{D_{fb}}{\theta+2} - 1\right) - \left(\frac{1}{r_D^{\theta+2}}\right)^{1-\frac{D_{fb}}{\theta+2}} \frac{(\theta+2)^2 \left[1-\frac{D_{fb}}{\theta+2}\right] \omega^{\frac{D_{fb}}{\theta+2}-1}}{\frac{D_{fb}}{\theta+2} - 1} t_D^{1-\frac{D_{fb}}{\theta+2}}. \quad \text{IV.71}$$

Evaluating IV.66 at $r_D = 1$, and substituting IV.71 results:

$$p_{wD}(t_D) = \left[\frac{\Gamma\left(\frac{D_{fb}}{\theta+2} - 1\right)}{(\theta+2)\Gamma\left(\frac{D_{fb}}{\theta+2}\right)} - \frac{(\theta+2)^{2v-1} \omega^{v-1}}{\left[\frac{D_{fb}}{\theta+2} - 1\right]\Gamma\left(\frac{D_{fb}}{\theta+2}\right)} t_D^v \right], \quad \text{IV.72}$$

where:

$$v = 1 - \frac{D_{fb}}{\theta+2}. \quad \text{IV.73}$$

A form of the recurrence formula is:

$$\frac{\Gamma(x-1)}{\Gamma(x)} = (x-1)^{-1}, \quad \text{IV.74}$$

therefore, eq. IV.72 is rewritten as:

$$p_{wD}(t_D) = \frac{1}{-v(\theta+2)} + \frac{(\theta+2)^{2v-1} \omega^{v-1}}{v\Gamma\left(\frac{D_{fb}}{\theta+2}\right)} t_D^v. \quad \text{IV.75}$$

IV.3. Approximate solutions at intermediate times: Interaction between porous media

a. Transient State with variable Interporous Skin

For intermediate times, the interaction between porous media takes place. For this period, transference function can be approximated as:

$$f(s) \approx A_{fD} [1 - \omega] \sqrt{\frac{\eta_{maD}}{H_D s}} \left(1 + \frac{S_{ma-fbD} \sqrt{H_D s}}{\sqrt{\eta_{maD}}} \right)^{-1}, \quad \text{IV.76}$$

therefore, eq. IV.28 is rewritten as:

$$\bar{P}_{wD}(s) = \frac{\left(1 + \frac{S_{ma-fbD}\sqrt{H_D s}}{\sqrt{\eta_{maD}}}\right)^{\frac{1}{2}} K_{\frac{1-\beta}{\theta+2}} \left(\frac{2}{\theta+2} \left(1 + \frac{S_{ma-fbD}\sqrt{H_D s}}{\sqrt{\eta_{maD}}}\right)^{-\frac{1}{2}} \sqrt{A_{fD}[1-\omega] \sqrt{\frac{\eta_{maD} s}{H_D}}}\right)}{s^{3/2} \left(A_{fD}[1-\omega] \sqrt{\frac{\eta_{maD}}{H_D s}} \right)^{\frac{1}{2}} K_{\frac{D_{fb}}{\theta+2}} \left(\frac{2}{\theta+2} \left(1 + \frac{S_{ma-fbD}\sqrt{H_D s}}{\sqrt{\eta_{maD}}}\right)^{-\frac{1}{2}} \sqrt{A_{fD}[1-\omega] \sqrt{\frac{\eta_{maD} s}{H_D}}}\right)}$$

IV.77

For small arguments, Bessel function in the denominator is approximated as:

$$K_{\frac{D_{fb}}{\theta+2}} \left(\frac{2}{\theta+2} \left(1 + \frac{S_{ma-fbD}\sqrt{H_D s}}{\sqrt{\eta_{maD}}}\right)^{-\frac{1}{2}} \sqrt{A_{fD}[1-\omega] \sqrt{\frac{\eta_{maD} s}{H_D}}}\right) \approx$$

$$\approx \frac{(\theta+2)^{\frac{D_{fb}}{\theta+2}}}{2} \left(1 + \frac{S_{ma-fbD}\sqrt{H_D s}}{\sqrt{\eta_{maD}}}\right)^{\frac{D_{fb}}{2[\theta+2]}} \left(A_{fD}[1-\omega] \sqrt{\frac{\eta_{maD} s}{H_D}} \right)^{-\frac{D_{fb}}{2[\theta+2]}} \Gamma\left(\frac{D_{fb}}{\theta+2}\right)$$

IV.78

Substituting eq. IV.78 in eq. IV.77:

$$\bar{P}_{wD}(s) = \frac{2 \left(A_{fD}[1-\omega] \sqrt{\frac{\eta_{maD}}{H_D}} \right)^{\frac{D_{fb}}{2[\theta+2]} \frac{1}{2}} \left(1 + \frac{S_{ma-fbD}\sqrt{H_D s}}{\sqrt{\eta_{maD}}}\right)^{\frac{1}{2} \frac{D_{fb}}{2[\theta+2]}}}{(\theta+2)^{\frac{D_{fb}}{\theta+2}} \Gamma\left(\frac{D_{fb}}{\theta+2}\right) \frac{s^{\frac{5}{4} \frac{D_{fb}}{4[\theta+2]}}}{s^{\frac{5}{4} \frac{D_{fb}}{4[\theta+2]}}}}$$

$$\cdot K_{\frac{1-\beta}{\theta+2}} \left(\frac{2}{\theta+2} \left(1 + \frac{S_{ma-fbD}\sqrt{H_D s}}{\sqrt{\eta_{maD}}}\right)^{-\frac{1}{2}} \sqrt{A_{fD}[1-\omega] \sqrt{\frac{\eta_{maD} s}{H_D}}}\right)$$

IV.79

For the $D_{fb} = \theta + 2$ case, the Bessel function in the numerator is approximated as:

$$K_0 \left(\frac{2}{\theta+2} \left(1 + \frac{S_{ma-fbD}\sqrt{H_D s}}{\sqrt{\eta_{maD}}}\right)^{\frac{1}{2}} \sqrt{A_{fD}[1-\omega] \sqrt{\frac{\eta_{maD} s}{H_D}}}\right) \approx$$

$$\approx - \left[\ln \left(\frac{1}{\theta+2} \left(1 + \frac{S_{ma-fbD}\sqrt{H_D s}}{\sqrt{\eta_{maD}}}\right)^{\frac{1}{2}} \sqrt{A_{fD}[1-\omega] \sqrt{\frac{\eta_{maD} s}{H_D}}}\right) + \gamma \right]$$

IV.80

thus, eq. IV.79 can be expressed as:

$$\bar{p}_{wD}(s) = \frac{2}{\theta+2} \left[-\frac{1}{4} \frac{\ln(s)}{s} - \frac{1}{2} \frac{\ln\left(A_{fD}[1-\omega] \sqrt{\frac{\eta_{maD}}{H_D}}\right)}{s} + \frac{\ln(\theta+2)}{s} + \frac{1}{2} \frac{\ln\left(1 + S_{ma-fbD} \sqrt{\frac{H_D s}{\eta_{maD}}}\right)}{s} - \frac{\gamma}{s} \right]. \quad \text{IV.81}$$

Taking the natural logarithmic expansion:

$$\ln\left(1 + S_{ma-fbD} \sqrt{\frac{H_D s}{\eta_{maD}}}\right) \approx S_{ma-fbD} \sqrt{\frac{H_D s}{\eta_{maD}}}, \quad \text{IV.82}$$

eq. IV.123 becomes:

$$\bar{p}_{wD}(s) = \frac{2}{\theta+2} \left[-\frac{1}{4} \frac{\ln(s)}{s} - \frac{1}{2} \frac{\ln\left(A_{fD}[1-\omega] \sqrt{\frac{\eta_{maD}}{H_D}}\right)}{s} + \frac{\ln(\theta+2)}{s} + \frac{1}{2} \frac{\left[S_{ma-fbD} \sqrt{\frac{H_D}{\eta_{maD}}} \right]}{\sqrt{s}} - \frac{\gamma}{s} \right], \quad \text{IV.83}$$

inverting to Real Space:

$$p_{wD}(t_D) = \frac{2}{\theta+2} \left[\frac{1}{4} \ln(t_D) - \frac{1}{2} \ln\left(A_{fD}[1-\omega] \sqrt{\frac{\eta_{maD}}{H_D}}\right) + \ln(\theta+2) + \frac{1}{2\sqrt{\pi}} S_{ma-fbD} \sqrt{\frac{H_D}{\eta_{maD}}} t_D^{-\frac{1}{2}} - 0.4329 \right] \quad \text{IV.84}$$

On the other hand, if $D_{fb} \neq \theta+2$, then the Bessel function in the denominator is approximated as:

$$\begin{aligned} K_{\frac{1-\beta}{\theta+2}} \left(\frac{2}{\theta+2} \left(1 + \frac{S_{ma-fbD} \sqrt{H_D s}}{\sqrt{\eta_{maD}}} \right)^{-\frac{1}{2}} \sqrt{A_{fD}[1-\omega] \sqrt{\frac{\eta_{maD} s}{H_D}}} \right) &\approx \\ &\approx \frac{(\theta+2)^{\frac{1-\beta}{\theta+2}}}{2} \left(1 + \frac{S_{ma-fbD} \sqrt{H_D s}}{\sqrt{\eta_{maD}}} \right)^{\frac{1-\beta}{2[\theta+2]}} \left(A_{fD}[1-\omega] \sqrt{\frac{\eta_{maD} s}{H_D}} \right)^{\frac{1-\beta}{2[\theta+2]}} \Gamma\left(\frac{1-\beta}{\theta+2}\right) \end{aligned} \quad \text{IV.85}$$

substituting eq. IV.85 in eq. IV.79:

$$\bar{p}_{wD}(s) = \frac{(\theta+2)^{\frac{1-\beta-D_{fb}}{\theta+2}} \Gamma\left(\frac{1-\beta}{\theta+2}\right) \left(A_{fD}[1-\omega] \sqrt{\frac{\eta_{maD}}{H_D}} \right)^{\frac{D_{fb}-[\theta+2]-[1-\beta]}{2[\theta+2]}} \left(1 + \frac{S_{ma-fbD} \sqrt{H_D s}}{\sqrt{\eta_{maD}}} \right)^{\frac{[\theta+2]-D_{fb}+[1-\beta]}{2[\theta+2]}}}{\Gamma\left(\frac{D_{fb}}{\theta+2}\right) s^{\frac{5}{4} - \frac{D_{fb}}{4[\theta+2]} + \frac{1-\beta}{4[\theta+2]}}}}, \quad \text{IV.86}$$

erraying, prior eq. reduces to:

$$\bar{p}_{wD}(s) = \frac{\Gamma\left(\frac{1-\beta}{\theta+2}\right) \left(A_{fD}[1-\omega] \sqrt{\frac{\eta_{maD}}{H_D}}\right)^{\frac{\beta-1}{\theta+2}} \left(1 + \frac{S_{ma-fbD} \sqrt{H_D} s}{\sqrt{\eta_{maD}}}\right)^{\frac{1-\beta}{\theta+2}}}{(\theta+2)^{\frac{2\beta+\theta}{\theta+2}} \Gamma\left(\frac{D_{fb}}{\theta+2}\right) s^{\frac{2\theta+5-\beta}{2[\theta+2]}}}, \quad \text{IV.87}$$

according to binomial series, eq. IV.87 becomes:

$$\bar{p}_{wD}(s) = \frac{\Gamma\left(\frac{1-\beta}{\theta+2}\right) \left(A_{fD}[1-\omega] \sqrt{\frac{\eta_{maD}}{H_D}}\right)^{\frac{D_{fb}-[\theta+2]}{\theta+2}}}{\Gamma\left(\frac{D_{fb}}{\theta+2}\right) (\theta+2)^{\frac{2D_{fb}-[\theta+2]}{\theta+2}}} \left[s^{\frac{D_{fb}-3[\theta+2]}{2[\theta+2]}} + \left[1 - \frac{D_{fb}}{\theta+2}\right] S_{ma-fbD} \sqrt{\frac{H_D}{\eta_{maD}}} s^{\frac{D_{fb}-2[\theta+2]}{2[\theta+2]}} \right], \quad \text{IV.88}$$

and, inverting to real space, and arraying, eq. IV.88 can be expressed as:

$$t_D^{\frac{v}{2}} p_{wD}(t_D) = \frac{\Gamma\left(\frac{1-\beta}{\theta+2}\right) \left(A_{fD}[1-\omega] \sqrt{\frac{\eta_{maD}}{H_D}}\right)^{v-1}}{\Gamma(v) \Gamma\left(\frac{3-v}{2}\right) (\theta+2)^{2v-1}} \left[\sqrt{t_D} + \frac{S_{ma-fbD} [1-v] \sqrt{\frac{H_D}{\eta_{maD}}} \Gamma\left(\frac{3-v}{2}\right)}{\Gamma\left(\frac{2-v}{2}\right)} \right]. \quad \text{IV.89}$$

It can be verified that, if $S_{ma-fbD} = 0$ this model converges to the transient interporous transference and the solution given in Appendix D.

b. Pseudosteady-state equivalence: Severe interporous skin

Similar to Cinco et al. (1985), pseudosteady-state is achieved when a highly damaged interface between matrix and fracture network exists. Therefore, transference function reduces to:

$$f(s) \approx \frac{A_{fD} \eta_{maD}}{S_{ma-fbD} H_D s}, \quad \text{IV.90}$$

thus, eq. IV.28 becomes:

$$\bar{p}_{wD}(s) = \frac{1}{s \sqrt{\frac{A_{fD} \eta_{maD}}{S_{ma-fbD} H_D}}} \frac{K_{\frac{1-\beta}{\theta+2}} \left(\frac{2}{\theta+2} \sqrt{\frac{A_{fD} \eta_{maD}}{S_{ma-fbD} H_D}} \right)}{K_{\frac{D_{fb}}{\theta+2}} \left(\frac{2}{\theta+2} \sqrt{\frac{A_{fD} \eta_{maD}}{S_{ma-fbD} H_D}} \right)}, \quad \text{IV.91}$$

for small arguments the Bessel function in the denominator is approximated as:

$$K_{\frac{D_{fb}}{\theta+2}} \left(\frac{2}{\theta+2} \sqrt{\frac{A_{fD}\eta_{maD}}{S_{ma-fbD}H_D}} \right) \approx \frac{1}{2} \left[\frac{\theta+2}{\sqrt{\frac{A_{fD}\eta_{maD}}{S_{ma-fbD}H_D}}} \right]^{\frac{D_{fb}}{\theta+2}} \Gamma \left(\frac{D_{fb}}{\theta+2} \right), \quad \text{IV.92}$$

hence, inverting to real space:

$$p_{wD}(t_D) = \frac{2}{(\theta+2)^{\frac{D_{fb}}{\theta+2}} \Gamma \left(\frac{D_{fb}}{\theta+2} \right) \left(\sqrt{\frac{A_{fD}\eta_{maD}}{S_{ma-fbD}H_D}} \right)^{1-\frac{D_{fb}}{\theta+2}}} K_{\frac{1-\beta}{\theta+2}} \left(\frac{2}{\theta+2} \sqrt{\frac{A_{fD}\eta_{maD}}{S_{ma-fbD}H_D}} \right), \quad \text{IV.93}$$

It can be observed that expression IV.93 corresponds to an independent of time value. Cinco-Ley et al. (1985) found a relationship between the interporous skin and other parameter of the transient interporous transference model with the pseudosteady-state's matrix-fracture interaction parameter. Extending such concept to the present work, it was found the following expression:

$$\lambda = \frac{A_{fD}\eta_{maD}}{S_{ma-fbD}H_D}. \quad \text{IV.94}$$

A simplified expression of eq. IV.93, when $D_{fb} = \theta + 2$ is given by:

$$p_{wD}(t_D) = \frac{2}{\theta+2} K_0 \left(\frac{2}{\theta+2} \sqrt{\frac{A_{fD}\eta_{maD}}{S_{ma-fbD}H_D}} \right), \quad \text{IV.95}$$

or, in terms of pseudosteady-state models' parameters:

$$p_{wD}(t_D) = \frac{2}{\theta+2} K_0 \left(\frac{2}{\theta+2} \sqrt{\lambda} \right), \quad \text{IV.96}$$

prior equation can be approximated as follows:

$$p_{wD}(t_D) = \frac{2}{\theta+2} \left[\ln(\theta+2) + \frac{1}{2} \ln(\lambda) - \gamma \right]. \quad \text{IV.97}$$

On the other hand, if $D_{fb} \neq \theta + 2$, then:

$$K_{\frac{1-\beta}{\theta+2}} \left(\frac{2}{\theta+2} \sqrt{\frac{A_{fD}\eta_{maD}}{S_{ma-fbD}H_D}} \right) \approx \frac{1}{2} \left[\frac{2}{\theta+2} \sqrt{\frac{S_{ma-fbD}H_D}{A_{fD}\eta_{maD}}} \right]^{\frac{1-\beta}{\theta+2}} \Gamma \left(\frac{1-\beta}{\theta+2} \right), \quad \text{IV.98}$$

and eq. IV.93 is reduced to:

$$p_{wD}(t_D) = \frac{(\theta+2)^{\frac{\theta+2-2D_{fb}}{\theta+2}} \Gamma \left(\frac{1-\beta}{\theta+2} \right) \left(\frac{S_{ma-fbD}H_D}{A_{fD}\eta_{maD}} \right)^{\frac{1-\beta}{\theta+2}}}{\Gamma \left(\frac{D_{fb}}{\theta+2} \right)}. \quad \text{IV.99}$$

In terms of pseudosteady-state models' parameters:

$$p_{wD}(t_D) = \frac{(\theta + 2)^{\frac{\theta+2-2D_{fb}}{\theta+2}} \Gamma\left(\frac{1-\beta}{\theta+2}\right) \lambda^{\frac{D_{fb}}{\theta+2}-1}}{\Gamma\left(\frac{D_{fb}}{\theta+2}\right)} \quad \text{IV.100}$$

IV.4. Approximate solutions at late times: Single System Behavior

At late times the double porosity system acts as a single one. Therefore, the transference function is approximated as:

$$f(s) \approx 1, \quad \text{IV.101}$$

and eq. IV.1 is reduced to:

$$\frac{\partial^2 p_{fbD}(r_D, t_D)}{\partial r_D^2} + \frac{\beta}{r_D} \frac{\partial p_{fbD}(r_D, t_D)}{\partial r_D} = r_D^\theta \frac{\partial p_{fbD}(r_D, t_D)}{\partial t_D}. \quad \text{IV.102}$$

For this case, an analogous procedure made for the early times case can be performed.

Thus, the solution for the late times case is given by:

$$p_{fbD}(r_D, t_D) = -\frac{r_D^{\theta+2-D_{fb}}}{(\theta+2)\Gamma\left(\frac{D_{fb}}{\theta+2}\right)} \Gamma\left(\frac{D_{fb}}{\theta+2}-1, \frac{r_D^{\theta+2}}{(\theta+2)^2 t_D}\right). \quad \text{IV.103}$$

Evaluating at wellbore:

$$p_{wD}(t_D) = -\frac{1}{(\theta+2)\Gamma\left(\frac{D_{fb}}{\theta+2}\right)} \Gamma\left(\frac{D_{fb}}{\theta+2}-1, \frac{1}{(\theta+2)^2 t_D}\right). \quad \text{IV.104}$$

Besides, if $D_{fb} = \theta + 2$, eq. IV.104 is approximated by the following expression:

$$p_{wD}(t_D) = \frac{1}{(\theta+2)} [\ln(t_D) + 2\ln(\theta+2) - \gamma]. \quad \text{IV.105}$$

It can be verified that, if $\theta = 0$, eq. IV.105 converges to the solution presented by Cinco-Ley et al. (1982).

On the other hand, for $D_{fb} \neq \theta + 2$ the approximation is given by:

$$p_{wD}(t_D) = \frac{1}{-v(\theta+2)} + \frac{(\theta+2)^{2v-1}}{v\Gamma\left(\frac{D_{fb}}{\theta+2}\right)} t_D^v. \quad \text{IV.106}$$

Chapter V

Validation and Application

In Chapter IV a general solution in Laplace space for the model developed in this thesis was developed. Such solution evaluated at wellbore is given by:

$$\bar{p}_{wD}(s) = \frac{K_{\frac{1-\beta}{\theta+2}} \left(\frac{2}{\theta+2} \sqrt{sf(s)} \right)}{s^{3/2} \sqrt{f(s)} K_{\frac{D_{fb}}{\theta+2}} \left(\frac{2}{\theta+2} \sqrt{sf(s)} \right)} \quad \text{V.1}$$

For computer-aided analysis, eq. V.1 is numerically inverted to real space (Stehfest, 1970) in order to analyze transient pressure data that shows fractal behavior.

Fig. V.1. shows the dimensionless pressure and the dimensionless pressure derivative function assuming free interaction between porous media, i.e., $S_{ma-fbD} = 0$ for different values of θ and D_{fb} . Under these circumstances, it can be observed that, for an idealized radial flow and fully connected system, i.e., $D_{fb} = 2$ and $\theta = 0$, respectively, this model converges to the model proposed by Cinco-Ley et al. (1982).

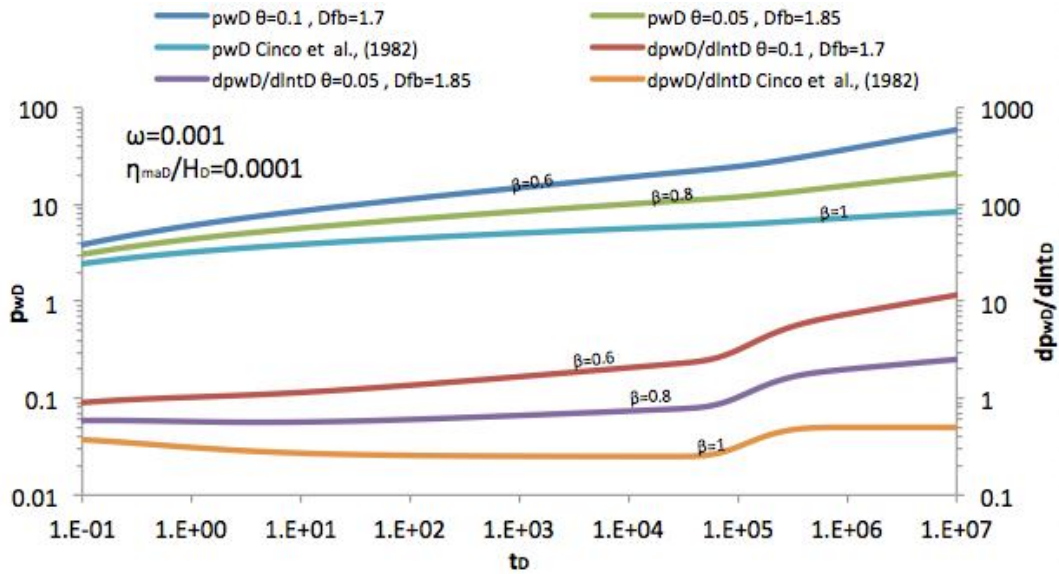


Fig. V.1. Pressure and pressure derivate function behavior for some values of D_{fb} , and θ without interporous skin and its convergence to the model proposed by Cinco-Ley et al., (1982).

In the available literature related to transient pressure analysis of fractal reservoir it has been stated that for the values $D_{fb} = 2$ and $\theta = 0$ the models converges to the well-known radial flow behavior. However, such behavior can be observed whenever the

condition $D_{fb} = \theta + 2$ be satisfied. **Fig. V.2.** shows a semilog plot of the dimensionless pressure behavior as a function of the dimensionless time for combinations that satisfy the $D_{fb} = \theta + 2$ condition. Hence, it can be observed that the dimensionless pressure for a idealized double porosity radial system perfectly connected (blue solid line) shows the same behavior of a double porosity spherical system poorly connected (green solid line).

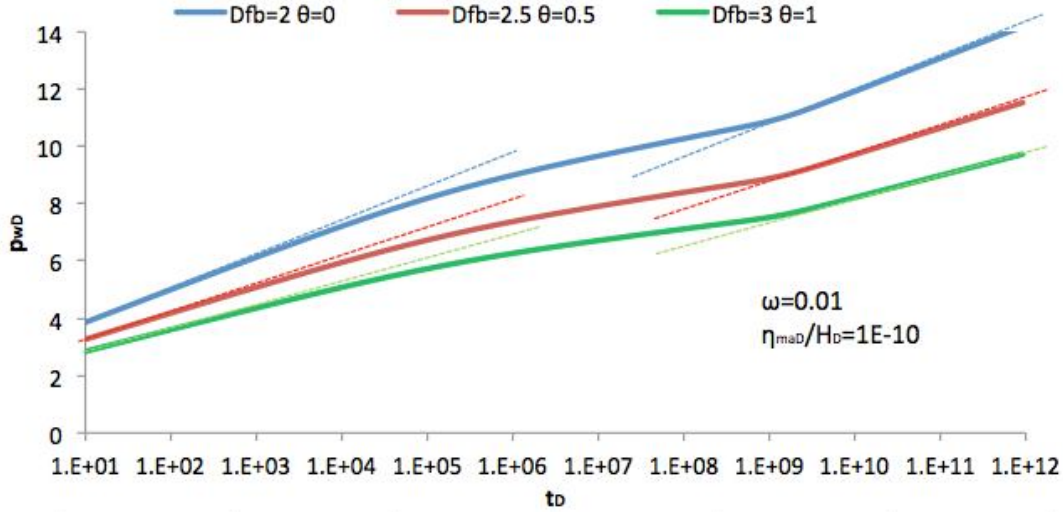


Fig. V.2. Semilog plot of the pressure behavior for some values of θ that satisfy the condition of $D_{fb} = \theta + 2$.

Besides, dotted lines in **Fig. V.2.** shows the convergence of the approximated solutions for early times:

$$p_{wD}(t_D) = \frac{1}{(\theta + 2)} [\ln(t_D) + 2 \ln(\theta + 2) - \ln(\omega) - \gamma], \quad \text{V.2}$$

and for late times:

$$p_{wD}(t_D) = \frac{1}{(\theta + 2)} [\ln(t_D) + 2 \ln(\theta + 2) - \gamma], \quad \text{V.3}$$

to the general solution for the shown cases.

Fig. V.3. shows the dimensionless pressure and the dimensionless pressure derivative function behavior of the proposed model when $D_{fb} \neq \theta + 2$, for different values of interporous skin and neglecting phenomena around wellbore. It can be observed that the higher the interporous skin the deeper the “valley” shape in the dimensionless pressure derivative function, which corresponds to the interaction between porous media.

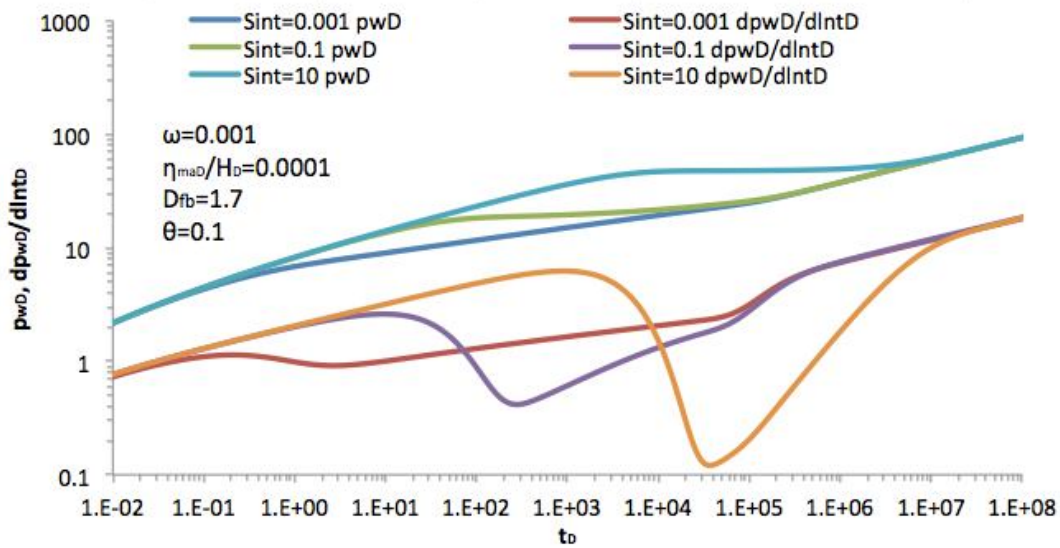


Fig. V.3. Impact of interporous skin in pressure and pressure derivative function, when $D_{fb} \neq \theta + 2$.

Fig. V.4. shows the log-log plot of the dimensionless pressure and dimensionless pressure derivative behavior of the proposed model for different values of interporous skin, such the condition $D_{fb} = \theta + 2$ is fulfilled. For this case $\theta = 0.2$ was used and the slope of the dimensionless pressure derivative function is equal to zero during the early and late times, so “apparent radial flow” behavior is observed. In addition, during intermediate times, the higher the interporous skin, the deeper the “valley” shape in the dimensionless pressure derivative function.

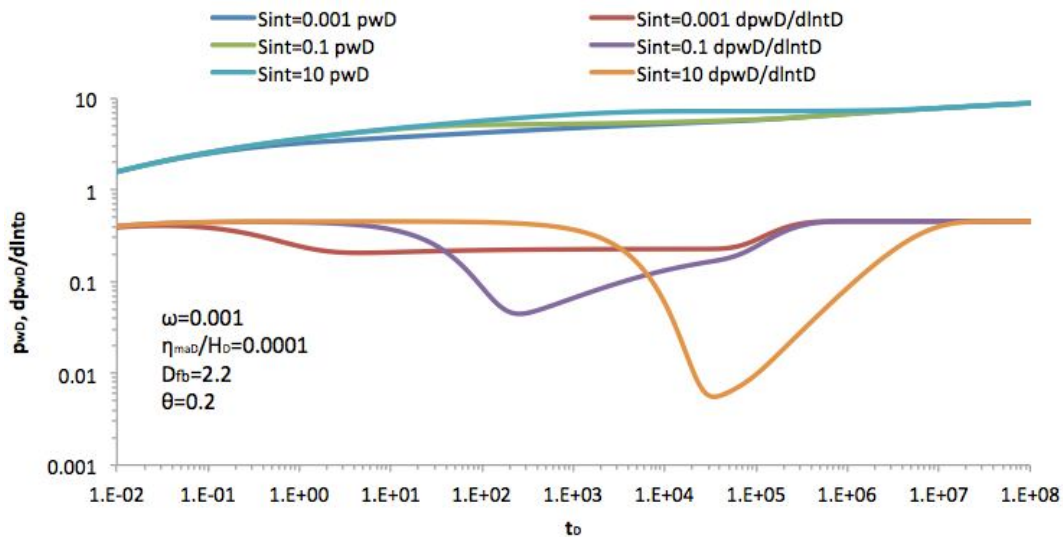


Fig. V.4. Impact of interporous skin in pressure and pressure derivative function, for $D_{fb} = \theta + 2$.

It was also mentioned that in order to include phenomena around wellbore to the proposed model, such as wellbore storage and skin around wellbore, eq. IV.29 should be used. **Fig. V.5.** and **Fig. V.6.** show the impact of these phenomena on the cases shown previously in **Fig. V.3.** and **Fig. V.4.**, respectively.

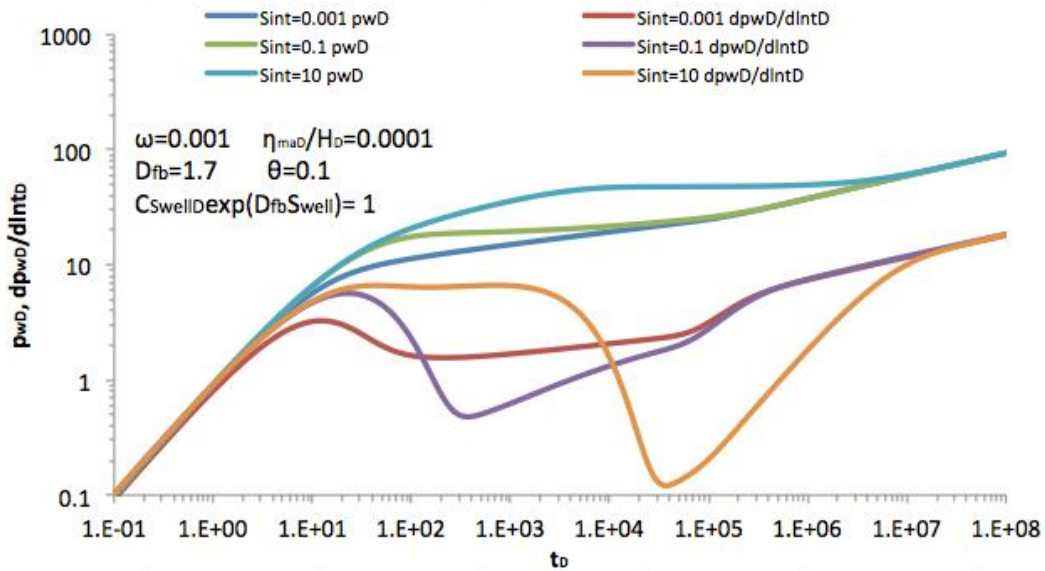


Fig. V.5. Behavior of pressure and pressure derivative function, when $D_{fb} \neq \theta + 2$, considering phenomena around wellbore.

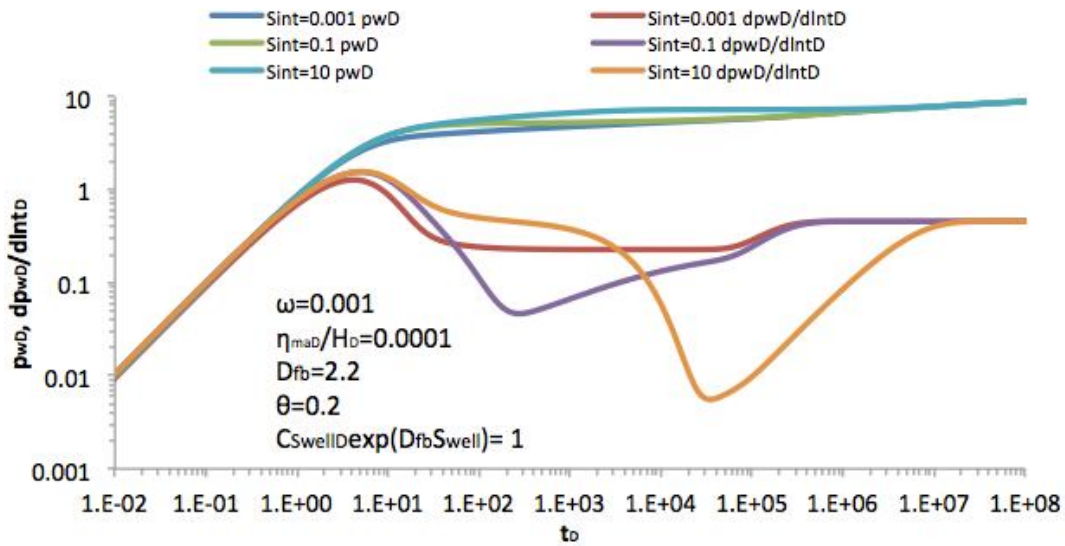


Fig. V.6. Behavior of pressure and pressure derivative function, when $D_{fb} = \theta + 2$, considering phenomena around wellbore.

Fig. V.7. shows the convergence of the approximate solutions at early, intermediate and late times, eq. IV.69, eq. IV.84 and eq. IV.105, respectively to the general solution, assuming no interporous skin. This semilog plot shows the typical behavior of a double porosity radial system, i.e., straight lines at early and late times and another straight line during intermediate times. However, the input values show that a flow geometry that tends to be spherical ($D_{fb} = 2.5$), with non-well connected flowing traces ($\theta = 0.5$) is equivalent to a radial flow, well-connected behavior. This type of behavior has been named *apparent radial flow*.

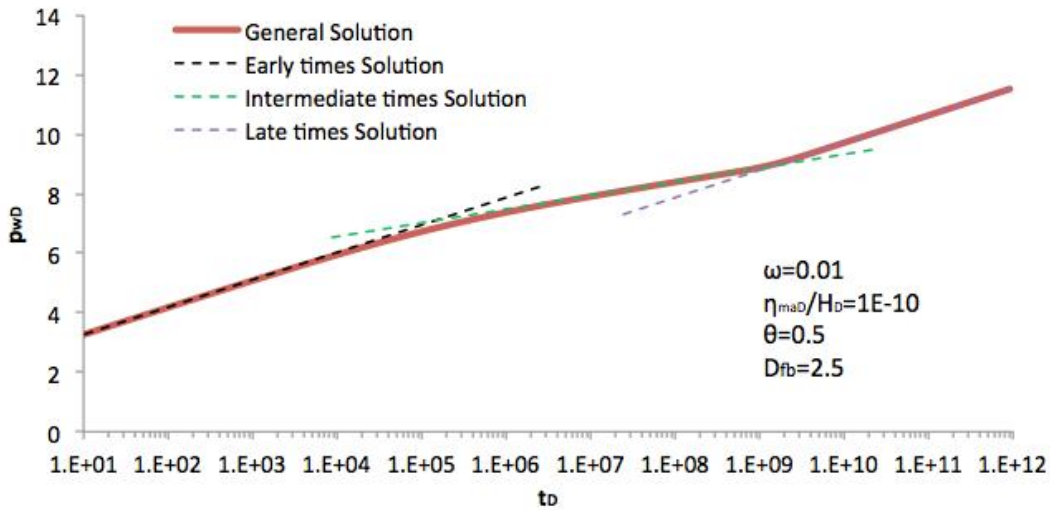


Fig. V.7. Convergence from the short, intermediate and long times solutions to the general solution, when $D_{fb} = \theta + 2$, with no interporous skin.

Analogously, **Fig. V.8.** shows the convergence of the approximate solutions at early, intermediate and late times, eq. IV.75, eq. IV.89 and eq. IV.106, respectively to the general solution, assuming no interporous skin, when $D_{fb} \neq \theta + 2$. For this case, all approximated solutions converge to the log-log straight line portions, corresponding to the fracture expansion, interaction between media and single system behavior.

Fig. V.8. exhibits the case shown in **Fig. V.6** but this time with a relative low interporous skin value. Except from the beginning of the approximated solution during intermediate times, it shows the same trend of the straight line portion of the general solution, and therefore this approximation might be useful to characterize the interporous skin and the matrix, if the non-linear regression is possible to be performed.

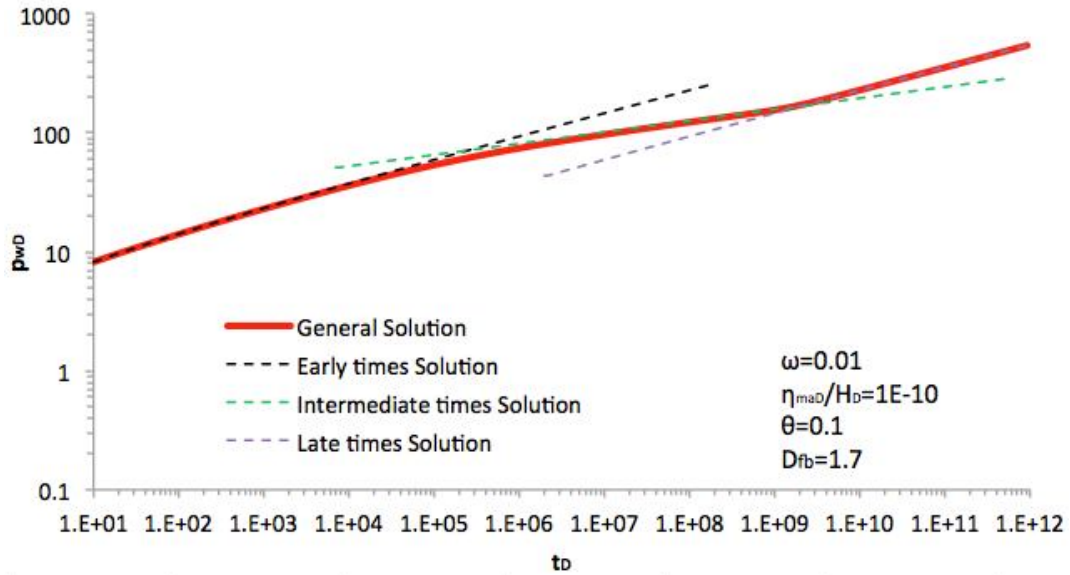


Fig. V.8. Convergence from the short, intermediate and long times solutions to the general solution, when $D_{fb} \neq \theta + 2$, with no interporous skin.

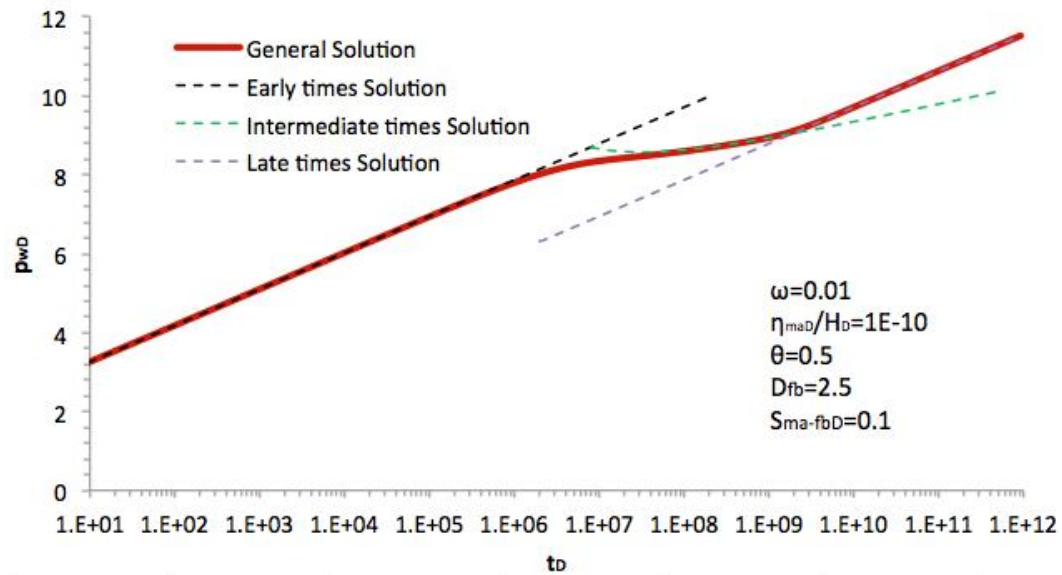


Fig. V.9. Convergence from the short, intermediate and long times solutions to the general solution, when $D_{fb} = \theta + 2$, with low interporous skin.

Fig. V.10. shows the case shown in Fig. V.8 with a relative low interporous skin value. For this case the convergence of the approximated solution during intermediate times to the general solution is observed.

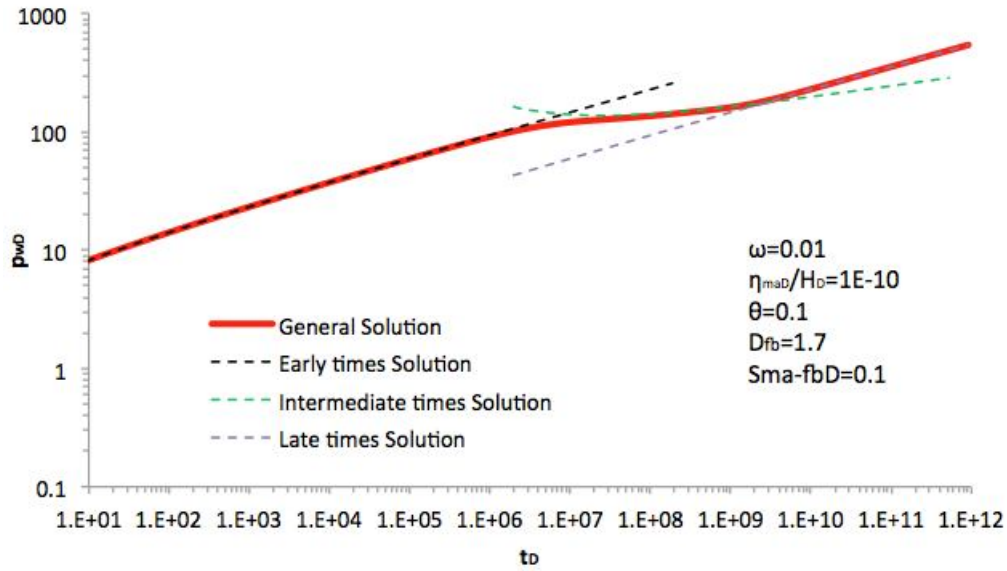


Fig. V.10. Convergence from the short, intermediate and long times solutions to the general solution, when $D_{fb} \neq \theta + 2$, with low interporous skin.

Fig. V.11. and **Fig. V.12.** show the convergence of the approximated solutions for severe interporous skin, i.e., pseudosteady state behavior to the general solution, for $D_{fb} = \theta + 2$ and $D_{fb} \neq \theta + 2$, respectively. The intermediate times behavior shows a flat slope and according to the equivalence given by eq. IV.94, the matrix-fracture interaction parameter, for both cases is $\lambda = 2 \times 10^{-11}$.

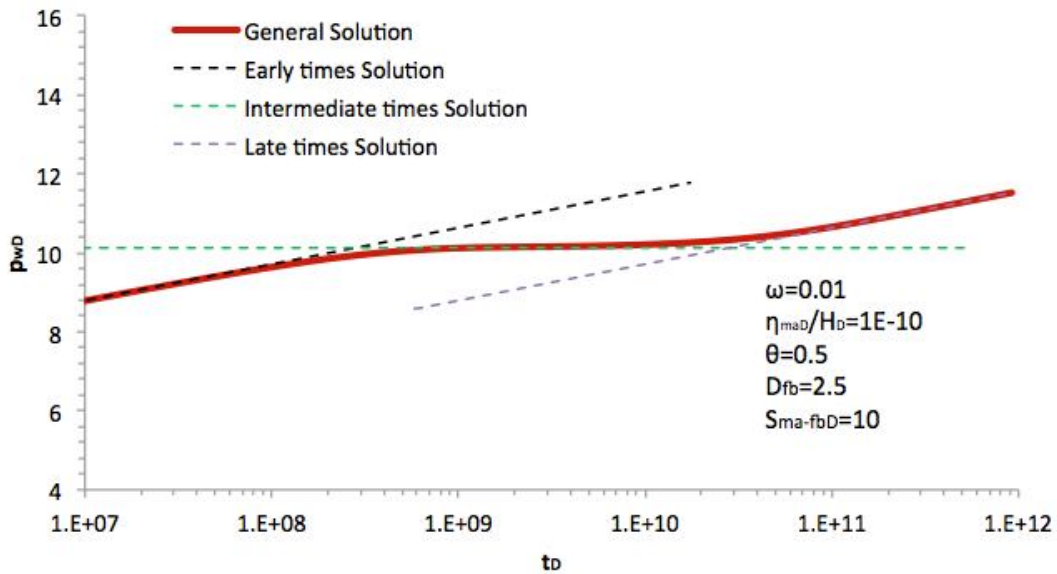


Fig. V.11. Convergence from the short, intermediate and long times solutions to the general solution, when $D_{fb} = \theta + 2$, with severe interporous skin (pseudosteady-state).

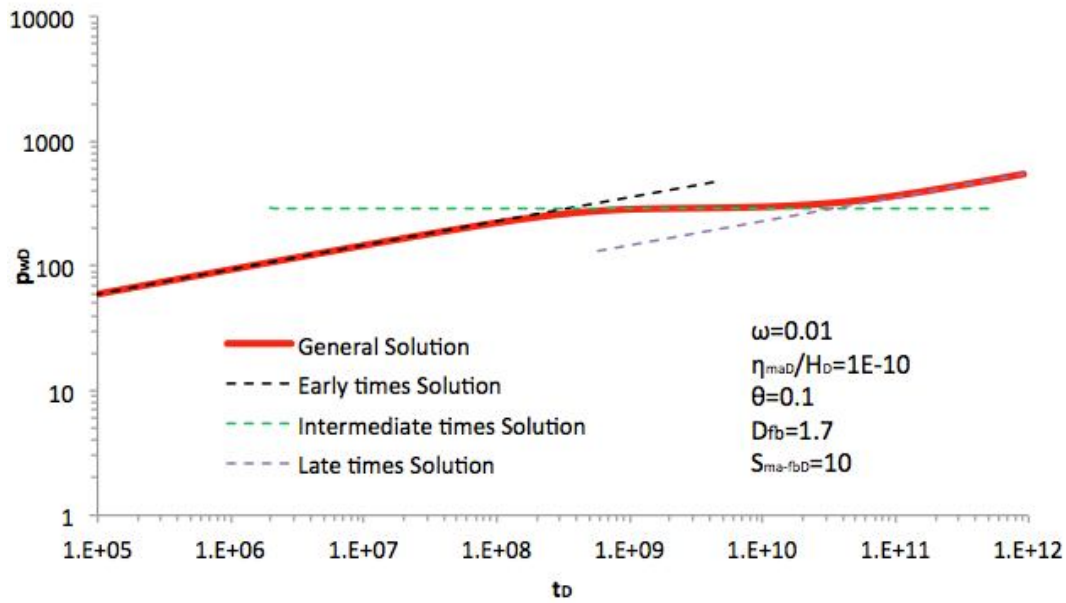


Fig. V.12. Convergence from the short, intermediate and long times solutions to the general solution, when $D_{fb} \neq \theta + 2$, with severe interporous skin (pseudosteady-state).

Example of Application

A drawdown test was performed in Well A. The behavior of pressure and pressure derivative function are shown in **Fig. V.13**. Reservoir and well data are given in **Table V.1**.

Table V.1. Reservoir and well data for the example.

Parameter	Quantity
q [bpd]	2,000
B_o [bbl@c.y/ bbl@c.s]	1.6
μ_o [cp]	6
r_w [ft]	0.5
ϕ_{fb} [fraction]	0.01

Pressure derivative function in **Fig. V.13** does not show the fractal fracture expansion, i.e., behavior at early times. Then, analyzing late time response (see **Fig. V.14**) and comparing such behavior with eq. IV. 106, it can be conclude that, $\nu \approx 0.8362$, hence, following relation between fractal parameters was deduced: $D_{fb} = 0.8362\theta + 1.6724$. Then, the methodology described by Flamenco et al. (2003)

was applied and resulting parameters are: $\theta_{\min} = 0$, $\theta_{\max} \approx 1.588$,
 $\left((\phi c_t)_i^{v-1} / a V_{uf} k_{fb}^v \right)_{\min} \approx 0.000127$ and $\left((\phi c_t)_i^{v-1} / a V_{uf} k_{fb}^v \right)_{\max} \approx 0.451$.

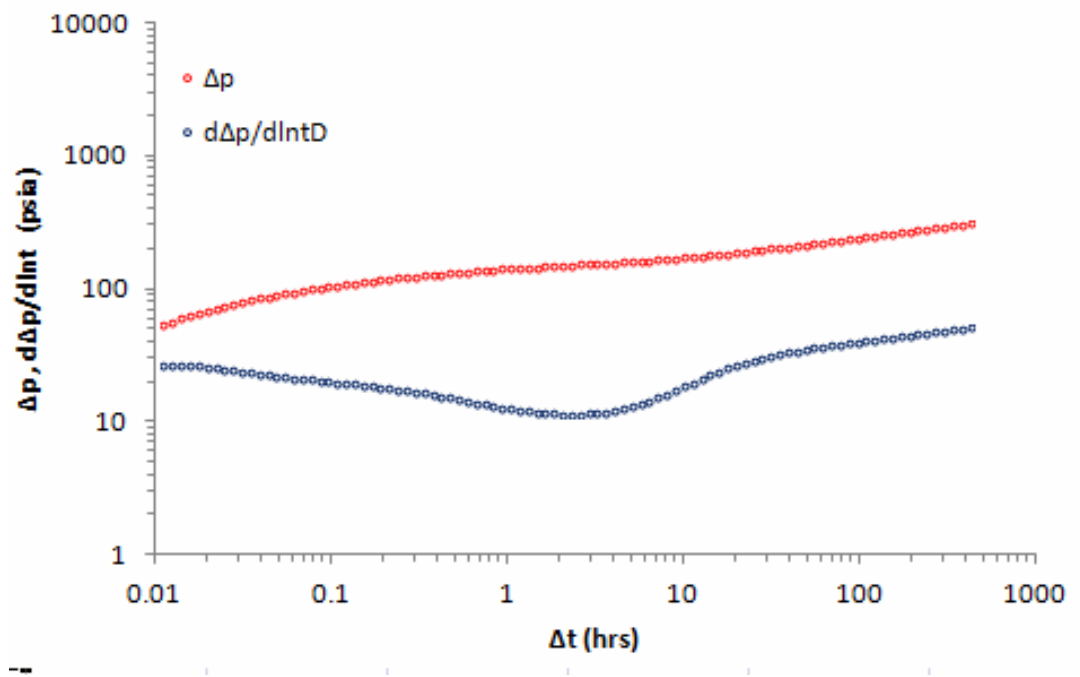


Fig. V.13. Pressure and pressure derivative function behavior for synthetic example.

Intermediate times can be analyzed plotting $t^{v/2} \Delta p(t)$ vs \sqrt{t} , and comparing it with the straight line given by eq. IV.89. Fig. IV.14 shows the $t^{v/2} \Delta p(t)$ vs \sqrt{t} plot for this example.

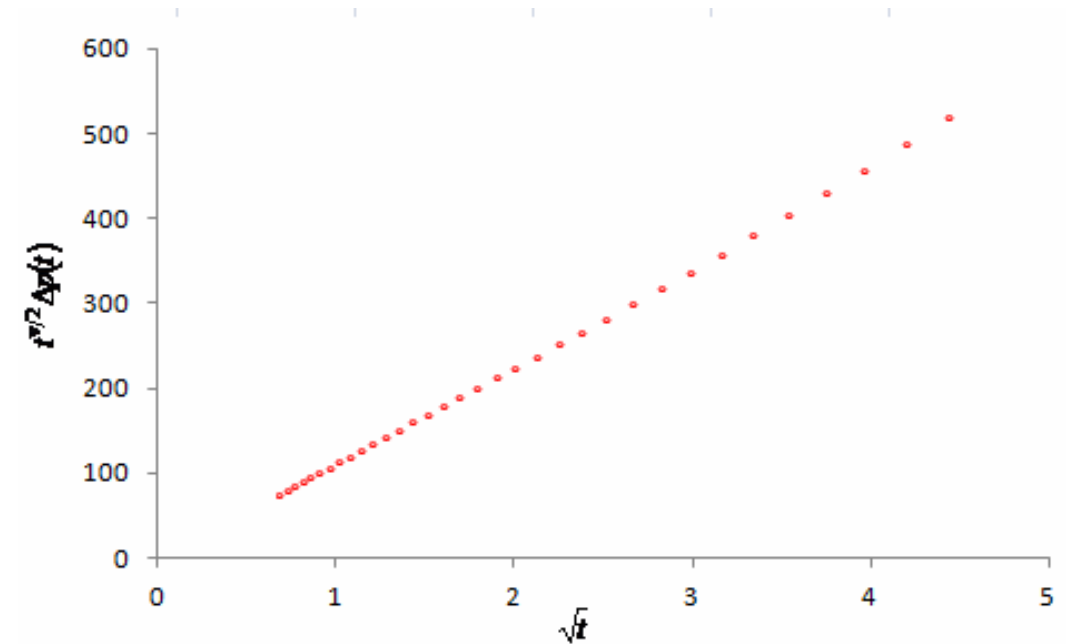


Fig. V.14. Log-log plot of the late time pressure behavior for synthetic example.

Fig. V.15. shows the adjusting $t^{v/2}\Delta p(t)$ vs \sqrt{t} straight-line plot for this example. Comparing straight line equation that fits the data with the eq. IV.89, it can be concluded that the transference between porous media is not free, i.e., exists an interporous skin between matrix and fractures. On the other hand, since intermediate times in **Fig. V.13** does not show a flat behavior, it can be concluded that the interporous transference is occurring under transient regime.

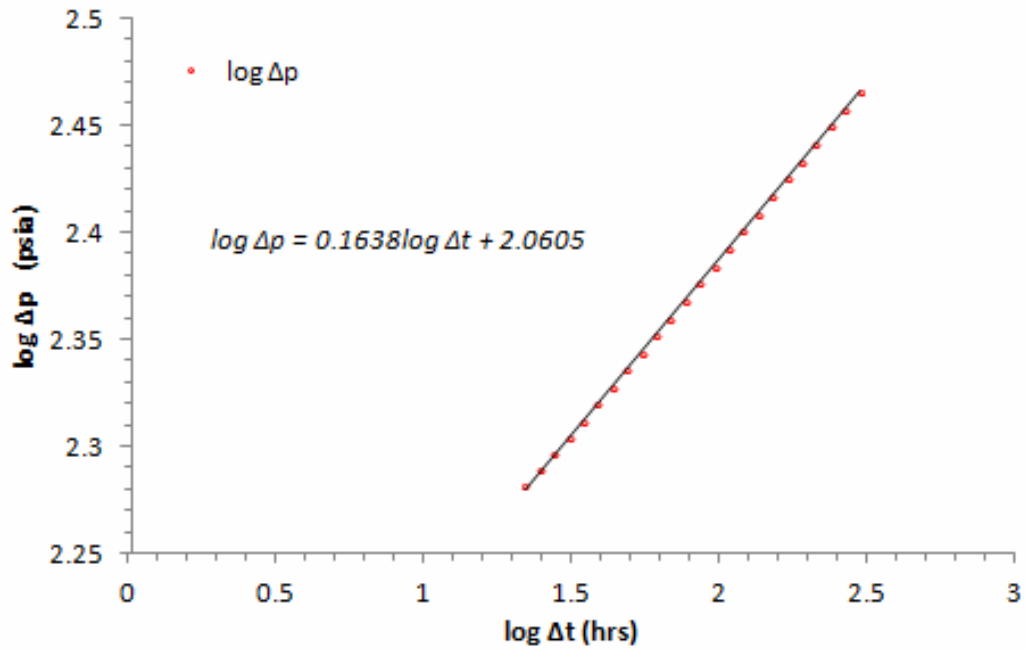


Fig. V.15. Specialized plot for intermediate times of the pressure behavior for synthetic example.

Chapter VI

Conclusions

1. A fractal flow model that describes transient interporous behavior in double porosity systems was developed. With this model it is possible to consider spheres or slabs as matrix blocks.
2. A general solution in Laplace space that describes the complete transient response of the fractal reservoirs, i.e. total expansion in fracture network, interaction between porous media and single system behavior, was developed.
3. Approximated analytical solutions in real space to describe pressure behavior during early, intermediate and late times were derived.
4. Solutions during intermediate times are used to characterize parameters useful for reservoir engineering studies; such as matrix block, fractal fracture network area per unit of bulk volume and interporous skin.
5. Main advantage of using fractal models is that these are the best suited to represent randomness in the fracture network distribution within the reservoir.
6. Advantages of using transient interporous transference models with interporous skin were discussed.

This page is intentionally left in blank.

References

- Acuña, J.A., Ershaghi, I. and Yortsos, Y.C., (1995), "Practical Application of Fractal Pressure-Transient Analysis in Naturally Fractured Reservoirs," *SPEFE 10 (3): 173-179*; Trans AIME, 299. SPE-24705-PA.
- Barenblatt, G.I., Zheltov, Iu, P. and Kochina, I.N., (1960), "Basic Concepts in the Theory of Seepage of Homogeneous Liquids in Fissured Rocks (strata)," *PMM* Vol. 24, No. 5, 852-864, in Russian.
- Barenblatt, G.I., Zheltov, Yu, P., (1960), "Fundamental equations of Filtration of Homogeneous Liquids in Fissured Rocks," *Soviet Physics Doklady* Vol. 5, 522-525.
- Barker, J.A.: "A Generalized Radial-Flow Model for Pumping Tests in Fractured Rock," *Water Resources Research*, 24, 1796-1804, 1988.
- Black, J.H. and K.L. Kipp: "Determination of hydrogeological parameters using sinusoidal test: A theoretical appraisal," *Water Resources Research*, 17(3), 686-692, 1981.
- Camacho-Velazquez, R., Fuentes-Cruz, G., and Vasquez-Cruz, M., (2008), "Decline-Curve Analysis of Fractured Reservoirs with Fractal Geometry." *SPE Res Eval & Eng* 11 (3): 606-619. SPE-104009-PA.
- Chang, J. and Y. Yortsos: "Pressure Transient Analysis of Fractal Reservoirs," *SPE Formation Evaluation*, (5) 31-38, 1990.
- Chang, J. and Y. Yortsos (1992), "A Note On Pressure-Transient Analysis Of Fractal Reservoirs," *paper SPE 25296, SPE Advanced Technology Series*, Vol. 1, No. 2, 170 – 171.
- Chatas, A.T.: "Unsteady spherical flow in petroleum reservoirs", *SPEJ* (6) 102-114, 1966.
- Cinco-Ley, H., Economides, M.J., Miller, F.G. (1979), "A parallelepiped Model to Analyze the Pressure Behavior of Geothermal Steam Wells Penetrating Vertical Fractures," *paper SPE 8231* presented at the SPE 54th Annual Technical Conference and Exhibition, Las Vegas, Sept. 23-26.

-
- Cinco-Ley, H., Samaniego V., F. (1982), "Pressure Transient Analysis for Naturally Fractured Reservoirs," *paper SPE 11026* presented at the SPE 57th Annual Fall Technical Conference and Exhibition, New Orleans, LA, Sept. 26-29.
- Cinco-Ley, H., Samaniego V., F., Kucuk, F., (1985), "The Pressure Transient Behavior for Naturally Fractured Reservoirs with Multiple Block Size," *paper SPE 14168* presented at the SPE 60th Annual Fall Technical Conference and Exhibition, Las Vegas, NV, Sept. 22-25.
- Cossio, M. (2012), "A Semi-Analytic Solution for Flow in Finite-Conductivity Vertical Fractures Using Fractal Theory," *paper SPE 163057-STU* presented at the SPE Annual Technical Conference and Exhibition, San Antonio, Texas, Oct. 8-10.
- De Swaan, O.A., (1976), "Analytic Solutions for Determining Naturally Fractured Reservoir Properties by Well Testing," *SPEJ Trans. AIME 261*, 117-122, June.
- Doe, T.W.: "Fractional Dimension Analysis of Constant-Pressure Well Tests", paper 22702 presented at the 66th Annual Technical Conference and Exhibition of the Society of Petroleum Engineers held in Dallas, TX, October 6-9, 1991.
- Flamenco-López, F., Camacho-Velázquez, R. (2003), "Determination of Fractal Parameters of Fracture Networks Using Pressure Transient Data," *paper SPE 82607, SPE Reservoir Evaluation & Engineering*, February.
- Gringarten, A.C., Bourdet, D.P., Landel., P.A., Kniazeff, V.J. (1979), "A Comparison Between Different Skin and Wellbore Storage Type-Curves for Early-Time Transient Analysis," *paper SPE 8205* presented at the SPE 54th Annual Technical Conference and Exhibition, Las Vegas, Sept. 23-26.
- Gringarten, A.C., (1987), "How To Recognize "Double Porosity" Systems from Well Tests," *paper SPE 16437, JPT*, June.
- Larsen, L., (2013) Private communication.
- Miller, F.G.: "Theory of Unsteady State Influx of Water in linear Reservoirs," *J. Inst. Pet.* **48**, 467, 1962.
- Moench, A.F. (1984), "Double-Porosity Models for a Fissured Groundwater Reservoir with Fracture Skin," *Water Resources Research*, Vol. 20, No. 7, 831-846.
- Najurieta, H.L., (1980), "A Theory for Pressure Transient Analysis in Naturally Fractured Reservoirs," *JPT 1241-1250*, July.

-
- Pulido, H., Samaniego, F., Rivera, J., Díaz, F., Galicia-Muñoz, G., (2006), “Well Test Analysis for Naturally Fractured Reservoirs with Transient Interporosity Matrix, Microfractures and Fractures Flow,” *Proceedings Thirty-first Workshop on Geothermal Reservoir Engineering* Stanford University, Stanford, California, January 22 – 24.
- Pulido, H., Samaniego, F., Galicia-Muñoz, G., Rivera, J., Velez, C. (2007), “Petrophysical Characterization of Carbonate Naturally Fractured Reservoirs for use in dual porosity simulators,” *Proceedings Thirty-Second Workshop on Geothermal Reservoir Engineering* Stanford University, Stanford, California, January 22 – 24.
- Pulido, H., Galicia-Muñoz, G., Valdes-Perez. A.R., Díaz-García F. (2011), “Improve Reserves Estimation using Interporosity Skin in Naturally Fractured Reservoirs ,” *Proceedings Thirty-Sixth Workshop on Geothermal Reservoir Engineering* Stanford University, Stanford, California, January 31 – February 2.
- Serra, K. V., Reynolds, A.C. and Raghavan, R., (1982), “New Pressure Transient Analysis Methods for Naturally Fractured Reservoirs,” *paper SPE 10780* presented at the SPE 1982 California Regional Meeting, San Francisco, California, March 24-26.
- Stehfest, H.: “Numerical inversion of Laplace transforms,” *Commun. ACM*, 13(1), 47-49, 1970.
- Streltsova, T.D., (1982), “Well Pressure Behavior of a Naturally Fractured Reservoirs,” *paper SPE 10782* presented at the SPE 1982 California Regional Meeting, San Francisco, California, March 24-26.
- Valdes-Perez. A.R., Pulido, H., Cinco-Ley., H., Galicia-Muñoz, G. (2011), “A New Bilinear Flow Model For Naturally Fractured Reservoirs with Transient Interporosity Transfer,” *Proceedings Thirty-Sixth Workshop on Geothermal Reservoir Engineering* Stanford University, Stanford, California, January 31 – February 2.
- Valdes-Perez. A.R., Pulido, H., Cinco-Ley., H., Galicia-Muñoz, G. (2012), “Discretization of the Resistivity, Capillary Pressure and Relative Permeability for Naturally Fractured Reservoirs,” *Proceedings Thirty-Seventh Workshop on*

Geothermal Reservoir Engineering Stanford University, Stanford, California,
January 30 – February 1.

Valdes-Perez. A.R., Pulido, H., Cinco-Ley., H., Larsen, L. (2013), “A New Double Porosity Fractal Model for Well Test Analysis with Transient Interporosity Transference for Petroleum and Geothermal Systems,” *Proceedings Thirty-Eighth Workshop on Geothermal Reservoir Engineering at Stanford University, Stanford, California, February 11-13.*

van Everdingen, A.F. and Hurst, W.: “Application of the Laplace Transformation to flow problems in Reservoirs,” *Trans. AIME*, **186**, 305-324B, 1949.

Warren, J.E. and Root, P.J., (1963), “The Behavior of Naturally Fractured Reservoirs,” *SPEJ Trans AIME, Vol. 228*, 245-255, September.

Appendix A

Generalized Radial Flow Model

A.1. Flow model development

Incoming oil mass into an object is given by:

$$m_{in} = \rho_o \bar{v} A \Delta t, \quad \text{A.1}$$

out coming oil mass from the same object is:

$$m_{out} = \rho_o \bar{v} A \Delta t + \Delta(\rho_o \bar{v} A) \Delta t, \quad \text{A.2}$$

then, cumulative oil mass into the object is:

$$m_{cum} = m_{out} - m_{in} = \Delta(\rho_o \bar{v} A) \Delta t. \quad \text{A.3}$$

On the other hand, mass of oil at a time t_1 is given by:

$$m_{t_1} = S_o \rho_o \phi V_{bulk}, \quad \text{A.4}$$

at a time t_2 :

$$m_{t_2} = S_o \rho_o \phi V_{bulk} + \Delta(S_o \rho_o \phi) V_{bulk}, \quad \text{A.5}$$

and, cumulative oil mass is given by:

$$m_{cum} = m_{t_2} - m_{t_1} = \Delta(S_o \rho_o \phi) V_{bulk}. \quad \text{A.6}$$

Equating eq. A.3 and A.6 results:

$$\Delta(\rho_o \bar{v} A) \Delta t = \Delta(S_o \rho_o \phi) V_{bulk}. \quad \text{A.7}$$

According to using definitions given in eq. I.4 and eq. I.6, and after mathematical manipulation eq. A.7 results:

$$\frac{1}{r^{d_e-1}} \frac{\partial(r^{d_e-1} \rho_o \bar{v})}{\partial r} = \frac{\partial(S_o \rho_o \phi)}{\partial t}. \quad \text{A.8}$$

Applying derivatives in both sides of eq. A.8:

$$\frac{1}{r^{d_e-1}} \left[r^{d_e-1} \rho_o \frac{\partial(\bar{v})}{\partial r} + \rho_o \bar{v} [d_e - 1] r^{d_e-2} + r^{d_e-1} \bar{v} \frac{\partial(\rho_o)}{\partial r} \right] = S_o \rho_o \frac{\partial(\phi)}{\partial t} + \phi \frac{\partial(S_o \rho_o)}{\partial t}. \quad \text{A.9}$$

Darcy's law states:

$$\bar{v} = \frac{k}{\mu} \frac{\partial p(r, t)}{\partial r}. \quad \text{A.10}$$

Substituting Darcy's law into eq. A.9 it results:

$$\begin{aligned} & \frac{1}{r^{d_e-1}} \frac{k\rho_o}{\mu} \left[r^{d_e-1} \frac{\partial}{\partial r} \left(\frac{\partial p(r,t)}{\partial r} \right) + r^{d_e-2} [d_e - 1] \frac{\partial p(r,t)}{\partial r} + \frac{r^{d_e-1}}{\rho_o} \left[\frac{\partial p(r,t)}{\partial r} \right] \frac{\partial(\rho_o)}{\partial r} \right] = \\ & = S_o \rho_o \phi \left[\frac{1}{\phi} \frac{\partial(\phi)}{\partial t} + \frac{1}{S_o \rho_o} \frac{\partial(S_o \rho_o)}{\partial t} \right] \end{aligned} \quad \text{A.11}$$

Using chain rule derivative of oil density regarding the radius can be written as:

$$\frac{\partial(\rho_o)}{\partial r} = \frac{\partial \rho_o}{\partial p(r,t)} \frac{\partial p(r,t)}{\partial r}, \quad \text{A.12}$$

Analogously with the porosity:

$$\frac{\partial \phi}{\partial t} = \frac{\partial \phi}{\partial p(r,t)} \frac{\partial p(r,t)}{\partial t}, \quad \text{A.13}$$

And:

$$\frac{\partial(S_o \rho_o)}{\partial t} = \frac{\partial(S_o \rho_o)}{\partial p} \frac{\partial p}{\partial t}. \quad \text{A.14}$$

Substituting eqs. from A.12 to A.14 and the definitions of compressibility of oil and compressibility of the formations, into eq. A.11 it results

$$\begin{aligned} & \frac{1}{r^{d_e-1}} \frac{k}{\mu} \left[r^{d_e-1} \frac{\partial}{\partial r} \left(\frac{\partial p(r,t)}{\partial r} \right) + r^{d_e-2} [d_e - 1] \frac{\partial p(r,t)}{\partial r} + r^{d_e-1} c_o \left(\frac{\partial p(r,t)}{\partial r} \right)^2 \right] = \\ & = S_o \phi [c_f + c_o] \frac{\partial p(r,t)}{\partial t} \end{aligned} \quad \text{A.15}$$

According to the definition of total compressibility of the formation for a single fluid (oil), eq. A.15, the diffusivity equation of a Generalized Radial Model results:

$$\frac{\partial^2 p(r,t)}{\partial r^2} + \frac{[d_e - 1]}{r} \frac{\partial p(r,t)}{\partial r} + c_o \left(\frac{\partial p(r,t)}{\partial r} \right)^2 = \frac{\phi \mu c_{if}}{k} \frac{\partial p(r,t)}{\partial t}. \quad \text{A.16}$$

Neglecting the quadratic pressure gradient term the following model is given:

$$\frac{\partial^2 p(r,t)}{\partial r^2} + \frac{[d_e - 1]}{r} \frac{\partial p(r,t)}{\partial r} = \frac{\phi \mu c_{if}}{k} \frac{\partial p(r,t)}{\partial t}. \quad \text{A.17}$$

Compact form of previous equation is:

$$\frac{1}{r^{d_e-1}} \frac{\partial}{\partial r} \left(r^{d_e-1} \frac{\partial p(r,t)}{\partial r} \right) = \frac{\phi \mu c_{if}}{k} \frac{\partial p(r,t)}{\partial t}. \quad \text{A.18}$$

A.2 Transformation to dimensionless variables for well test analysis

Following dimensionless variables has been state. Dimensionless radius:

$$r_D = \frac{r}{r_w}, \quad \text{A.19}$$

dimensionless time:

$$t_D = \frac{k}{\phi\mu c_i r_w^2} t, \quad \text{A.20}$$

dimensionless pressure:

$$p_D(r_D, t_D) = \frac{Ak[p_i - p(r, t)]}{qB_o\mu r_w^{2-d_e}}. \quad \text{A.21}$$

Using chain rule, first derivative of pressure regarding the distance can be written as follows:

$$\frac{\partial p(r, t)}{\partial r} = \frac{\partial p(r, t)}{p_D(r_D, t_D)} \frac{dr_D}{dr} \frac{\partial p_D(r_D, t_D)}{\partial r_D}. \quad \text{A.22}$$

The first derivative of pressure regarding dimensionless pressure is:

$$\frac{\partial p(r, t)}{\partial p_D(r_D, t_D)} = -\frac{qB_o\mu r_w^{2-d_e}}{Ak}. \quad \text{A.23}$$

On the other hand, derivative of dimensionless radius regarding radius is:

$$\frac{dr_D}{dr} = \frac{1}{r_w}, \quad \text{A.24}$$

hence:

$$\frac{\partial p(r, t)}{\partial r} = -\frac{qB_o\mu r_w^{1-d_e}}{Ak} \frac{\partial p_D(r_D, t_D)}{\partial r_D}. \quad \text{A.25}$$

Taking second derivative regarding radius of eq. A.25:

$$\frac{\partial^2 p(r, t)}{\partial r^2} = -\frac{qB_o\mu r_w^{-d_e}}{Ak} \frac{\partial^2 p_D(r_D, t_D)}{\partial r_D^2}. \quad \text{A.26}$$

Analogously, first derivative of pressure regarding time can be expressed, which is given by:

$$\frac{\partial p(r, t)}{\partial t} = -\frac{qB_o\mu r_w^{2-d_e}}{Ak} \frac{k}{\phi\mu c_i r_w^2} \frac{\partial p_D(r_D, t_D)}{\partial t_D}. \quad \text{A.27}$$

Substituting eq. A.19, A.25, A.26 and A.27 into eq. A.17 results:

$$\frac{\partial^2 p_D(r_D, t_D)}{\partial r_D^2} + \frac{d_e - 1}{r_D} \frac{\partial p_D(r_D, t_D)}{\partial r_D} = \frac{\partial p_D(r_D, t_D)}{\partial t_D}. \quad \text{A.28}$$

It can be verified that, when $d_e = 1$ GRF, eq. A.28, it takes the form of the linear flow model; when $d_e = 2$ it converges to the radial flow model and to the spherical flow model when $d_e = 3$.

A.3. General solution in Laplace space assuming constant rate

In order to have a well test analysis model for the Generalized Radial Flow Model, eq. A.28, the following conditions have been set:

$$\text{initial condition:} \quad p_D(r_D, t_D = 0) = 0, \quad \text{A.29}$$

$$\text{inner Boundary:} \quad \frac{\partial p_D(1, t_D)}{\partial t_D} = -1, \quad \text{A.30}$$

$$\text{outer boundary:} \quad \lim_{r_D \rightarrow \infty} (p_D(r_D, t_D)) = 0. \quad \text{A.31}$$

Applying Laplace transform to eq. A.28 and according to initial condition, it results:

$$\frac{d^2 \bar{p}_D(r_D, s)}{dr_D^2} + \frac{d_e - 1}{r_D} \frac{d\bar{p}_D(r_D, s)}{dr_D} - s\bar{p}_D(r_D, s) = 0. \quad \text{A.32}$$

The following transform function has been set:

$$\bar{p}_D(r_D, s) = \bar{G}_D(z), \quad \text{A.33}$$

and the transformation variables:

$$z = r_D \sqrt{s}. \quad \text{A.34}$$

Hence:

$$\frac{dz}{dr_D} = \sqrt{s}. \quad \text{A.35}$$

Moreover, parameter ν is established:

$$\nu = 1 - \frac{d_e}{2}. \quad \text{A.36}$$

$$2 - 2\nu = d_e. \quad \text{A.37}$$

Applying the variable transformations, the following expression is obtained:

$$z^2 \frac{\partial^2 \bar{G}_D(z)}{\partial z^2} + [1 - 2\nu]z \frac{\partial \bar{G}_D(z)}{\partial z} - z^2 \bar{G}_D(z) = 0. \quad \text{A.38}$$

Moreover, to equalize the coefficient of the first derivative to one the following expression is proposed:

$$\bar{G}_D(z) = z^\nu B_D(z). \quad \text{A.39}$$

then, eq. 31 in terms of eq. 39 is:

$$z^2 \frac{d^2 B_D(z)}{dz^2} + z \frac{dB_D(z)}{dz} - [v^2 + z^2] B_D(z) = 0. \quad \text{A.40}$$

Its solution is given by:

$$B_D(z) = c_1 I_v(z) + c_2 K_v(z), \quad \text{A.41}$$

Or, in terms of eq. A.39:

$$\bar{G}_D(z) = c_1 z^v I_v(z) + c_2 z^v K_v(z), \quad \text{A.42}$$

therefore previous eq. can be expressed in terms of $\bar{p}_D(r_D, s)$ and $r_D \sqrt{s}$:

$$\bar{p}_D(r_D, s) = c_1 (r_D \sqrt{s})^v I_v(r_D \sqrt{s}) + c_2 (r_D \sqrt{s})^v K_v(r_D \sqrt{s}). \quad \text{A.43}$$

Applying outer boundary condition, a bounded solution is obtained:

$$\bar{p}_D(r_D, s) = c_2 (r_D \sqrt{s})^v K_v(r_D \sqrt{s}). \quad \text{A.44}$$

and, applying the inner boundary condition, a particular solution is obtained:

$$\bar{p}_D(r_D, s) = \frac{r_D^v K_v(r_D \sqrt{s})}{s^{3/2} K_{v-1}(\sqrt{s})}. \quad \text{A.45}$$

According to:

$$v = 1 - \frac{d_e}{2}, \quad \text{A.46}$$

then:

$$\bar{p}_D(r_D, s) = \frac{r_D^{2-d_e} K_{2-d_e}(r_D \sqrt{s})}{s^{3/2} K_{\frac{d_e}{2}}(\sqrt{s})}. \quad \text{A.47}$$

A.4. Solution in real space using similarity transform

Establishing the following transformation function:

$$Z_{3D} = (d_e)^{2-\frac{2}{d_e}} p_D(r_D, t_D), \quad \text{A.48}$$

or:

$$p_D(r_D, t_D) = (d_e)^{\frac{2}{d_e}-2} Z_{2D}. \quad \text{A.49}$$

Besides:

$$\tau_3 = \frac{1}{d_e} r_D^{d_e}, \quad \text{A.50}$$

and:

$$\kappa_3 = d_e^{2-\frac{2}{d_e}} t_D. \tag{A.51}$$

Applying an analogous procedure as the one showed in Chapter IV, the following approximation in real space was obtained:

$$p_D(r_D, t_D) = -\frac{r_D^{2-d_e}}{2\Gamma\left(\frac{d_e}{2}\right)} \Gamma\left(\frac{d_e}{2}-1, \frac{r_D^2}{4t_D}\right). \tag{A.52}$$

Appendix B

Pressure Transient Analysis of Fractal Reservoirs assuming Pseudo-Steady State Interporosity Transfer

In this appendix, the development of the Fractal Reservoir Model proposed by Chang et al., (1990) is demonstrated. For this demonstration is very important to keep in mind the definition of the *Geometry Factor* given by eq. I.20.

B.1. Model development

Incoming oil mass into an object is given by:

$$m_{in} = \rho_o q_o \Delta t, \quad \text{B.1}$$

out coming oil mass from the same object is:

$$m_{out} = \rho_o q_o \Delta t + \Delta(\rho_o q_o) \Delta t, \quad \text{B.2}$$

oil mass contribution from the Euclidean matrix:

$$m_{ma} = \rho_o \bar{q}_{ma} \Delta t, \quad \text{B.3}$$

then, cumulative oil mass into the object is:

$$m_{cum} = m_{out} - m_{in} + \rho_o \bar{q}_{ma} \Delta t = \Delta(\rho_o q_o) \Delta t + \rho_o \bar{q}_{ma} \Delta t. \quad \text{B.4}$$

On the other hand, mass of oil at a time t_1 is given by:

$$m_{t_1} = S_o \rho_o \phi_{fb} V_{bulk}, \quad \text{B.5}$$

at a time t_2 :

$$m_{t_2} = S_o \rho_o \phi_{fb} V_{bulk} + \Delta(S_o \rho_o \phi_{fb}) V_{bulk}, \quad \text{B.6}$$

and, cumulative oil mass is given by:

$$m_{cum} = m_{t_2} - m_{t_1} = \Delta(S_o \rho_o \phi_{fb}) V_{bulk}. \quad \text{B.7}$$

Equating eq. B.4 and B.7 results:

$$\Delta(\rho_o q_o) \Delta t + \rho_o \bar{q}_{ma} \Delta t = \Delta(S_o \rho_o \phi_{fb}) V_{bulk}. \quad \text{B.8}$$

According to the definition of bulk volume, eq. B.8 becomes:

$$\Delta(\rho_o q_o) \Delta t + \rho_o \bar{q}_{ma} \Delta t = \Delta(S_o \rho_o \phi_{fb}) \left[\alpha_{d_e} r^{d_e-1} b^{3-d_e} \Delta r \right], \quad \text{B.9}$$

arraying previous equation:

$$\frac{1}{\alpha_{d_e} r^{d_e-1} b^{3-d_e}} \frac{\Delta(\rho_o q_o)}{\Delta r} + \frac{\rho_o \bar{q}_{ma}}{V_{bulk}} = \frac{\Delta(S_o \rho_o \phi_{fb})}{\Delta t}. \quad \text{B.10}$$

Matrix flow rate per unit of bulk is defined:

$$q_{ma}^* = \frac{\bar{q}_{ma}}{V_{bulk}}. \quad \text{B.11}$$

Taking the limits Δr and Δt to zero, and arraying eq. B.10 becomes:

$$\frac{\partial(\rho_o q_o)}{\partial r} + \alpha_{d_e} r^{d_e-1} b^{3-d_e} \rho_o q_{ma}^* = \alpha_{d_e} r^{d_e-1} b^{3-d_e} \frac{\partial(S_o \rho_o \phi_{fb})}{\partial t}. \quad \text{B.12}$$

Inserting Darcy's equation in fractal form into previous equation, it results:

$$\frac{\partial}{\partial r} \left(\rho_o \frac{a V_{uf} k_{fb} r^\beta}{\phi_{fb} \mu} \frac{\partial p_{fb}}{\partial r} \right) + \alpha_{d_e} r^{d_e-1} b^{3-d_e} \rho_o q_{ma}^* = \alpha_{d_e} r^{d_e-1} b^{3-d_e} \frac{\partial(S_o \rho_o \phi_{fb})}{\partial t}. \quad \text{B.13}$$

Besides, matrix flow rate due to expansion effects is given by:

$$q_{ma} = \phi_{ma} c_{ima} V_{bulk} \frac{\partial p_{ma}}{\partial t}, \quad \text{B.14}$$

hence, matrix flow rate per unit of bulk is:

$$q_{ma}^* = \frac{q_{ma}}{V_{bulk}} = \phi_{ma} c_{ima} \frac{\partial p_{ma}}{\partial t}. \quad \text{B.15}$$

Based on matrix flow rate per unit of bulk, eq. B.13 is rewritten as:

$$\frac{\partial}{\partial r} \left(\rho_o \frac{a V_{uf} k_{fb} r^\beta}{\phi_{fb} \mu} \frac{\partial p_{fb}}{\partial r} \right) + \alpha_{d_e} r^{d_e-1} b^{3-d_e} \rho_o \phi_{ma} c_{ima} \frac{\partial p_{ma}}{\partial t} = \alpha_{d_e} r^{d_e-1} b^{3-d_e} \frac{\partial(S_o \rho_o \phi_{fb})}{\partial t}, \quad \text{B.16}$$

applying the derivatives in eq. B.16:

$$\begin{aligned} & \frac{a V_{uf} k_{fb}}{\phi_{fb} \mu} \left[\rho_o r^\beta \frac{\partial^2 p_{fb}}{\partial r^2} + \frac{\beta \rho_o r^\beta}{r} \frac{\partial p_{fb}}{\partial r} + r^\beta \frac{\partial p_{fb}}{\partial r} \frac{\partial \rho_o}{\partial r} \right] + \\ & + \alpha_{d_e} r^{d_e-1} b^{3-d_e} \rho_o \phi_{ma} c_{ima} \frac{\partial p_{ma}}{\partial t} = \alpha_{d_e} r^{d_e-1} b^{3-d_e} \left[\phi_{fb} \frac{\partial(S_o \rho_o)}{\partial t} + S_o \rho_o \frac{\partial(\phi_{fb})}{\partial t} \right]. \end{aligned} \quad \text{B.17}$$

According to chain rule:

$$\frac{\partial \rho_o}{\partial r} = \frac{\partial \rho_o}{\partial p_{fb}} \frac{\partial p_{fb}}{\partial r}, \quad \text{B.18}$$

$$\frac{\partial S_o \rho_o}{\partial t} = \frac{\partial S_o \rho_o}{\partial p_{fb}} \frac{\partial p_{fb}}{\partial t}, \quad \text{B.19}$$

$$\frac{\partial \phi_{fb}}{\partial t} = \frac{\partial \phi_{fb}}{\partial p_{fb}} \frac{\partial p_{fb}}{\partial t}, \quad \text{B.20}$$

substituting eqs. B.18, B.19 and B.20 into B.17, and using the definitions of compressibility of oil and fractured formation, B.17 is rewritten as follows:

$$\frac{aV_{uf}k_{fb}\rho_o}{\phi_{fb}\mu} \left[r^\beta \frac{\partial^2 p_{fb}}{\partial r^2} + \frac{\beta r^\beta}{r} \frac{\partial p_{fb}}{\partial r} + r^\beta c_o \left(\frac{\partial p_{fb}}{\partial r} \right)^2 \right] +$$

B.21

$$+ \alpha_{d_e} r^{d_e-1} b^{3-d_e} \rho_o \phi_{ma} c_{tma} \frac{\partial p_{ma}}{\partial t} = \alpha_{d_e} r^{d_e-1} b^{3-d_e} \phi_{fb} S_o \rho_o [c_o + c_{fb}] \frac{\partial p_{fb}}{\partial t}$$

assuming single phase flow, total compressibility is defined as:

$$c_{tfb} = c_o + c_{fb}, \quad \text{B.22}$$

and neglecting quadratic gradient pressure and according to definition of fracture network porosity, prior equation becomes:

$$\frac{\partial}{\partial r} \left(\frac{aV_{uf}k_{fb}r^\beta}{\phi_{fb}\mu} \frac{\partial p_{fb}}{\partial r} \right) + \alpha_{d_e} r^{d_e-1} b^{3-d_e} \phi_{ma} c_{tma} \frac{\partial p_{ma}}{\partial t} = ar^{D_{fb}-1} V_{uf} c_{tfb} \frac{\partial p_{fb}}{\partial t}. \quad \text{B.23}$$

B.2. Transformation to dimensionless variables

Following dimensionless variables has been state. Dimensionless radius:

$$r_D = \frac{r}{r_w}, \quad \text{B.24}$$

dimensionless time:

$$t_D = \frac{k_{fb}}{\phi_{fb}\mu c_{tfb} r_w^{2+\theta}} \left[1 + \frac{\alpha_{d_e} b^{3-d_e} r_w^{d_e-D_{fb}} \phi_{ma} c_{tma}}{aV_{uf} c_{tfb}} \right] t, \quad \text{B.25}$$

dimensionless pressure in the fracture network:

$$p_{fbD}(r_D, t_D) = \frac{aV_{uf}k_{fb} [p_i - p_{fb}(r, t)]}{q\mu r_w^{1-\beta} \phi_{fb}}, \quad \text{B.26}$$

similarly, for pressure within the matrix:

$$p_{maD}(r_D, t_D) = \frac{aV_{uf}k_{fb} [p_i - p_{ma}(r, t)]}{q\mu r_w^{1-\beta} \phi_{fb}}. \quad \text{B.27}$$

Using chain rule, first derivative of pressure in the fracture network regarding the distance can be written as follows:

$$\frac{\partial p_{fb}(r, t)}{\partial r} = \frac{\partial p_{fb}(r, t)}{p_{fbD}(r_D, t_D)} \frac{dr_D}{dr} \frac{\partial p_{fbD}(r_D, t_D)}{\partial r_D}. \quad \text{B.28}$$

Based on dimensionless pressure definition, pressure as a function of radius and time is expressed as:

$$p_{fb}(r, t) = p_i - \frac{q\mu r_w^{1-\beta} \phi_{fb}}{aV_{uf} k_{fb}} p_{fbD}(r_D, t_D), \quad \text{B.29}$$

which first derivative regarding dimensionless pressure in fracture network is:

$$\frac{\partial p_{fb}(r, t)}{\partial p_{fbD}(r_D, t_D)} = - \frac{q\mu r_w^{1-\beta} \phi_{fb}}{aV_{uf} k_{fb}}. \quad \text{B.30}$$

Based on the dimensionless radius definition, derivative of dimensionless radius regarding radius is:

$$\frac{dr_D}{dr} = \frac{1}{r_w}, \quad \text{B.31}$$

then, eq. B.28 becomes:

$$\frac{\partial p_{fb}(r, t)}{\partial r} = - \frac{q\mu r_w^{-\beta} \phi_{fb}}{aV_{uf} k_{fb}} \frac{\partial p_{fbD}(r_D, t_D)}{\partial r_D}. \quad \text{B.32}$$

Taking second derivative regarding radius of eq. B.32:

$$\frac{\partial^2 p_{fb}(r, t)}{\partial r^2} = - \frac{q\mu r_w^{-\beta-1} \phi_{fb}}{aV_{uf} k_{fb}} \frac{\partial^2 p_{fbD}(r_D, t_D)}{\partial r_D^2}. \quad \text{B.33}$$

Moreover, first derivative of pressure regarding time can be expressed:

$$\frac{\partial p_{fb}(r, t)}{\partial t} = \frac{\partial p_{fb}(r, t)}{p_{fbD}(r_D, t_D)} \frac{dt_D}{dt} \frac{\partial p_{fbD}(r_D, t_D)}{\partial t_D}, \quad \text{B.34}$$

substituting:

$$\frac{\partial p_{fb}(r, t)}{\partial t} = - \frac{q r_w^{1-\beta}}{aV_{uf} c_{ifb} r_w^{2+\theta} \left[1 + \frac{\alpha_{de} b^{3-d_e} r_w^{d_e-D_{fb}} \phi_{ma} c_{ima}}{aV_{uf} c_{ifb}} \right]} \frac{\partial p_{fbD}(r_D, t_D)}{\partial t_D}. \quad \text{B.35}$$

Analogously, for the derivative of pressure within matrix regarding to time:

$$\frac{\partial p_{ma}(r, t)}{\partial t} = - \frac{q r_w^{1-\beta}}{aV_{uf} c_{ifb} r_w^{2+\theta} \left[1 + \frac{\alpha_{de} b^{3-d_e} r_w^{d_e-D_{fb}} \phi_{ma} c_{ima}}{aV_{uf} c_{ifb}} \right]} \frac{\partial p_{maD}(r_D, t_D)}{\partial t_D}. \quad \text{B.36}$$

Substituting eq. B.24, B.32, B.33, B.35 and B.36 into eq. B.28 results:

$$\frac{1}{r_D^{D_{fb}-1}} \frac{\partial}{\partial r_D} \left(r_D^\beta \frac{\partial p_{fbD}(r_D, t_D)}{\partial r_D} \right) = r_D^{d_e-D_{fb}} [1 - \omega_{ps}] \frac{\partial p_{maD}(r_D, t_D)}{\partial t_D} + \omega_{ps} \frac{\partial p_{fbD}(r_D, t_D)}{\partial t_D}, \quad \text{B.37}$$

where:

ω_{ps} = storage coefficient is defined as follows:

$$\omega_{ps} = \frac{aV_{uf}c_{ifb}}{aV_{uf}c_{ifb} + \alpha_{d_e} b^{3-d_e} r_w^{d_e-D_{fb}} \phi_{ma} c_{ima}}. \quad \text{B.38}$$

On the other hand, flow rate from matrix to fracture network per unit bulk volume is given by the expression:

$$q_{ma}^* = \frac{q_{ma}}{V_{bulk}} = \frac{A_{ma-f} v_{ma}}{V_{bulk}}. \quad \text{B.39}$$

Area of matrix exposed to flow can be defined as:

$$A_{ma-f} = \frac{a[D_{fb} - 1] V_{uf} \Delta r}{r^2} r^{D_{fb}}, \quad \text{B.40}$$

velocity of oil coming out from matrix can be expressed using Darcy's law:

$$v_{ma} = \frac{k_{ma}}{\mu} \left[\frac{p_{fb} - p_{ma}}{l_{ma}} \right]. \quad \text{B.41}$$

Based on eq. B.39, B.40 and the definition of bulk volume, flow rate from matrix to fracture network per unit bulk volume can be expressed as follows:

$$q_{ma}^* = \tau_1 r^{D'_{fb}-1} \frac{k_{ma}}{\mu} \left[\frac{p_{fb} - p_{ma}}{l_{ma-f}} \right], \quad \text{B.42}$$

where:

l_{ma-f} = average distance between the matrix and the fractal fracture network;

τ_1 is a constant defined by:

$$\tau_1 = \frac{a[D_{fb} - 1] V_{uf}}{\alpha_{d_e} b^{3-d_e}}, \quad \text{B.43}$$

and,

$$D'_{fb} = D_{fb} - d_e. \quad \text{B.44}$$

Besides, distance between the matrix and the fracture network can be represented as:

$$l_{ma-f} = \tau_2 r^{D''_{fb}}, \quad \text{B.45}$$

where:

$$\tau_2 = a[D_{fb} - 1] [D_{fb} - 2] \Delta r V_{uf}, \quad \text{B.46}$$

and:

$$D''_{fb} = D_{fb} - 3. \quad \text{B.47}$$

Hence, eq. B.42 is rewritten as follows:

$$q_{ma}^* = \frac{\sigma k_{ma}}{\mu} [p_{fb} - p_{ma}], \quad \text{B.48}$$

where shape factor σ , is given by:

$$\sigma = \frac{\tau_1 r^{D'_{fb} - D''_{fb} - 1}}{\tau_2}. \quad \text{B.49}$$

Equating B.11 and B.48 results:

$$\frac{\partial p_{ma}}{\partial t} = \frac{\sigma k_{ma}}{\phi_{ma} c_{tma} \mu} [p_{fb} - p_{ma}]. \quad \text{B.50}$$

Expressing prior eq. in dimensionless variables:

$$\frac{\partial p_{maD}(r_D, t_D)}{\partial t_D} = \frac{\lambda'}{r_D^\Phi} [p_{fbD}(r_D, t_D) - p_{maD}(r_D, t_D)]. \quad \text{B.51}$$

An alternative way to present prior equation is:

$$\frac{\partial p_{maD}(r_D, t_D)}{\partial t_D} = \frac{\lambda}{[1 - \omega_{ps}] r_D^\Phi} [p_{fbD}(r_D, t_D) - p_{maD}(r_D, t_D)], \quad \text{B.52}$$

where:

$$\lambda' = \frac{\lambda}{1 - \omega_{ps}} = \frac{\tau_1 r_w^{2+\theta-\Phi} k_{ma} \phi_{fb} c_{tfb}}{\tau_2 \phi_{ma} c_{tma} k_{fb}} \left[1 + \frac{\alpha_{d_e} b^{3-d_e} r_w^{d_e - D'_{fb}} \phi_{ma} c_{tma}}{a V_{uf} c_{tfb}} \right], \quad \text{B.53}$$

and:

$$\Phi = D'_{fb} + 1 - D''_{fb}. \quad \text{B.54}$$

Appendix C

Pressure Transient Analysis of Fractal Reservoirs with Transient Interporous Transference (Olaewaju, 1996)

C.1. Model development

The procedure for the development of this model is the same as describe in for Chang et al.'s model (1990) in Appendix B, until eq. B.13, which is given by:

$$\frac{\partial}{\partial r} \left(\rho_o \frac{aV_{uf} k_{fb} r^\beta}{\phi_{fb} \mu} \frac{\partial p_{fb}}{\partial r} \right) + \alpha_{d_e} r^{d_e-1} b^{3-d_e} \rho_o q_{ma}^* = \alpha_{d_e} r^{d_e-1} b^{3-d_e} \frac{\partial (S_o \rho_o \phi_{fb})}{\partial t} \quad C.1$$

After applying the derivatives in eq. C.1, it results:

$$\begin{aligned} & \frac{aV_{uf} k_{fb}}{\phi_{fb} \mu} \left[\rho_o r^\beta \frac{\partial^2 p_{fb}(r,t)}{\partial r^2} + \rho_o \beta r^{\beta-1} \frac{\partial p_{fb}(r,t)}{\partial r} + r^\beta \frac{\partial p_{fb}(r,t)}{\partial r} \frac{\partial \rho_o}{\partial r} \right] + \\ & + \alpha_{d_e} r^{d_e-1} b^{3-d_e} \rho_o q_{ma}^* = \alpha_{d_e} r^{d_e-1} b^{3-d_e} \left[\phi_{fb} \frac{\partial (S_o \rho_o)}{\partial t} + S_o \rho_o \frac{\partial (\phi_{fb})}{\partial t} \right] \end{aligned} \quad C.2$$

According to chain rule:

$$\frac{\partial \rho_o}{\partial r} = \frac{\partial \rho_o}{\partial p_{fb}} \frac{\partial p_{fb}}{\partial r}, \quad C.3$$

$$\frac{\partial S_o \rho_o}{\partial t} = \frac{\partial S_o \rho_o}{\partial p_{fb}} \frac{\partial p_{fb}}{\partial t}, \quad C.4$$

$$\frac{\partial \phi_{fb}}{\partial t} = \frac{\partial \phi_{fb}}{\partial p_{fb}} \frac{\partial p_{fb}}{\partial t}, \quad C.5$$

substituting, eq. C.3, C.4, C.5 and, using the definitions of oil and formation compressibility, eq. C.2 becomes:

$$\begin{aligned} & \frac{aV_{uf} k_{fb}}{\phi_{fb} \mu} \left[r^\beta \frac{\partial^2 p_{fb}(r,t)}{\partial r^2} + \beta r^{\beta-1} \frac{\partial p_{fb}(r,t)}{\partial r} + r^\beta c_o \left(\frac{\partial p_{fb}(r,t)}{\partial r} \right)^2 \right] + \alpha_{d_e} r^{d_e-1} b^{3-d_e} q_{ma}^* = \\ & = \alpha_{d_e} r^{d_e-1} b^{3-d_e} \phi_{fb} S_o [c_o + c_{fb}] \frac{\partial p_{fb}(r,t)}{\partial t} \end{aligned} \quad C.6$$

Assuming single phase flow, and according to the total compressibility definition, eq. C.6 is written as:

$$\frac{\alpha V_{uf} k_{fb}}{\phi_{fb} \mu} \left[r^\beta \frac{\partial^2 p_{fb}(r,t)}{\partial r^2} + \beta r^{\beta-1} \frac{\partial p_{fb}(r,t)}{\partial r} + r^\beta c_o \left(\frac{\partial p_{fb}(r,t)}{\partial r} \right)^2 \right] + \alpha_{d_e} r^{d_e-1} b^{3-d_e} q_{ma}^* =$$

$$= \alpha_{d_e} r^{d_e-1} b^{3-d_e} \phi_{fb} c_{ifb} \frac{\partial p_{fb}(r,t)}{\partial t}$$

Neglecting quadratic gradient pressure, prior equation becomes:

$$\frac{1}{r^{D_{fb}-1}} \frac{\partial}{\partial r} \left(r^\beta \frac{\partial p_{fb}(r,t)}{\partial r} \right) - \frac{k_{ma} A_{fb}}{k_{fb}} \int_0^t \frac{\partial p_{fb}(\tau)}{d\tau} (\nabla \Delta p_{uma})_{sur} d\tau = \frac{1}{\eta_{fb}} \frac{\partial p_{fb}(r,t)}{\partial t}$$

where:

$$q_{ma}^* = -\frac{k_{ma}}{\mu} A_{fb} \int_0^t \frac{\partial p_{fb}(\tau)}{d\tau} (\nabla \Delta p_{uma})_{sur} d\tau,$$

A_{fb} = exposed to flow area which is defined as:

$$A_{fb} = \frac{1}{h_{ma}};$$

η_{fb} = hydraulic diffusivity coefficient is defined as:

$$\eta_{fb} = \frac{k_{fb}}{\phi_{fb} \mu c_{ifb}},$$

and pressure gradient is given by:

$$(\nabla \Delta p_{uma})_{sur} = \frac{3}{h_{ma}} \sum_{n=1}^{\infty} e^{-\frac{4k_{ma} r_w^{\theta+2} (\phi_{c_t})_t (2n+1)\pi^2 [t_D-\tau]}{\phi_{ma} c_{ima} k_{fb} h_{ma}^2}}$$

C.2. Dimensionless variables transformation

Following dimensionless variables are established. Dimensionless radius:

$$r_D = \frac{r}{r_w},$$

dimensionless position at the matrix:

$$z_D = \frac{2z}{h_{ma}}.$$

Dimensionless time:

$$t_D = \frac{k_{fb}}{(\phi_{c_t})_t \mu r_w^{2+\theta}} t,$$

where:

$$(\phi_{c_t})_t = \phi_{fb} c_{ifb} + \phi_{ma} c_{ima}.$$

Dimensionless pressure in the fracture network:

$$p_{fbD}(r_D, t_D) = \frac{aV_{uf}k_{fb}[p_{fb}(r, t) - p_i]}{q\mu r_w^{1-\beta}\phi_{fb}}, \quad \text{C.17}$$

similarly, for pressure within the matrix:

$$p_{maD}(r_D, t_D) = \frac{aV_{uf}k_{fb}[p_{ma}(r, t) - p_i]}{q\mu r_w^{1-\beta}\phi_{fb}}. \quad \text{C.18}$$

Using chain rule, first derivative of pressure in the fracture network regarding the distance can be written as follows:

$$\frac{\partial p_{fb}(r, t)}{\partial r} = \frac{\partial p_{fb}(r, t)}{p_{fbD}(r_D, t_D)} \frac{dr_D}{dr} \frac{\partial p_{fbD}(r_D, t_D)}{\partial r_D}. \quad \text{C.19}$$

Applying the derivatives, C.19 becomes:

$$\frac{\partial p_{fb}(r, t)}{\partial r} = \frac{q\mu r_w^{-\beta}\phi_{fb}}{aV_{uf}k_{fb}} \frac{\partial p_{fbD}(r_D, t_D)}{\partial r_D}. \quad \text{C.20}$$

The second derivative regarding radius of eq. C.20 is given by:

$$\frac{\partial^2 p_{fb}(r, t)}{\partial r^2} = \frac{q\mu r_w^{-\beta-1}\phi_{fb}}{aV_{uf}k_{fb}} \frac{\partial^2 p_{fbD}(r_D, t_D)}{\partial r_D^2}. \quad \text{C.21}$$

Analogously, first derivative of pressure regarding time is:

$$\frac{\partial p_{fb}(r, t)}{\partial t} = \left[\frac{q\mu r_w^{1-\beta}\phi_{fb}}{aV_{uf}k_{fb}} \right] \left[\frac{k_{fb}}{(\phi c_t)_t \mu r_w^{2+\theta}} \right] \frac{\partial p_{fbD}(r_D, t_D)}{\partial t_D}. \quad \text{C.22}$$

And,

$$\frac{\partial p_{fb}(r, \tau)}{\partial \tau} = \left[\frac{q\mu r_w^{1-\beta}\phi_{fb}}{aV_{uf}k_{fb}} \right] \frac{\partial p_{fbD}(r_D, t_D)}{\partial t_D}. \quad \text{C.23}$$

Substituting C.13, C.20, C.21, C.22, C.23 in C.30 and arraying, the following expression is obtained:

$$\begin{aligned} & \frac{\partial^2 p_{fbD}(r_D, t_D)}{\partial r_D^2} + \frac{\beta}{r_D} \frac{\partial p_{fbD}(r_D, t_D)}{\partial r_D} - r_D^{-\theta} \frac{k_{ma}A_{fb}r_w^{\theta+2}}{k_{fb}} \int_0^t \frac{\partial p_{fbD}(r_D, t_D)}{\partial \tau} (\nabla \Delta p_{uma})_{sur} d\tau = \\ & = r_D^{-\theta} \left[\frac{\phi_{fb}c_{ifb}}{(\phi c_t)_t} \right] \frac{\partial p_{fbD}(r_D, t_D)}{\partial t_D} \end{aligned} \quad \text{C.24}$$

Considering strata as matrix blocks, eq. C.12, then:

$$\frac{\partial^2 p_{fbD}(r_D, t_D)}{\partial r_D^2} + \frac{\beta}{r_D} \frac{\partial p_{fbD}(r_D, t_D)}{\partial r_D} - \frac{r_D^\theta \lambda}{3} \int_0^t \frac{\partial p_{fbD}(r_D, t_D)}{\partial \tau} \sum_{n=1}^{\infty} e^{-\frac{\lambda(2n+1)\pi^2[t_D-\tau]}{3[1-\omega]}} d\tau =$$

$$= r_D^\theta \omega \frac{\partial p_{fbD}(r_D, t_D)}{\partial t_D} \quad , \quad \text{C.25}$$

where *interporosity flow coefficient* is defined as:

$$\lambda = \frac{12k_{ma}r_w^{\theta+2}}{h_{ma}k_{fb}}; \quad \text{C.26}$$

dimensionless storativity ratio:

$$\omega = \frac{\phi_{fb}c_{ifb}}{(\phi c_t)_i}. \quad \text{C.27}$$

C.3. General solution in Laplace space assuming constant rate

In order to have a well test analysis model for the Fractal Reservoir Model assuming free interaction transference between matrix and fractures, the following conditions have been set:

Initial condition for fracture network: $p_{fbD}(r_D, t_D = 0) = 0,$ C.28

inner boundary: $r_D^\beta \frac{\partial p_{fbD}(1, t_D)}{\partial t_D} = -1,$ C.29

outer boundary: $\lim_{r_D \rightarrow \infty} (p_D(r_D, t_D)) = 0.$ C.30

Applying Laplace transform to eq. C.57 and according to initial condition, it becomes:

$$r_D^2 \frac{d^2 \bar{p}_{fbD}(r_D, s)}{dr_D^2} + [1 - 2\delta] r_D \frac{d\bar{p}_{fbD}(r_D, s)}{dr_D} - sr_D^{\theta+2} f(s) \bar{p}_{fbD}(r_D, s) = 0. \quad \text{C.31}$$

where:

$$f(s) = \omega + [1 - \omega] \sqrt{\frac{\lambda}{3s[1-\omega]}} \tanh\left(\sqrt{\frac{3s[1-\omega]}{\lambda}}\right), \quad \text{C.32}$$

and:

$$\delta = \frac{1 - \beta}{2}. \quad \text{C.33}$$

Establishing the following transform function:

$$\bar{p}_D(r_D, s) = \bar{G}_D(z), \quad \text{C.34}$$

and the transformation variable:

$$z = \frac{2\sqrt{sf(s)}}{\theta + 2} r_D^{\frac{\theta+2}{2}}, \quad \text{C.35}$$

a transformation of variables takes places. Using definitions given by eq. C.34 and eq. C.35 the following expression is obtained:

$$z^2 \frac{\partial^2 \bar{G}_D(z)}{\partial z^2} + [1 - 2\nu]z \frac{\partial \bar{G}_D(z)}{\partial z} - z^2 \bar{G}_D(z) = 0, \quad \text{C.36}$$

where:

$$\nu = \frac{1 - \beta}{\theta + 2}. \quad \text{C.37}$$

To equalize the coefficient of the first derivative to one the following expression is proposed:

$$\bar{G}_D(z) = \frac{z^\nu}{\psi} B_D(z), \quad \text{C.38}$$

where:

$$\psi = \left(\frac{2\sqrt{sf(s)}}{\theta + 2} \right)^{\frac{1-\beta}{\theta+2}}. \quad \text{C.39}$$

Applying the transformations given by eq. C.38 and C.39, eq. C.36 can be written as:

$$z^2 \frac{d^2 B_D(z)}{dz^2} + z \frac{dB_D(z)}{dz} - [v^2 + z^2] B_D(z) = 0. \quad \text{C.40}$$

Solution of eq. 40 is given by:

$$B_D(z) = c_1 I_\nu(z) + c_2 K_\nu(z), \quad \text{C.41}$$

or, in terms of eq. C.38:

$$\bar{G}_D(z) = \frac{z^\nu}{\psi} [c_1 I_\nu(z) + c_2 K_\nu(z)], \quad \text{C.42}$$

and, in terms of $\bar{p}_D(r_D, s)$ and $r_D \sqrt{s}$, the solution is:

$$\bar{p}_D(r_D, s) = r_D^{\frac{1-\beta}{2}} \left[c_1 I_{\frac{1-\beta}{\theta+2}} \left(\frac{2\sqrt{sf(s)}}{\theta + 2} r_D^{\frac{\theta+2}{2}} \right) + c_2 K_{\frac{1-\beta}{\theta+2}} \left(\frac{2\sqrt{sf(s)}}{\theta + 2} r_D^{\frac{\theta+2}{2}} \right) \right]. \quad \text{C.43}$$

Applying outer boundary condition, it can be deduced that:

$$c_1 = 0, \quad \text{C.44}$$

hence bounded solution is:

$$\bar{p}_D(r_D, s) = c_2 r_D^{\frac{1-\beta}{2}} K_{\frac{1-\beta}{\theta+2}} \left(\frac{2\sqrt{sf(s)}}{\theta + 2} r_D^{\frac{\theta+2}{2}} \right). \quad \text{C.45}$$

Applying the inner boundary condition it is concluded that:

$$c_2 = -\frac{1}{s^{3/2} \sqrt{f(s)} K_{\frac{D_{fb}}{\theta+2}} \left(\frac{2\sqrt{sf(s)}}{\theta+2} \right)}. \quad \text{C.46}$$

Then, particular solution is given by:

$$\bar{p}_D(r_D, s) = \frac{r_D^{\frac{1-\beta}{2}} K_{\frac{1-\beta}{\theta+2}} \left(\frac{2\sqrt{sf(s)}}{\theta+2} r_D^{\frac{\theta+2}{2}} \right)}{s^{3/2} \sqrt{f(s)} K_{\frac{D_{fb}}{\theta+2}} \left(\frac{2\sqrt{sf(s)}}{\theta+2} \right)}. \quad \text{C.47}$$

Hence, dimensionless pressure at wellbore is:

$$\bar{p}_{wD}(s) = \frac{K_{\frac{1-\beta}{\theta+2}} \left(\frac{2}{\theta+2} \sqrt{sf(s)} \right)}{s^{3/2} \sqrt{f(s)} K_{\frac{D_{fb}}{\theta+2}} \left(\frac{2}{\theta+2} \sqrt{sf(s)} \right)}. \quad \text{C.48}$$

Appendix D

Pressure Transient Analysis of Fractal Reservoirs assuming Free Interaction Interporosity Transfer

D.1. Model development

The development of this model follows the same steps as shown in Appendix B, until eq. B.13, given by:

$$\frac{\partial}{\partial r} \left(\rho_o \frac{aV_{uf} k_{fb} r^\beta}{\phi_{fb} \mu} \frac{\partial p_{fb}}{\partial r} \right) + \alpha_{d_e} r^{d_e-1} b^{3-d_e} \rho_o q_{ma}^* = \alpha_{d_e} r^{d_e-1} b^{3-d_e} \frac{\partial (S_o \rho_o \phi_{fb})}{\partial t}. \quad D.1$$

Applying the derivatives in eq. D.1:

$$\begin{aligned} & \frac{aV_{uf} k_{fb}}{\phi_{fb} \mu} \left[\rho_o r^\beta \frac{\partial^2 p_{fb}(r,t)}{\partial r^2} + \rho_o \beta r^{\beta-1} \frac{\partial p_{fb}(r,t)}{\partial r} + r^\beta \frac{\partial p_{fb}(r,t)}{\partial r} \frac{\partial \rho_o}{\partial r} \right] + \\ & + \alpha_{D_{fb}} r^{D_{fb}-1} b^{3-D_{fb}} \rho_o q_{ma}^* = \alpha_{D_{fb}} r^{D_{fb}-1} b^{3-D_{fb}} \left[\phi_{fb} \frac{\partial (S_o \rho_o)}{\partial t} + S_o \rho_o \frac{\partial (\phi_{fb})}{\partial t} \right]. \end{aligned} \quad D.2$$

According to chain rule:

$$\frac{\partial \rho_o}{\partial r} = \frac{\partial \rho_o}{\partial p_{fb}} \frac{\partial p_{fb}}{\partial r}, \quad D.3$$

$$\frac{\partial S_o \rho_o}{\partial t} = \frac{\partial S_o \rho_o}{\partial p_{fb}} \frac{\partial p_{fb}}{\partial t}, \quad D.4$$

$$\frac{\partial \phi_{fb}}{\partial t} = \frac{\partial \phi_{fb}}{\partial p_{fb}} \frac{\partial p_{fb}}{\partial t}. \quad D.5$$

Substituting eq. D.3, eq. D.4 and eq. D.5 in eq. D.2 and using the definitions of oil and formation compressibility, eq. D.2 becomes:

$$\begin{aligned} & \frac{aV_{uf} k_{fb}}{\phi_{fb} \mu} \left[r^\beta \frac{\partial^2 p_{fb}(r,t)}{\partial r^2} + \beta r^{\beta-1} \frac{\partial p_{fb}(r,t)}{\partial r} + r^\beta c_o \left(\frac{\partial p_{fb}(r,t)}{\partial r} \right)^2 \right] + \alpha_{D_{fb}} r^{D_{fb}-1} b^{3-D_{fb}} q_{ma}^* = \\ & = \alpha_{D_{fb}} r^{D_{fb}-1} b^{3-D_{fb}} \phi_{fb} S_o [c_o + c_{fb}] \frac{\partial p_{fb}(r,t)}{\partial t} \end{aligned} \quad D.6$$

Assuming single phase flow, and according to the total compressibility definition, eq. D.6 is written as:

$$\frac{\alpha V_{uf} k_{fb}}{\phi_{fb} \mu} \left[r^\beta \frac{\partial^2 p_{fb}(r,t)}{\partial r^2} + \beta r^{\beta-1} \frac{\partial p_{fb}(r,t)}{\partial r} + r^\beta c_o \left(\frac{\partial p_{fb}(r,t)}{\partial r} \right)^2 \right] + \alpha_{D_{fb}} r^{D_{fb}-1} b^{3-D_{fb}} q_{ma}^* =$$

$$= \alpha_{D_{fb}} r^{D_{fb}-1} b^{3-D_{fb}} \phi_{fb} c_{ifb} \frac{\partial p_{fb}(r,t)}{\partial t}$$

D.7

Neglecting quadratic gradient pressure, prior equation becomes:

$$r^\beta \frac{\partial^2 p_{fb}(r,t)}{\partial r^2} + \beta r^{\beta-1} \frac{\partial p_{fb}(r,t)}{\partial r} + r^{D_{fb}-1} \frac{\mu}{k_{fb}} q_{ma}^* = r^{D_{fb}-1} \frac{c_{ifb} \phi_{fb} \mu}{k_{fb}} \frac{\partial p_{fb}(r,t)}{\partial t}.$$

D.8

Where:

$$q_{ma}^* = -\frac{k_{ma} A_{fb}}{\mu} \int_0^t \frac{\partial p_{fb}(\tau)}{d\tau} (\nabla \Delta p_{uma})_{sur} d\tau.$$

D.9

If slab matrix blocks are assumed, area exposed to flow is defined as:

$$A_{fb} = \frac{2}{h_{ma} + h_f};$$

D.10

or, if cube matrix blocks are assumed:

$$A_{fb} = \frac{6h_{ma}^2}{(h_{ma} + h_f)^3}.$$

D.11

Substituting eq. D.9 into D.8:

$$\frac{1}{r^{D_{fb}-1}} \frac{\partial}{\partial r} \left(r^\beta \frac{\partial p_{fb}(r,t)}{\partial r} \right) - \frac{k_{ma} A_{fb}}{k_{fb}} \int_0^t \frac{\partial p_{fb}(\tau)}{d\tau} (\nabla \Delta p_{uma})_{sur} d\tau = \frac{1}{\eta_{fb}} \frac{\partial p_{fb}(r,t)}{\partial t},$$

D.12

where hydraulic diffusivity coefficient is defined as:

$$\eta_{fb} = \frac{k_{fb}}{\phi_{fb} \mu c_{ifb}}.$$

D.13

D.2. Transformation to dimensionless variables

Following dimensionless variables has been state. Dimensionless radius:

$$r_D = \frac{r}{r_w},$$

D.14

dimensionless time:

$$t_D = \frac{k_{fb}}{(\phi c_t)_i \mu r_w^{2+\theta}} t,$$

D.15

where:

$$(\phi c_i)_t = \phi_{fb} c_{ifb} + \phi_{ma} c_{ima}. \quad D.16$$

Dimensionless pressure in the fracture network:

$$p_{fbD}(r_D, t_D) = \frac{a V_{uf} k_{fb} [p_i - p_{fb}(r, t)]}{q \mu r_w^{1-\beta} \phi_{fb}}, \quad D.17$$

similarly, for pressure within the matrix:

$$p_{maD}(r_D, t_D) = \frac{a V_{uf} k_{fb} [p_i - p_{ma}(r, t)]}{q \mu r_w^{1-\beta} \phi_{fb}}. \quad D.18$$

Using chain rule, first derivative of pressure in the fracture network regarding the distance can be written as follows:

$$\frac{\partial p_{fb}(r, t)}{\partial r} = \frac{\partial p_{fb}(r, t)}{p_{fbD}(r_D, t_D)} \frac{dr_D}{dr} \frac{\partial p_{fbD}(r_D, t_D)}{\partial r_D}. \quad D.19$$

Applying the derivatives, eq. D.19 becomes:

$$\frac{\partial p_{fb}(r, t)}{\partial r} = - \frac{q \mu r_w^{-\beta} \phi_{fb}}{a V_{uf} k_{fb}} \frac{\partial p_{fbD}(r_D, t_D)}{\partial r_D}. \quad D.20$$

Taking second derivative of eq. D.20 regarding radius, it results:

$$\frac{\partial^2 p_{fb}(r, t)}{\partial r^2} = - \frac{q \mu r_w^{-\beta-1} \phi_{fb}}{a V_{uf} k_{fb}} \frac{\partial^2 p_{fbD}(r_D, t_D)}{\partial r_D^2}. \quad D.21$$

Moreover, first derivative of pressure regarding time can be expressed:

$$\frac{\partial p_{fb}(r, t)}{\partial t} = \left[- \frac{q \mu r_w^{1-\beta} \phi_{fb}}{a V_{uf} k_{fb}} \right] \left[\frac{k_{fb}}{(\phi c_i)_t \mu r_w^{2+\theta}} \right] \frac{\partial p_{fbD}(r_D, t_D)}{\partial t_D}. \quad D.22$$

and,

$$\frac{\partial p_{fb}(r, \tau)}{\partial \tau} = - \frac{q \mu r_w^{1-\beta} \phi_{fb}}{a V_{uf} k_{fb}} \frac{\partial p_{fbD}(r_D, t_D)}{\partial \tau}. \quad D.23$$

Substituting D.14, D.20, D.21, D.22, and D.23 in D.12, it becomes:

$$\begin{aligned} & \frac{\partial^2 p_{fbD}(r_D, t_D)}{\partial r_D^2} + \frac{\beta}{r_D} \frac{\partial p_{fbD}(r_D, t_D)}{\partial r_D} - r_D^\theta A_{fD} [1 - \omega] \int_0^{t_D} \frac{\partial p_{fbD}(r_D, \tau)}{\partial \tau} F(\eta_{maD}, H_D, t_D - \tau) d\tau = \\ & = r_D^\theta \omega \frac{\partial p_{fbD}(r_D, t_D)}{\partial t_D} \end{aligned} \quad D.24$$

where, *dimensionless storativity ratio*, ω is defined as:

$$\omega = \frac{\phi_{fb} c_{ifb}}{(\phi c_t)_t}; \quad \text{D.25}$$

dimensionless matrix hydraulic diffusivity:

$$\eta_{maD} = \frac{k_{ma} (\phi c_t)_t}{\phi_{ma} c_{ima} k_{fb}}; \quad \text{D.26}$$

block size ratio:

$$H_D = \frac{r_w^2}{h_{ma}^2}; \quad \text{D.27}$$

dimensionless fracture area, A_{fD} :

$$A_{fD} = \frac{A_{fb} h_{ma} V_b r_w^\theta}{V_{ma}}. \quad \text{D.28}$$

Fluid transfer function, assuming slabs:

$$F(\eta_{maD}, H_D, t_D - \tau) = \frac{4\eta_{maD}}{H_D} \sum_{n=1}^{\infty} e^{-\frac{\eta_{maD}(2n+1)^2 \pi^2 [t_D - \tau]}{H_D}}, \quad \text{D.29}$$

or, if spheres as matrix blocks, fluid transfer function is:

$$F(\eta_{maD}, H_D, t_D - \tau) = \frac{4\eta_{maD}}{H_D} \sum_{n=1}^{\infty} e^{-\frac{4\eta_{maD} n^2 \pi^2 [t_D - \tau]}{H_D}}. \quad \text{D.30}$$

D.3. General solution in Laplace space assuming constant rate

In order to have a well test analysis model for the Fractal Reservoir Model assuming free interaction transfer between matrix and fractures, the following conditions have been set:

Initial condition for fracture network: $p_{fbD}(r_D, t_D = 0) = 0,$ D.31

inner Boundary: $r_D^\beta \frac{\partial p_{fbD}(1, t_D)}{\partial t_D} = -1,$ D.32

outer boundary: $\lim_{r_D \rightarrow \infty} (p_D(r_D, t_D)) = 0.$ D.33

Applying Laplace transform to eq. D.24 yields:

$$\begin{aligned} \frac{d^2 p_{fbD}(r_D, t_D)}{dr_D^2} + \frac{\beta}{r_D} \frac{dp_{fbD}(r_D, t_D)}{dr_D} - r_D^\theta A_{fD} [1 - \omega] \bar{F}(\eta_{maD}, H_D, s) s \bar{p}_{fbD}(r_D, s) = \\ = r_D^\theta \omega [s \bar{p}_{fbD}(r_D, s) - p_{fbD}(r_D, 0)] \end{aligned} \quad \text{D.34}$$

where, for slab matrix blocks:

$$\bar{F}(\eta_{maD}, H_D, s) = \sqrt{\frac{\eta_{maD}}{H_D s}} \tanh\left(\frac{1}{2} \sqrt{\frac{H_D s}{\eta_{maD}}}\right), \quad \text{D.35}$$

And, for spheres as matrix blocks:

$$\bar{F}(\eta_{maD}, H_D, s) = \sqrt{\frac{\eta_{maD}}{H_D s}} \left[\coth\left(\frac{1}{2} \sqrt{\frac{H_D s}{\eta_{maD}}}\right) - 2 \sqrt{\frac{\eta_{maD}}{H_D s}} \right]. \quad \text{D.36}$$

Applying initial condition in eq. D.34, and arraying:

$$r_D^2 \frac{d^2 \bar{p}_{fbD}(r_D, s)}{dr_D^2} + \beta r_D \frac{d\bar{p}_{fbD}(r_D, s)}{dr_D} - s r_D^{\theta+2} f(s) \bar{p}_{fbD}(r_D, s) = 0, \quad \text{D.37}$$

where:

$$f(s) = A_{fD} [1 - \omega] \bar{F}(\eta_{maD}, H_D, s) + \omega. \quad \text{D.38}$$

Parameter δ is established:

$$\delta = \frac{1 - \beta}{2}. \quad \text{D.39}$$

then:

$$r_D^2 \frac{d^2 \bar{p}_{fbD}(r_D, s)}{dr_D^2} + [1 - 2\delta] r_D \frac{d\bar{p}_{fbD}(r_D, s)}{dr_D} - s r_D^{\theta+2} f(s) \bar{p}_{fbD}(r_D, s) = 0. \quad \text{D.40}$$

The following transform function has been set:

$$\bar{p}_D(r_D, s) = \bar{G}_D(z), \quad \text{D.41}$$

and the transformation variable:

$$z = \frac{2\sqrt{sf(s)}}{\theta + 2} r_D^{\frac{\theta+2}{2}}. \quad \text{D.42}$$

Using definitions given by eq. D.40 and eq. D.41 the following expression is obtained:

$$z^2 \frac{\partial^2 \bar{G}_D(z)}{\partial z^2} + [1 - 2v] z \frac{\partial \bar{G}_D(z)}{\partial z} - z^2 \bar{G}_D(z) = 0. \quad \text{D.43}$$

where,

$$v = \frac{1 - \beta}{\theta + 2}. \quad \text{D.44}$$

To equalize the coefficient of the first derivative to one the following expression is proposed:

$$\bar{G}_D(z) = \frac{z^v}{\psi} B_D(z), \quad \text{D.45}$$

where:

$$\psi = \left(\frac{2\sqrt{sf(s)}}{\theta + 2} \right)^{\frac{1-\beta}{\theta+2}}. \quad \text{D.46}$$

Applying the transformations given by eq. C.45 and C.46, eq. C.43 can be written as:

$$z^2 \frac{d^2 B_D(z)}{dz^2} + z \frac{dB_D(z)}{dz} - [v^2 + z^2] B_D(z) = 0. \quad \text{D.47}$$

Its solution is given by:

$$B_D(z) = c_1 I_\nu(z) + c_2 K_\nu(z), \quad \text{D.48}$$

or, in terms of eq. D.85:

$$\bar{G}_D(z) = \frac{z^\nu}{\psi} [c_1 I_\nu(z) + c_2 K_\nu(z)], \quad \text{D.49}$$

and, in terms of $\bar{p}_D(r_D, s)$ and $r_D \sqrt{s}$, solution is:

$$\bar{p}_D(r_D, s) = r_D^{\frac{1-\beta}{2}} \left[c_1 I_{\frac{1-\beta}{\theta+2}} \left(\frac{2\sqrt{sf(s)}}{\theta+2} r_D^{\frac{\theta+2}{2}} \right) + c_2 K_{\frac{1-\beta}{\theta+2}} \left(\frac{2\sqrt{sf(s)}}{\theta+2} r_D^{\frac{\theta+2}{2}} \right) \right]. \quad \text{D.50}$$

Applying outer boundary condition, it can be deduced that:

$$c_1 = 0, \quad \text{D.51}$$

And, bounded solution is:

$$\bar{p}_D(r_D, s) = c_2 r_D^{\frac{1-\beta}{2}} K_{\frac{1-\beta}{\theta+2}} \left(\frac{2\sqrt{sf(s)}}{\theta+2} r_D^{\frac{\theta+2}{2}} \right). \quad \text{D.52}$$

Applying the inner boundary condition it is concluded that:

$$c_2 = - \frac{1}{s^{3/2} \sqrt{f(s)} K_{\frac{D_{fb}}{\theta+2}} \left(\frac{2\sqrt{sf(s)}}{\theta+2} \right)}, \quad \text{D.53}$$

then, particular solution is given by:

$$\bar{p}_D(r_D, s) = \frac{r_D^{\frac{1-\beta}{2}} K_{\frac{1-\beta}{\theta+2}} \left(\frac{2\sqrt{sf(s)}}{\theta+2} r_D^{\frac{\theta+2}{2}} \right)}{s^{3/2} \sqrt{f(s)} K_{\frac{D_{fb}}{\theta+2}} \left(\frac{2\sqrt{sf(s)}}{\theta+2} \right)}, \quad \text{D.54}$$

at wellbore:

$$\bar{p}_{wD}(s) = \frac{K_{\frac{1-\beta}{\theta+2}} \left(\frac{2}{\theta+2} \sqrt{sf(s)} \right)}{s^{3/2} \sqrt{f(s)} K_{\frac{D_{fb}}{\theta+2}} \left(\frac{2}{\theta+2} \sqrt{sf(s)} \right)}. \quad \text{D.55}$$

D.4. Approximate solutions at short times: Total Expansion in the Fracture Network

At short times, only the fracture network is acting:

$$f(s) \approx \omega, \quad \text{D.56}$$

Therefore, eq. D.24 is reduced to:

$$\frac{\partial^2 p_{fbD}(r_D, t_D)}{\partial r_D^2} + \frac{\beta}{r_D} \frac{\partial p_{fbD}(r_D, t_D)}{\partial r_D} = r_D^\theta \omega \frac{\partial p_{fbD}(r_D, t_D)}{\partial t_D}. \quad \text{D.57}$$

Establishing the following transformation function:

$$Z_{4D} = \omega (D_{fb})^{2-\frac{[\theta+2]}{D_{fb}}} p_{fbD}(r_D, t_D), \quad \text{D.58}$$

or:

$$p_{fbD}(r_D, t_D) = \omega^{-1} (D_{fb})^{\frac{[\theta+2]}{D_{fb}}-2} Z_{4D}. \quad \text{D.59}$$

besides:

$$\tau_4 = \frac{1}{D_{fb}} r_D^{D_{fb}}, \quad \text{D.60}$$

and:

$$\kappa_4 = D_{fb}^{2-\frac{[\theta+2]}{D_{fb}}} t_D. \quad \text{D.61}$$

The procedure to obtain this approximate solution is analogous to the one shown in section IV.4 of Chapter 4 in the main text. Therefore, the founded approximate solution is given by:

$$p_{fbD}(r_D, t_D) = -\frac{r_D^{\theta+2-D_{fb}}}{(\theta+2)\Gamma\left(\frac{D_{fb}}{\theta+2}\right)} \Gamma\left(\frac{D_{fb}}{\theta+2}-1, \frac{\omega r_D^{\theta+2}}{(\theta+2)^2 t_D}\right). \quad \text{D.62}$$

In order to have simplified solutions relatively easy to use, two cases must be defined. The first case is given by the condition $D_{fb} = \theta + 2$. If that is the case and evaluated in $r_D = 1$, eq. D.62 becomes:

$$p_{wD}(t_D) = -\frac{1}{(\theta+2)} \Gamma\left(0, \frac{\omega}{(\theta+2)^2 t_D}\right). \quad \text{D.63}$$

According to incomplete gamma function convergences, prior expression can be expressed as:

$$p_{wD}(t_D) = -\frac{1}{(\theta+2)} E_i\left(\frac{\omega}{(\theta+2)^2 t_D}\right), \quad \text{D.64}$$

where:

$E_i(x)$ = integral exponential.

For small arguments of the integral exponential, eq. D.64 can be approximated as:

$$p_{wD}(t_D) = \frac{1}{(\theta + 2)} [\ln(t_D) + 2 \ln(\theta + 2) - \ln(\omega) - \gamma], \quad \text{D.65}$$

where:

γ = Euler's constant.

On the other hand, for $D_{fb} \neq \theta + 2$ the following approximation was used, based on the incomplete gamma function definition:

$$\Gamma(a, x) \approx \Gamma(a) - \frac{x^a}{a} + \frac{x^{a+1}}{[a+1]}, \quad \text{D.66}$$

hence, incomplete gamma function for this problem is approximated as:

$$\Gamma\left(\frac{D_{fb}}{\theta + 2} - 1, \frac{\omega r_D^{\theta+2}}{(\theta + 2)^2 t_D}\right) = \Gamma\left(\frac{D_{fb}}{\theta + 2} - 1\right) - \left(\frac{1}{r_D^{\theta+2}}\right)^{1 - \frac{D_{fb}}{\theta+2}} \frac{(\theta + 2)^2 \left[1 - \frac{D_{fb}}{\theta+2}\right] \omega^{\frac{D_{fb}}{\theta+2} - 1} t_D^{1 - \frac{D_{fb}}{\theta+2}}}{\frac{D_{fb}}{\theta + 2} - 1}. \quad \text{D.67}$$

Substituting D.67 in eq. D.62 and evaluating in $r_D = 1$:

$$p_{wD}(t_D) = \left[\frac{\Gamma\left(\frac{D_{fb}}{\theta + 2} - 1\right)}{(\theta + 2) \Gamma\left(\frac{D_{fb}}{\theta + 2}\right)} - \frac{(\theta + 2)^{2v-1} \omega^{v-1}}{\left[\frac{D_{fb}}{\theta + 2} - 1\right] \Gamma\left(\frac{D_{fb}}{\theta + 2}\right)} t_D^v \right], \quad \text{D.68}$$

where:

$$v = 1 - \frac{D_{fb}}{\theta + 2}, \quad \text{D.69}$$

Recurrence formula of gamma function can be written as:

$$\frac{\Gamma(x-1)}{\Gamma(x)} = (x-1)^{-1}. \quad \text{D.70}$$

Therefore, eq. D.68 is rewritten as:

$$p_{wD}(t_D) = \frac{1}{-v(\theta + 2)} + \frac{(\theta + 2)^{2v-1} \omega^{v-1}}{v \Gamma\left(\frac{D_{fb}}{\theta + 2}\right)} t_D^v. \quad \text{D.71}$$

It can be verified that, if there is no anomaly in conductivity in fractal object, i.e., $\theta = 0$ and a homogeneous reservoir is assumed, i.e., $\omega = 1$, prior equations converges to the generalized radial flow model solution, given in Appendix A.

D.5. Approximate solutions at intermediate times: Interaction between porous media

For intermediate times, the interaction between porous media takes place. For this period, transference function can be approximated as:

$$f(s) \approx A_{fD} [1 - \omega] \sqrt{\frac{\eta_{maD}}{H_D s}}, \quad D.72$$

Therefore, eq. D.55 is rewritten as:

$$\bar{p}_{wD}(s) = \frac{1}{s^{3/2} \left(A_{fD} [1 - \omega] \sqrt{\frac{\eta_{maD}}{H_D s}} \right)^{\frac{1}{2}} \frac{K_{\frac{1-\beta}{\theta+2}} \left(\frac{2}{\theta+2} \sqrt{A_{fD} [1 - \omega] \sqrt{\frac{\eta_{maD} s}{H_D}}} \right)}{K_{\frac{D_{fb}}{\theta+2}} \left(\frac{2}{\theta+2} \sqrt{A_{fD} [1 - \omega] \sqrt{\frac{\eta_{maD} s}{H_D}}} \right)}}. \quad D.73$$

For small arguments, Bessel function in the denominator is approximated as:

$$K_{\frac{D_{fb}}{\theta+2}} \left(\frac{2}{\theta+2} \sqrt{A_{fD} [1 - \omega] \sqrt{\frac{\eta_{maD} s}{H_D}}} \right) \approx \frac{(\theta+2)^{\frac{D_{fb}}{\theta+2}}}{2} \left(A_{fD} [1 - \omega] \sqrt{\frac{\eta_{maD} s}{H_D}} \right)^{-\frac{D_{fb}}{2[\theta+2]}} \Gamma \left(\frac{D_{fb}}{\theta+2} \right). \quad D.74$$

Substituting eq. D.74 in eq. D.73:

$$\bar{p}_{wD}(s) = \frac{2 \left(A_{fD} [1 - \omega] \sqrt{\frac{\eta_{maD}}{H_D}} \right)^{\frac{D_{fb}}{2[\theta+2]} \frac{1}{2}}}{(\theta+2)^{\frac{D_{fb}}{\theta+2}} \Gamma \left(\frac{D_{fb}}{\theta+2} \right) s^{\frac{5}{4} - \frac{D_{fb}}{4[\theta+2]}}} K_{\frac{1-\beta}{\theta+2}} \left(\frac{2}{\theta+2} \sqrt{A_{fD} [1 - \omega] \sqrt{\frac{\eta_{maD} s}{H_D}}} \right). \quad D.75$$

For the $D_{fb} = \theta+2$ case, the Bessel function in the numerator is approximated as:

$$K_0 \left(\frac{2}{\theta+2} \sqrt{A_{fD} [1 - \omega] \sqrt{\frac{\eta_{maD} s}{H_D}}} \right) \approx - \left[\ln \left(\frac{1}{\theta+2} \sqrt{A_{fD} [1 - \omega] \sqrt{\frac{\eta_{maD} s}{H_D}}} \right) + \gamma \right], \quad D.76$$

thus, eq. D.75 can be expressed as:

$$\bar{p}_{wD}(s) = \frac{2}{\theta+2} \left[-\frac{1}{4} \frac{\ln(s)}{s} - \frac{1}{2} \frac{\ln \left(A_{fD} [1 - \omega] \sqrt{\frac{\eta_{maD}}{H_D}} \right)}{s} + \frac{\ln(\theta+2)}{s} - \frac{\gamma}{s} \right]. \quad D.77$$

Inverting to Real Space:

$$p_{wD}(t_D) = \frac{2}{\theta+2} \left[\frac{1}{4} \ln(t_D) - \frac{1}{2} \ln \left(A_{fD} [1 - \omega] \sqrt{\frac{\eta_{maD}}{H_D}} \right) + \ln(\theta+2) - 0.4329 \right]. \quad D.78$$

On the other hand, if $D_{fb} \neq \theta + 2$, then the Bessel function in the denominator is approximated as:

$$K_{\frac{1-\beta}{\theta+2}} \left(\frac{2}{\theta+2} \left(1 + \frac{S_{ma-fbD} \sqrt{H_D S}}{\sqrt{\eta_{maD}}} \right)^{\frac{1}{2}} \sqrt{A_{fD} [1-\omega] \sqrt{\frac{\eta_{maD} S}{H_D}}} \right) \approx \frac{(\theta+2)^{\frac{1-\beta}{\theta+2}}}{2} \left(A_{fD} [1-\omega] \sqrt{\frac{\eta_{maD} S}{H_D}} \right)^{\frac{1-\beta}{2[\theta+2]}} \Gamma \left(\frac{1-\beta}{\theta+2} \right) \quad D.79$$

substituting eq. D.79 in eq. D.75:

$$\bar{p}_{wD}(s) = \frac{(\theta+2)^{\frac{1-\beta-D_{fb}}{\theta+2}} \Gamma \left(\frac{1-\beta}{\theta+2} \right) \left(A_{fD} [1-\omega] \sqrt{\frac{\eta_{maD}}{H_D}} \right)^{\frac{D_{fb}-[\theta+2]-[1-\beta]}{2[\theta+2]}}}{\Gamma \left(\frac{D_{fb}}{\theta+2} \right) s^{\frac{5}{4} - \frac{D_{fb}}{4[\theta+2]} + \frac{1-\beta}{4[\theta+2]}}}, \quad D.80$$

since:

$$D_{fb} = \beta + \theta + 1, \quad D.81$$

then

$$\bar{p}_{wD}(s) = \frac{\Gamma \left(\frac{1-\beta}{\theta+2} \right) \left(A_{fD} [1-\omega] \sqrt{\frac{\eta_{maD}}{H_D}} \right)^{\frac{\beta-1}{\theta+2}}}{(\theta+2)^{\frac{2\beta+\theta}{\theta+2}} \Gamma \left(\frac{D_{fb}}{\theta+2} \right) s^{\frac{2\theta+5-\beta}{2[\theta+2]}}}. \quad D.82$$

Inverting to real space:

$$p_{wD}(t_D) = \frac{\Gamma \left(\frac{1-\beta}{\theta+2} \right) \left(A_{fD} [1-\omega] \sqrt{\frac{\eta_{maD}}{H_D}} \right)^{\frac{D_{fb}-[\theta+2]}{\theta+2}}}{\Gamma \left(\frac{D_{fb}}{\theta+2} \right) \Gamma \left(\frac{3}{2} - \frac{D_{fb}}{2[\theta+2]} \right) (\theta+2)^{\frac{2D_{fb}-[\theta+2]}{\theta+2}}} t_D^{\frac{1}{2} - \frac{D_{fb}}{2[\theta+2]}}. \quad D.83$$

D.6. Approximate solutions at large times: Single System Behavior

At short times, only the fracture network is acting:

$$f(s) \approx 1, \quad D.84$$

and eq. D.24 is reduced to:

$$\frac{\partial^2 p_{fbD}(r_D, t_D)}{\partial r_D^2} + \frac{\beta}{r_D} \frac{\partial p_{fbD}(r_D, t_D)}{\partial r_D} = r_D^\theta \frac{\partial p_{fbD}(r_D, t_D)}{\partial t_D}. \quad D.85$$

Applying an analogous procedure as shown in section D.4, the following solution was developed:

$$p_{fbD}(r_D, t_D) = -\frac{r_D^{\theta+2-D_{fb}}}{(\theta+2)\Gamma\left(\frac{D_{fb}}{\theta+2}\right)} \Gamma\left(\frac{D_{fb}}{\theta+2}-1, \frac{r_D^{\theta+2}}{(\theta+2)^2 t_D}\right). \quad \text{D.86}$$

In order to have simplified solutions relatively easy to use, two cases must be defined. The first case is given by the condition $D_{fb} = \theta + 2$. If that is the case, eq. D.86 and evaluated in $r_D = 1$, it becomes:

$$p_{wD}(t_D) = -\frac{1}{(\theta+2)} \Gamma\left(0, \frac{1}{(\theta+2)^2 t_D}\right). \quad \text{D.87}$$

According to incomplete gamma function convergences, prior expression can be expressed as:

$$p_{wD}(t_D) = -\frac{1}{(\theta+2)} E_i\left(\frac{1}{(\theta+2)^2 t_D}\right), \quad \text{D.88}$$

where:

$E_i(x)$ = integral exponential.

For small arguments of the integral exponential, eq. D.88 can be approximated as:

$$p_{wD}(t_D) = \frac{1}{(\theta+2)} [\ln(t_D) + 2 \ln(\theta+2) - \gamma], \quad \text{D.89}$$

where:

γ = Euler's constant.

On the other hand, for $D_{fb} \neq \theta + 2$ incomplete gamma function can be expressed as:

$$\Gamma(a, x) \approx \Gamma(a) - \frac{x^a}{a} + \frac{x^{a+1}}{[a+1]}. \quad \text{D.90}$$

Hence, incomplete gamma function for this problem is approximated as:

$$\Gamma\left(\frac{D_{fb}}{\theta+2}-1, \frac{r_D^{\theta+2}}{(\theta+2)^2 t_D}\right) = \Gamma\left(\frac{D_{fb}}{\theta+2}-1\right) - \left(\frac{1}{r_D^{\theta+2}}\right)^{1-\frac{D_{fb}}{\theta+2}} \frac{(\theta+2)^2 \left[1-\frac{D_{fb}}{\theta+2}\right]}{\frac{D_{fb}}{\theta+2}-1} t_D^{\frac{D_{fb}}{\theta+2}}. \quad \text{D.91}$$

Substituting D.91 in eq. D.86 and evaluating in $r_D = 1$:

$$p_{wD}(t_D) = \left[\frac{\Gamma\left(\frac{D_{fb}}{\theta+2}-1\right)}{(\theta+2)\Gamma\left(\frac{D_{fb}}{\theta+2}\right)} - \frac{(\theta+2)^{2\nu-1}}{\left[\frac{D_{fb}}{\theta+2}-1\right]\Gamma\left(\frac{D_{fb}}{\theta+2}\right)} t_D^\nu \right], \quad \text{D.92}$$

where:

$$v = 1 - \frac{D_{fb}}{\theta + 2}. \quad \text{D.93}$$

Recurrence formula states can be expressed as:

$$\frac{\Gamma(x-1)}{\Gamma(x)} = (x-1)^{-1}, \quad \text{D.94}$$

Therefore, eq. D.92 is rewritten as:

$$p_{wD}(t_D) = \frac{1}{-v(\theta + 2)} + \frac{(\theta + 2)^{2v-1}}{v\Gamma\left(\frac{D_{fb}}{\theta + 2}\right)} t_D^v. \quad \text{D.95}$$

D.7. Convergence to Cinco-Ley and Samaniego (1982)

This model satisfies the $D_{fb} = \theta + 2$ condition, due to the fractal dimension of fracture network, D_{fb} , converges to the Euclidian radial dimension ($D_{fb} = 2$) and the anomaly in conductivity in fractal object, θ , is zero. Therefore, for early times, D.65 reduces to:

$$p_{wD}(t_D) = \frac{1}{2} [\ln(t_D) + 2 \ln(2) - \ln(\omega) - \gamma], \quad \text{D.96}$$

where:

$$\gamma = 0.5772156649, \quad \text{D.97}$$

Arraying:

$$p_{wD}(t_D) = \frac{1}{2} \left[\ln\left(\frac{t_D}{\omega}\right) + 0.8091 \right]. \quad \text{D.98}$$

Analogously, for intermediate times eq. D.78 reduces to:

$$p_{wD}(t_D) = \frac{1}{4} \ln(t_D) - \frac{1}{2} \ln\left(A_{fD} [1 - \omega] \sqrt{\frac{\eta_{maD}}{H_D}}\right) + 0.2602. \quad \text{D.99}$$

And, for late times, eq. D.89 becomes:

$$p_{wD}(t_D) = \frac{1}{2} [\ln(t_D) + 0.8091]. \quad \text{D.100}$$

Summary:

A double porosity flow model assuming a fractal reservoir and transient interporosity transference was developed. Diffusivity equation describing such flow on its dimensionless form is given by eq. D.24:

$$\frac{\partial^2 p_{fbD}(r_D, t_D)}{\partial r_D^2} + \frac{\beta}{r_D} \frac{\partial p_{fbD}(r_D, t_D)}{\partial r_D} - r_D^\theta A_{fD} [1 - \omega] \int_0^{t_D} \frac{\partial p_{fbD}(r_D, \tau)}{\partial \tau} F(\eta_{maD}, H_D, t_D - \tau) d\tau =$$

$$= r_D^\theta \omega \frac{\partial p_{fbD}(r_D, t_D)}{\partial t_D}$$

The solution in Laplace Space for the previous equation, assuming infinite reservoir and constant flow rate at wellbore is given by eq. D.54:

$$\bar{p}_D(r_D, s) = \frac{r_D^{\frac{1-\beta}{2}} K_{\frac{1-\beta}{\theta+2}} \left(\frac{2\sqrt{sf(s)}}{\theta+2} r_D^{\frac{\theta+2}{2}} \right)}{s^{3/2} \sqrt{f(s)} K_{\frac{D_{fb}}{\theta+2}} \left(\frac{2\sqrt{sf(s)}}{\theta+2} \right)},$$

where transference function is defined by eq. D.38:

$$f(s) = A_{fD} [1 - \omega] \bar{F}(\eta_{maD}, H_D, s) + \omega.$$

The analytical solution when the fracture network is under expansion (short times) is given by eq. D.62:

$$p_{fbD}(r_D, t_D) = - \frac{r_D^{\theta+2-D_{fb}}}{(\theta+2) \Gamma\left(\frac{D_{fb}}{\theta+2}\right)} \Gamma\left(\frac{D_{fb}}{\theta+2} - 1, \frac{\omega r_D^{\theta+2}}{(\theta+2)^2 t_D}\right).$$

It was shown that two approximations can be obtained, depending on the values of D_{fb} and θ . If, $D_{fb} = \theta + 2$ the approximation is given by eq. D.65:

$$p_{wD}(t_D) = \frac{1}{(\theta+2)} [\ln(t_D) + 2 \ln(\theta+2) - \ln(\omega) - \gamma].$$

The convergence to Cinco-Ley et al.'s model (1982) is based on this case. It results when $\theta = 0$, and consequently $D_{fb} = 2$. The result of this case is depicted in eq. D.98:

$$p_{wD}(t_D) = \frac{1}{2} \left[\ln\left(\frac{t_D}{\omega}\right) + 0.8091 \right].$$

On the other hand, if $D_{fb} \neq \theta + 2$ the approximated solution for short times is given by eq. D.71:

$$p_{wD}(t_D) = \frac{1}{-v(\theta+2)} + \frac{(\theta+2)^{2v-1} \omega^{v-1}}{v \Gamma\left(\frac{D_{fb}}{\theta+2}\right)} t_D^v.$$

For the interaction period two approximations can be obtained, depending on the values of D_{fb} and θ . If, $D_{fb} = \theta + 2$ the approximation is given by eq. D.174:

$$p_{wD}(t_D) = \frac{2}{\theta + 2} \left[\frac{1}{4} \ln(t_D) - \frac{1}{2} \ln \left(A_{fD} [1 - \omega] \sqrt{\frac{\eta_{maD}}{H_D}} \right) + \ln(\theta + 2) - 0.4329 \right].$$

Again, the convergence to Cinco-Ley et al.'s model (1982) results when $\theta = 0$, and consequently $D_{fb} = 2$. The result of this case is given by eq. D.99:

$$p_{wD}(t_D) = \frac{1}{4} \ln(t_D) - \frac{1}{2} \ln \left(A_{fD} [1 - \omega] \sqrt{\frac{\eta_{maD}}{H_D}} \right) + 0.2602.$$

On the other hand, the $D_{fb} \neq \theta + 2$ case is given by eq. D.83:

$$p_{wD}(t_D) = \frac{\Gamma\left(\frac{1-\beta}{\theta+2}\right) \left(A_{fD} [1 - \omega] \sqrt{\frac{\eta_{maD}}{H_D}} \right)^{\frac{D_{fb} - [\theta+2]}{\theta+2}}}{\Gamma\left(\frac{D_{fb}}{\theta+2}\right) \Gamma\left(\frac{3}{2} - \frac{D_{fb}}{2[\theta+2]}\right) (\theta+2)^{\frac{2D_{fb} - [\theta+2]}{\theta+2}}} t_D^{\frac{1}{2} - \frac{D_{fb}}{2[\theta+2]}}.$$

The analytical solution for the single system behavior (late times) is given by eq. D.86:

$$p_{fbD}(r_D, t_D) = - \frac{r_D^{\theta+2-D_{fb}}}{(\theta+2) \Gamma\left(\frac{D_{fb}}{\theta+2}\right)} \Gamma\left(\frac{D_{fb}}{\theta+2} - 1, \frac{r_D^{\theta+2}}{(\theta+2)^2 t_D}\right).$$

Analogously to the previous cases, if $D_{fb} = \theta + 2$ the approximation is given by eq. D.89:

$$p_{wD}(t_D) = \frac{1}{(\theta+2)} [\ln(t_D) + 2 \ln(\theta+2) - \gamma].$$

The convergence to Cinco-Ley et al.'s model (1982) is based on this case. It results when $\theta = 0$, and consequently $D_{fb} = 2$. The result of this case is depicted in eq. D.100:

$$p_{wD}(t_D) = \frac{1}{2} [\ln(t_D) + 0.8091].$$

On the other hand, if $D_{fb} \neq \theta + 2$ the approximated solution for short times is given by eq. D.95:

$$p_{wD}(t_D) = \frac{1}{-v(\theta+2)} + \frac{(\theta+2)^{2v-1} \omega^{v-1}}{v \Gamma\left(\frac{D_{fb}}{\theta+2}\right)} t_D^v.$$

Appendix E

Modified Transient Matrix-Response Model (Larsen, 2013)

The approach from Appendix C can be recast in a different form which comes closer to the Pseudosteady-state (PSS) model and has a similar late-time behavior, which Olarewaju's model (1996) does not. To this end, note that in a direct comparison of standard PSS and transient Euclidean slab models with flow equations, from Warren and Root (1963):

$$\frac{k_{fb}}{\mu} \frac{1}{r} \frac{\partial}{\partial r} \left(r \frac{\partial p_{fb}}{\partial r} \right) = \phi_{fb} c_{tfb} \frac{\partial p_{fb}}{\partial t} + \phi_{ma} c_{tma} \frac{\partial p_{ma}}{\partial t}, \quad E.1$$

on the other hand, from Serra et al. (1982):

$$\frac{k_{fb}}{\mu} \frac{1}{r} \frac{\partial}{\partial r} \left(r \frac{\partial p_{fb}}{\partial r} \right) = \phi_{fb} c_{tfb} \frac{\partial p_{fb}}{\partial t} - \frac{k_{ma}}{\mu h_1} \left(\frac{\partial p_{ma}}{\partial z} \right)_{z=0}. \quad E.2$$

we can get from the PSS model to the transient model by replacing the “storage term” in the matrix by the “flux term” from the matrix. With the same approach we should be able to modify the PSS model proposed by Chang et al. (1990) combining it with the model proposed by Olarewaju (1996):

$$\frac{1}{r_D^{\beta+\theta}} \frac{\partial}{\partial r_D} \left(r_D^\beta \frac{\partial p_{fbD}}{\partial r_D} \right) = \omega \frac{\partial p_{fbD}}{\partial t_D} - [1 - \omega] r_D^{d_e - D_{fb}} \frac{\lambda}{3} \frac{\partial p_{maD}}{\partial z_D}. \quad E.3$$

Following Laplace transformation and steps similar to those in Appendices C and D, the following equation can be derived:

$$\frac{1}{r_D^{\beta-\theta}} \frac{d}{dr_D} \left(r_D^\beta \frac{d\bar{p}_{fbD}}{dr_D} \right) = \left[\omega s + \frac{\lambda}{3} r_D^{d_e - D_{fb}} \sqrt{\alpha s} \tanh(L_D \sqrt{\alpha s}) \right] \bar{p}_{fbD}, \quad E.4$$

where:

$$L_D^2 \alpha = \frac{3[1 - \omega]}{\lambda}, \quad E.5$$

then, for small values of ω , we can ignore the first term inside the brackets and it is reduced to:

$$\frac{1}{r_D^{\beta-\theta}} \frac{d}{dr_D} \left(r_D^\beta \frac{d\bar{p}_{fbD}}{dr_D} \right) = \frac{\lambda}{3} r_D^{d_e - D_{fb}} \sqrt{\alpha s} \tanh(L_D \sqrt{\alpha s}) \bar{p}_{fbD}. \quad E.6$$

This page is intentionally left in blank.

Appendix F

Wellbore Storage for Fractal Models

F. 1. Wellbore Storage

Total flow rate is given by:

$$q = q_{wb}(t) + q_{sf}(t), \quad \text{F.1}$$

where:

$$q_{wb}(t) = \text{rate in wellbore,}$$

and:

$$q_{sf}(t) = \text{sandface rate.}$$

Multiplying F.1 by B_o :

$$qB_o = q_{wb}(t)B_o + q_{sf}(t)B_o. \quad \text{F.2}$$

Rate in wellbore is given by:

$$q_{wb}(t)B_o = -24c_{wb}V_{wb} \frac{dp_{wf}(t)}{dt}. \quad \text{F.3}$$

Storage coefficient is defined as:

$$C = c_{wb}V_{wb}, \quad \text{F.4}$$

substituting storage coefficient in F.3 results:

$$qB_o = -24C \frac{dp_{wf}(t)}{dt} + q_{sf}(t)B_o. \quad \text{F.5}$$

On the other hand, sandface rate is given by the equation:

$$q_{sf}(t)B_o = \frac{\alpha_n b^{3-n} k_{fb}}{\mu} \left(r^{n-\theta-1} \frac{\partial p_{fb}}{\partial r} \right)_{r=r_w}. \quad \text{F.6}$$

Therefore, substituting prior equation into F.5:

$$qB_o = -24C \frac{dp_{wf}(t)}{dt} + \frac{\alpha_n b^{3-n} k_{fb}}{\mu} \left(r^{n-\theta-1} \frac{\partial p_{fb}}{\partial r} \right)_{r=r_w}. \quad \text{F.7}$$

Dimensionless time is defined as:

$$t_D = \frac{k_{fb}}{(\phi c_i)_i \mu r_w^{2+\theta}} t, \quad \text{F.8}$$

where:

$$(\phi c_i)_i = \phi_{fb} c_{ifb} + \phi_{ma} c_{ima}. \quad \text{F.9}$$

Besides, dimensionless pressure in the fracture network is given by:

$$p_{fbD}(r_D, t_D) = \frac{aV_{uf}k_{fb}[p_i - p_{fb}(r, t)]}{q\mu r_w^{1-\beta}\phi_{fb}}. \quad \text{F.10}$$

Hence, using dimensionless variables definitions:

$$\frac{\partial p_{fb}(r, t)}{\partial t} = \left[-\frac{qB_o\mu r_w^{1-\beta}\phi_{fb}}{aV_{uf}k_{fb}} \right] \left[\frac{k_{fb}}{(\phi c_t)_t \mu r_w^{2+\theta}} \right] \frac{\partial p_{fbD}(r_D, t_D)}{\partial t_D}, \quad \text{F.11}$$

and,

$$\frac{\partial p_{fb}(r, t)}{\partial r} = -\frac{qB_o\mu r_w^{-\beta}\phi_{fb}}{aV_{uf}k_{fb}} \frac{\partial p_{fbD}(r_D, t_D)}{\partial r_D}. \quad \text{F.12}$$

Substituting F.11 and F.12 in F.7, it becomes:

$$1 = 24C \frac{r_w^{-D_{fb}}\phi_{fb}}{aV_{uf}(\phi c_t)_t} \frac{\partial p_{wD}(t_D)}{\partial t_D} - \frac{\phi_{fb}r_w^{n-D_{fb}}\alpha_n b^{3-n}}{aV_{uf}} \left(r_D^{n-\theta-1} \frac{\partial p_{fbD}(r_D, t_D)}{\partial r_D} \right)_{r_D=1}. \quad \text{F.13}$$

According to the fractal fracture network porosity definition:

$$\phi_{fb} = \frac{ar^{D_{fb}-n}V_{uf}}{\alpha_n b^{3-n}}, \quad \text{F.14}$$

Eq. F.13 becomes:

$$1 = \frac{24\phi_{fb}C}{aV_{uf}(\phi c_t)_t r_w^{D_{fb}}} \frac{\partial p_{wD}(t_D)}{\partial t_D} - \left(r_D^\beta \frac{\partial p_{fbD}(r_D, t_D)}{\partial r_D} \right)_{r_D=1}. \quad \text{F.15}$$

Dimensionless wellbore storage for fractal reservoirs is defined as:

$$C_D = \frac{24\phi_{fb}C}{aV_{uf}(\phi c_t)_t r_w^{D_{fb}}}. \quad \text{F.16}$$

Hence:

$$\left(r_D^\beta \frac{\partial p_{fbD}(r_D, t_D)}{\partial r_D} \right)_{r_D=1} = C_D \frac{\partial p_{wD}(t_D)}{\partial t_D} - 1. \quad \text{F.17}$$

F. 2. Wellbore Storage in Damaged Zone

Wellbore Storage in the entire damaged zone in a fractal reservoir is given by:

$$C_{Swell} = C + \frac{aV_{uf}(\phi c_t)_t r_{we}^{D_{fb}}}{24\phi_{fb}} - \frac{aV_{uf}(\phi c_t)_t r_w^{D_{fb}}}{24\phi_{fb}}, \quad \text{F.18}$$

Where:

r_{we} = effective wellbore radius, it is defined as:

$$r_{we} = r_w e^{-Swell} . \quad F.19$$

Substituting effective wellbore radius definition in F.18, the following expression results:

$$C_{Swell} = C + \frac{aV_{uf}(\phi c_t)_t r_w^{D_{fb}}}{24\phi_{fb}} \left[e^{-D_{fb}Swell} - 1 \right]. \quad F.20$$

According to dimensionless wellbore storage for fractal reservoirs definition:

$$C_D = \frac{24\phi_{fb}C}{aV_{uf}(\phi c_t)_t r_w^{D_{fb}}}, \quad F.21$$

eq. F.20 becomes:

$$\frac{24\phi_{fb}}{aV_{uf}(\phi c_t)_t r_w^{D_{fb}}} C_{Swell} = C_D + e^{-D_{fb}Swell} - 1. \quad F.22$$

Dimensionless Wellbore Storage in the damaged zone in a fractal reservoir is defined as:

$$C_{SwellD} = \frac{24\phi_{fb}C_{Swell}}{aV_{uf}(\phi c_t)_t r_w^{D_{fb}}}, \quad F.23$$

substituting prior definition in F.22:

$$C_{SwellD} e^{D_{fb}Swell} = [C_D - 1] e^{D_{fb}Swell} + 1. \quad F.24$$

This page is intentionally left in blank.

Appendix G

Constant Rate Solutions with Boundary Effects

In Chapter III the development of a dimensionless diffusivity equation for a double porosity fractal reservoir was shown. It is given by:

$$\begin{aligned} \frac{\partial^2 p_{fbD}(r_D, t_D)}{\partial r_D^2} + \frac{\beta}{r_D} \frac{\partial p_{fbD}(r_D, t_D)}{\partial r_D} - r_D^\theta A_{fD} [1 - \omega] \int_0^{t_D} \frac{\partial p_{maD}(r_D, \tau)}{\partial \tau} F(\eta_{maD}, H_D, t_D - \tau) d\tau = \\ , G.1 \\ = r_D^\theta \omega \frac{\partial p_{fbD}(r_D, t_D)}{\partial t_D} \end{aligned}$$

and its general solution in Laplace space and approximate solutions in real space, assuming an infinite reservoir, was shown in Chapter IV.

This appendix shows the solutions of the fractal model when it is affected by radial boundary effects, i.e., constant pressure and closed reservoirs. For both cases the initial condition is the same as the one used in the infinite fractal reservoir, i.e.:

$$p_{fbD}(r_D, t_D = 0) = 0, \quad G.2$$

hence general solution for eq. G.1 in Laplace space, considering initial condition given by eq. G.2 is:

$$\bar{p}_D(r_D, s) = r_D^{\frac{1-\beta}{2}} \left[c_3 I_{\frac{1-\beta}{\theta+2}}(g(s)r_D^\varepsilon) + c_4 K_{\frac{1-\beta}{\theta+2}}(g(s)r_D^\varepsilon) \right]. \quad G.3$$

where:

$$g(s) = \frac{2\sqrt{sf(s)}}{\theta + 2}, \quad G.4$$

function $f(s)$ is given by:

$$f(s) = \frac{A_{fD} [1 - \omega] \bar{F}(\eta_{maD}, H_D, s)}{1 + \frac{H_D S_{ma-\beta D}}{\eta_{maD}} \bar{F}(\eta_{maD}, H_D, s) s} + \omega, \quad G.5$$

and:

$$\varepsilon = \frac{\theta + 2}{2}. \quad G.6$$

G.1. Constant rate solution of a fractal reservoir model assuming transient interporosity Transference and constant pressure boundary

When a reservoir is affected by a large aquifer or a cap gas, it is subjected to an outer constant pressure boundary. Such case is stated and solve as follows:

inner Boundary:
$$r_D^\beta \frac{\partial p_{fbD}(1, t_D)}{\partial t_D} = -1, \quad \text{G.7}$$

outer boundary:
$$p_D(L_D, t_D) = 0. \quad \text{G.8}$$

Applying outer boundary condition, G.8:

$$\bar{p}_D(L_D, s) = L_D^2 \left[c_3 I_{\frac{1-\beta}{\theta+2}}(g(s)L_D^\varepsilon) + c_4 K_{\frac{1-\beta}{\theta+2}}(g(s)L_D^\varepsilon) \right], \quad \text{G.9}$$

hence:

$$c_3 I_{\frac{1-\beta}{\theta+2}}(g(s)L_D^\varepsilon) + c_4 K_{\frac{1-\beta}{\theta+2}}(g(s)L_D^\varepsilon) = 0. \quad \text{G.10}$$

and:

$$c_3 = -c_4 \frac{K_{\frac{1-\beta}{\theta+2}}(g(s)L_D^\varepsilon)}{I_{\frac{1-\beta}{\theta+2}}(g(s)L_D^\varepsilon)}. \quad \text{G.11}$$

Applying the derivative regarding r_D in eq. G.3, it can be verified that:

$$\frac{d\bar{p}_D(r_D, s)}{dr_D} = c_3 r_D^{\frac{-\beta-1}{2}} \left[g(s)\varepsilon r_D^\varepsilon I_{\frac{1-\beta}{\theta+2}-1}(g(s)r_D^\varepsilon) \right] + c_4 r_D^{\frac{-\beta-1}{2}} \left[g(s)\varepsilon r_D^\varepsilon K_{\frac{1-\beta}{\theta+2}-1}(g(s)r_D^\varepsilon) \right]. \quad \text{G.12}$$

Applying inner boundary condition:

$$r_D^\beta \frac{d\bar{p}_D(r_D = 1, s)}{dr_D} = c_3 \left[g(s)\varepsilon I_{\frac{1-\beta}{\theta+2}-1}(g(s)) \right] + c_4 \left[g(s)\varepsilon K_{\frac{1-\beta}{\theta+2}-1}(g(s)) \right], \quad \text{G.13}$$

therefore:

$$c_3 I_{\frac{1-\beta}{\theta+2}-1}(g(s)) + c_4 K_{\frac{1-\beta}{\theta+2}-1}(g(s)) = -\frac{1}{sg(s)\varepsilon}. \quad \text{G.14}$$

Substituting eq. G.11 into G.14:

$$\left[-c_4 \frac{K_{\frac{1-\beta}{\theta+2}}(g(s)L_D^\varepsilon)}{I_{\frac{1-\beta}{\theta+2}}(g(s)L_D^\varepsilon)} \right] I_{\frac{1-\beta}{\theta+2}-1}(g(s)) + c_4 K_{\frac{1-\beta}{\theta+2}-1}(g(s)) = -\frac{1}{sg(s)\varepsilon}, \quad \text{G.15}$$

hence:

$$c_4 = \frac{1}{sg(s)\varepsilon \left[K_{\frac{1-\beta}{\theta+2}}(g(s)) - \frac{K_{\frac{1-\beta}{\theta+2}}(g(s)L_D^\varepsilon)I_{\frac{1-\beta}{\theta+2}}(g(s))}{I_{\frac{1-\beta}{\theta+2}}(g(s)L_D^\varepsilon)} \right]}, \quad \text{G.16}$$

therefore:

$$c_3 = \frac{1}{sg(s)\varepsilon \left[K_{\frac{1-\beta}{\theta+2}}(g(s)) - \frac{K_{\frac{1-\beta}{\theta+2}}(g(s)L_D^\varepsilon)I_{\frac{1-\beta}{\theta+2}}(g(s))}{I_{\frac{1-\beta}{\theta+2}}(g(s)L_D^\varepsilon)} \right]} \frac{K_{\frac{1-\beta}{\theta+2}}(g(s)L_D^\varepsilon)}{I_{\frac{1-\beta}{\theta+2}}(g(s)L_D^\varepsilon)}. \quad \text{G.17}$$

Pressure at wellbore is given by:

$$\bar{p}_{wD}(s) = c_3 I_{\frac{1-\beta}{\theta+2}}(g(s)r_D^\varepsilon) + c_4 K_{\frac{1-\beta}{\theta+2}}(g(s)r_D^\varepsilon), \quad \text{G.18}$$

where constants c_3 and c_4 are given by eqs. G.17 and G.16, respectively.

G.2. Constant Rate Solution of a closed Fractal Reservoir Model assuming Transient Interporosity Transference

When one is dealing with a closed reservoir e.g., an impermeable fault, such case has to be stated as follows:

$$\text{inner boundary:} \quad r_D^\beta \frac{\partial p_{\beta D}(1, t_D)}{\partial t_D} = -1, \quad \text{G.19}$$

$$\text{outer boundary:} \quad \frac{\partial p_D(L_D, t_D)}{\partial r_D} = 0. \quad \text{G.20}$$

Applying the derivative regarding r_D in eq. G.3:

$$\frac{d\bar{p}_D(r_D, s)}{dr_D} = c_5 r_D^{-\beta-1} \left[g(s)\varepsilon r_D^\varepsilon I_{\frac{1-\beta}{\theta+2}}(g(s)r_D^\varepsilon) \right] + c_6 r_D^{-\beta-1} \left[g(s)\varepsilon r_D^\varepsilon K_{\frac{1-\beta}{\theta+2}}(g(s)r_D^\varepsilon) \right]. \quad \text{G.21}$$

Applying inner boundary condition in eq. G.21:

$$r_D^\beta \frac{d\bar{p}_D(r_D = 1, s)}{dr_D} = c_5 \left[g(s)\varepsilon I_{\frac{1-\beta}{\theta+2}}(g(s)) \right] + c_6 \left[g(s)\varepsilon K_{\frac{1-\beta}{\theta+2}}(g(s)) \right], \quad \text{G.22}$$

therefore:

$$c_5 I_{\frac{1-\beta}{\theta+2}}(g(s)) + c_6 K_{\frac{1-\beta}{\theta+2}}(g(s)) = -\frac{1}{sg(s)\varepsilon}. \quad \text{G.23}$$

Applying outer boundary condition to eq. G.21:

$$\frac{d\bar{p}_D(L_D, s)}{dr_D} = c_5 L_D^{\frac{-\beta-1}{2}} \left[g(s) \varepsilon L_D^\varepsilon I_{\frac{1-\beta}{\theta+2}} \left(g(s) L_D^\varepsilon \right) \right] + c_6 L_D^{\frac{-\beta-1}{2}} \left[g(s) \varepsilon L_D^\varepsilon K_{\frac{1-\beta}{\theta+2}} \left(g(s) L_D^\varepsilon \right) \right] = 0, \quad \text{G.24}$$

hence:

$$c_5 = -c_6 \frac{K_{\frac{1-\beta}{\theta+2}} \left(g(s) L_D^\varepsilon \right)}{I_{\frac{1-\beta}{\theta+2}} \left(g(s) L_D^\varepsilon \right)}. \quad \text{G.25}$$

Substituting c_5 into eq. G.23 results:

$$c_6 = - \frac{1}{sg(s) \varepsilon \left[K_{\frac{1-\beta}{\theta+2}} \left(g(s) \right) - \frac{K_{\frac{1-\beta}{\theta+2}} \left(g(s) L_D^\varepsilon \right) I_{\frac{1-\beta}{\theta+2}} \left(g(s) \right)}{I_{\frac{1-\beta}{\theta+2}} \left(g(s) L_D^\varepsilon \right)} \right]}, \quad \text{G.26}$$

and:

$$c_5 = \frac{K_{\frac{1-\beta}{\theta+2}} \left(g(s) L_D^\varepsilon \right)}{sg(s) \varepsilon \left[K_{\frac{1-\beta}{\theta+2}} \left(g(s) \right) - \frac{K_{\frac{1-\beta}{\theta+2}} \left(g(s) L_D^\varepsilon \right) I_{\frac{1-\beta}{\theta+2}} \left(g(s) \right)}{I_{\frac{1-\beta}{\theta+2}} \left(g(s) L_D^\varepsilon \right)} \right] I_{\frac{1-\beta}{\theta+2}} \left(g(s) L_D^\varepsilon \right)}. \quad \text{G.27}$$

Pressure at wellbore is given by:

$$\bar{p}_{wD}(s) = c_5 I_{\frac{1-\beta}{\theta+2}} \left(g(s) r_D^\varepsilon \right) + c_6 K_{\frac{1-\beta}{\theta+2}} \left(g(s) r_D^\varepsilon \right), \quad \text{G.28}$$

where constants c_5 and c_6 are given by eqs. G.27 and G.26, respectively.
